Behaviour of steel I-beams reinforced while under load

Masoud Mohammadzadeh

A Thesis in

The Department

of

Building Civil and Environmental Engineering

Presented in Partial Fulfillment of the Requirements

For the Degree of

Doctor of Philosophy (Civil Engineering) at

Concordia University

Montréal, Québec, Canada

October 2022

CONCORDIA UNIVERSITY

SCHOOL OF GRADUATE STUDIES

This is to certify that the thesis prepared

By: Masoud Mohammadzadeh

Entitled: Behaviour of steel I-beams reinforced while under load

and submitted in partial fulfillment of the requirements for the degree of

Doctor Of Philosophy Civil Engineering

complies with the regulations of the University and meets the accepted standards with respect to originality and quality.

Signed by the final examining committee:

_____ Chair
Dr. Yuhong Yan

_____ Thesis Supervisor
Dr. Anjan Bhowmick

_____ Examiner
Dr. Lucia Tirca

_____ Examiner
Dr. Emre Erkmen

_____ Examiner
Dr. Mehdi Hojjati

_____ External Examiner
Dr. M. Shahria Alam

Approved by _____
Dr. Mazdak Nik-Bakht , Graduate Program Director

«2022-12-09» _____
Dr. Mourad Debbabi , Dean

ABSTRACT

Behaviour of steel I-beams reinforced while under load

Masoud Mohammadzadeh, Ph.D.

Concordia University, 2022

Steel beams often require reinforcing while they are under load. This may be due to inappropriate design, defective constructions, structure aging, additional bearing requirements, material deterioration, or accidental damage. A common method for reinforcing steel members is by attaching a steel cover plate onto the existing structure by welding. This strengthening technique can increase the stiffness and strength and can also change the structural behaviour and failure mode of the strengthened steel beam. Very limited research has been conducted on the strengthening of steel beams while they are in service. This research presents a Finite element (FE) based study on steel I-beams welded with steel cover plates while under load. The details of the development of the FE models are presented and the developed models are validated by comparing them against available experimental test results of steel beams reinforced while under load. With the validated FE models, a series of steel I-beams reinforced with steel cover plates at the bottom flanges are analyzed. The considered failures for these beams are cross-section yielding and lateral-torsional buckling limit state flexural resistance. The behaviour and ultimate capacity of simply supported I-beams subjected to positive moment; and continuous-span I-beams subjected to negative moment by welding a cover plate while under load are studied. For the simply supported I-beams, the effects of different parameters, such as residual stress patterns in the I-beam and cover plate, welding residual stress, type of welding patterns, and the difference in steel grades between the I-beam and reinforcing plate, on the behaviour of the steel I-beams reinforced while under load are investigated numerically. FE analysis shows that with increased preload, the capacity of the I-beam reinforced under load reduces when the failure mode of the beam is lateral-torsional buckling (LTB). On the other hand, the variation of the preload has an insignificant effect on the behaviour and ultimate strength of the reinforced beam when the reinforced beam fails in flexural yielding. Moreover, the flexural capacities of reinforced simply supported I-beams with welded cover plates obtained from FE analyses are compared with the capacities predicted by the American (AISC 360-16) and Canadian (CAN/CSA-S16-19) steel design standards. FE analysis shows that AISC 360-16, when the effect of loading height is considered, can reasonably predict the capacity of simply supported I-beams reinforced with welded cover plate at the bottom flange.

In addition, the effects of welding heat, welding sequence, and weld length on the residual welding deformation and behaviour of simply supported steel I-beams reinforced while under load are investigated by considering welding procedure simulation. It is observed that an appropriate welding sequence and weld length can reduce the residual lateral deformations induced from welding a reinforcing plate to the bottom flange of the preloaded I-beam and thus control the unfavorable welding effects. Based on the analyses, a welding segment length of L/9, where L is the length of the beam, is recommended for practical applications. In addition, the effects of initial geometric imperfection and preload level on the welding residual deformation and the behaviour of the reinforced beams are studied numerically. FE analysis shows that the direction and magnitude of initial geometrical imperfection can change the value and direction of the residual deformation resulting from welding.

Finally, the numerical study includes the preloaded steel I-beams reinforced with steel cover plates welded to the compression flanges of the continuous-span beams. Three-point loading condition is considered to simulate continuous span bridges. FE analyses show that adding a cover plate to each span of the beam can increase the ultimate capacity and stiffness of the beam. Also, the reinforcement can prevent the beam from lateral torsional buckling failure mode and the beam can reach its capacity. Furthermore, similar to simply supported beams, the preloading level has an insignificant effect on the behaviour and ultimate capacity of the continuous-span beam reinforced with a cover plate welded to the compression flange.

Acknowledgments

It is my pleasure to express my gratitude to numerous people who helped me to undertake and complete the journey of Ph.D. candidacy. Without their support and help, this dissertation would not have been possible.

First and foremost, I would like to thank my supervisor, Dr. Anjan Bhowmick, for his guidance, and encouragement and for allowing me to continue my studies under his supervision. Dr. Bhowmick was always accessible and willing to help and support me with my research. It has been an honour and privilege to work and learn from Dr. Bhowmick.

I would like to acknowledge the financial support from Gina Cody School of Engineering and Computer Science, Concordia University, Montreal, Canada and the Natural Sciences and Engineering Research Council of Canada.

My deepest gratitude goes to my parents, Shokoufeh and Sadyar for their love, support and patience in all my endeavors. I also thank my sister, Solmaz, my brother, Milad and my in-laws for their endless support during my Ph.D. I am blessed to have such a wonderful family.

Last but not least, words fail me to express my appreciation to my wife, Mahsa. She dedicated so much of her time and effort to make it easier for me to focus on doing my research and completing this dissertation over the past four years of my study.

Dedication

Dedicated with infinite love to my Father, Mother,

Wife,

Sister and Brother

Co-Authorship

This thesis has been prepared in accordance with the regulations for a manuscript-based thesis format. This research presents numerical work carried out solely by Masoud Mohammadzadeh. Advice and guidance were provided for the whole thesis by the academic supervisor Dr. Anjan Bhowmick. This thesis consists of the following chapters:

- Chapter 3
  Mohammadzadeh, M., Bhowmick, A.K. Behavior of steel I-beams reinforced while under load. Engineering Structures 2022; 257 (6):114080.
- Chapter 4
  Mohammadzadeh, M., Bhowmick, A.K. Reinforcing preloaded steel I-beams by considering welding heat effects and geometric imperfections. Canadian Journal of Civil Engineering 2022; Submitted.
- Chapter 5
  Mohammadzadeh, M., Bhowmick, A.K. Reinforcing of steel I-beams with welded cover plates in the negative bending moment region. Journal of Bridge Engineering 2022; Submitted

1. Contents

List of Tables

List of Figures

1. INTRODUCTION

1.1. BACKGROUND AND PROBLEM DEFINITION

Reinforcing existing steel beams is often unavoidable due to the change of the primary function of the structure or additional applied loads. Replacement of the beams is more expensive and time-consuming which can be avoided by reinforcing and increasing their capacity. On the other hand, beams that require strengthening often are in service and complete relieving of their loads is not either possible or not economical. Thus, steel beams may need to be reinforced while under load.

Research on steel beams reinforced with welded steel plates while under load is very limited. Liu and Gannon (2007) first studied the behaviour of steel beams reinforced under load by conducting tests on steel I-beams reinforced with welded cover plates. Two different reinforcing patterns, one where a plate was welded to the bottom flange of the beam section along its length (pattern A) and the other where two plates were welded against tips of the flanges of the beam section along its length (pattern B), were considered and the specimens were tested for different preload levels. It was observed that increasing the preload resulted in a decrease in lateral-torsional buckling strength for beams with pattern A reinforcement (plate welded to the bottom flange) than the same specimen strengthened under no preload.

It was also reported that the variation of the preload level has an insignificant effect on the ultimate resistance and behaviour of beams with flexural yielding failure (pattern B). Furthermore, Liu and Gannon (2009) continued their investigation by conducting parametric studies on the effects of the preload magnitude, initial imperfection, length of the cover plate, the span of the beam and lateral restraint on the reinforcement of the steel beams. In their numerical study, a reduction of resistance of beams with lateral-torsional buckling failure by increasing preload was indicated for beams with type A reinforcement. Liang et al. (2015) conducted a detailed experimental investigation on the I-steel beams reinforced while under load by welding cover plates on the top and bottom flanges. In their research, the procedures of reinforcement, preloading and welding of reinforcing plates and their effects were studied. Three reinforced I-beams with preload levels 0, 37% and 74% of the unreinforced beam capacity were investigated. It was reported that for the beam with the 37% preload level, the failure was lateral-torsional buckling and the ultimate capacity was reduced comparing with the capacity of the reinforced beam without preloading. However, for the reinforced beam with the 74% preloading level, the ultimate capacity increased. The failure mode for this beam was flange local buckling. Thus, no clear and definable relationship was obtained between the preload and strength of the reinforced beam from the study of Liang et al. (2015).

1.2. RESEARCH SIGNIFICANCE AND MOTIVATION

Many steel buildings and bridges in Canada are in serious need of rehabilitation or strengthening. This is either due to the increased load caused by the new utilization of the structures or due to the publication of new design codes that dictate higher demands on existing structures or structural elements. Beams are often required to be reinforced after they have been placed in service and are loaded with dead loads and partial live loads. When the bottom flange of the I-beam is easily accessible, the most economical option is to weld a cover plate to the bottom flange. Currently, there are no specific design guidelines available in North American design standards for steel beams reinforced under load, although many steel beams have been strengthened. The design procedure generally involves selecting a cover plate that is able to resist the additional factored moment applied in the beam. While the current practice is simple, it is not clear to the designer how the reinforced beam will behave if locked-in stresses due to dead loads are present during the reinforcement. In addition, if the cover plate is welded, there can be welding residual stresses which might cause non-uniform yielding in the reinforced beam. Another issue is that beams in many existing structures are often of lower grade steel than the more modern steels used for reinforcement, and this can complicate the design and analysis of the reinforced beam further.

Furthermore, the presence of local but intense heat induced by welding the cover plate to the beam is the other vital parameter in the behaviour of beams reinforced while under. The local heating induced by welding can cause transient and permanent deflections in the beams. Also, this intense heat might change the behaviour and reduce the capacity of the beams reinforced by welding a cover plate temporarily or permanently. It is not clear to the building and bridge designers how the welding and intense local heat from welding affects the behaviour of reinforced beams with locked-in stresses due to service loads present during the welding process.

In the continuous steel beams, a challenging issue is to reinforce steel beams subjected to negative moments while they are under preloading. In the negative moment region in composite steel bridges, usually, it is assumed that the concrete slab does not carry any tension stress. Besides, lateral restraint of the compression flange is provided just by cross-frames. Therefore, the beam is susceptible to lateral-torsional buckling failure mode while subjected to a negative bending moment. If the lateral-torsional buckling failure is prevented, the pier section can reach its plastic capacity, which would allow the formation of the second hinge at the midspan, and this could increase the load-carrying capacity of the beam significantly. In addition, in continuous beams using different reinforcing plate lengths (cut-off

point), can have a significant effect on the behaviour of preloaded steel beams reinforced by welding cover-plates to the compression flange.

Structural engineers have long been asking for guidance to check the strength of I-shape beams reinforced under load.

1.3. OBJECTIVES AND SCOPE OF THE WORK

The overall objective of this research is to investigate behaviour of steel I-beams reinforced with cover plates welded to the bottom flanges of the I-beams when the beams are under load. The study includes three sub-objectives which are as follows:

1) To investigate behaviour of simply supported steel I-beams strengthened with welded cover plate (bottom flange in tension) considering welding effects and effects of pre-loadings.
2) To study behaviour of steel I-beams strengthened while under load considering weld heat effects and geometric imperfections
3) To study reinforcing of steel I-beams with welded cover plates in the negative bending moment region

In order to achieve the objectives a detailed numerical study on simply supported and continuous-span steel I-beams welded with steel cover plates while under load is conducted. Finite element models are developed to conduct parametric studies to investigate the effects of important parameters such as initial residual stress distributions and magnitudes, welding residual stress, preloading level, material grade difference between the I-beam and the reinforcing plate, loading pattern, geometrical imperfection, welding type; continuous or intermittent welding on the strength weld sequence, weld length and weld residual deformations on the behaviour and ultimate capacity of simply supported I-beams reinforced by welding a cover plate at tension flange. Furthermore, the numerical study considers the effectiveness of reinforcing continuous-span I-beams by welding cover plates at the compression flange location in changing the failure mode of the beams from LTB to cross-section yielding. Also, the effect of cover plate length and the cut-off point is studied in this study. The parametric studies are conducted for the beams with cross-section yielding and lateral torsional buckling failure modes, respectively.

1.4. THESIS LAYOUT

The thesis consists of 6 chapters as follows:

- Chapter 1 includes an introduction that consists of background and problem definition, research significance and motivation, and the objective and scope of the work.

- Chapter 2 includes the literature review, a brief review of reinforcing steel columns while under load and a comprehensive review of reinforcing steel beams while under load.
- Chapter 3 discusses "Behaviour of steel I-beams reinforced while under load". In this chapter, a series of simply supported steel I-beams reinforced with cover plates welded at the bottom flanges are analyzed. Also, the effects of different parameters, such as residual stress patterns in the I-beam and cover plate, welding residual stress, type of welding patterns, and the difference in steel grades between I-beam and reinforcing plate, on the behaviour of the steel I-beams reinforced while under load are investigated numerically. Finally, the flexural capacities of reinforced I-beams with welded cover plates obtained from FE analyses are compared with the capacities predicted by the American (AISC 360-16) and Canadian (CAN/CSA-S16-19) steel design standards.
- Chapter 4 includes "Analysis of steel I-beams strengthened while under load- considering weld heat effects". This chapter presents a finite element (FE) based study on the behaviour of preloaded steel I-beams reinforced with welded cover plates at the bottom flanges of beams considering welding procedure simulation. This chapter investigates the effects of welding heat, welding sequence and weld length on the residual welding deformation and behaviour of steel I-beams reinforced while under load. In addition, the effects of initial geometric imperfection and preload level on the welding residual deformation and the behaviour of the reinforced beams are studied numerically in chapter 4.
- Chapter 5 discusses "Reinforcing of steel I-beams with welded cover plates in the negative bending moment region". This chapter presents a numerical study on preloaded steel I-beams reinforced with steel cover plates welded at the compression flanges of the beams. A series of steel I-beams are analyzed to study the behaviour of I-beams strengthened by welding a cover plate at the compression flange. Three-point loading condition was considered to simulate continuous span bridges.

- Chapter 6 presents a summary of the research project, the main contributions, conclusions, and recommendations for future work.

2. GENERAL BACKGROUND

2.1. REINFORCING OF STEEL COLUMNS WHILE UNDER LOAD

Most of the research conducted about the reinforcing of steel structures while under load, are related to the strengthening of columns by welding cover plate to the preloaded columns. Nagaraja Rao and Lamber Tall (1962) carried out an experimental test on the stub column and pin-end column while under load with the ASTM-A7 material and investigate the effects of preloading, welding sequence and residual stresses due to welding on the behaviour of the columns. It was seen that during welding operation the length of a column underload, increased and during cooling, decreased. In addition, the distribution of the residual stress changed by welding. Furthermore, welding did not change the ultimate stress of the columns. Tall (1989) continued this research and recommended a welding pattern to obtain the maximum effect of reinforcement by plate. Tall (1989) noted that the strength of columns is identical for both reinforced columns under load and no load. Also, they indicated that the residual stress has an insignificant role in the strength of columns reinforced while under load. Thus, there is no need to use intermittent welds for reinforcing to decrease residual stress effects. Tide (1990) challenged Tall's conclusion and suggested that thermal input should be controlled, and intermittent welds are needed. Marzouk and Mohan (1990) believed that the distribution and magnitude of residual stresses have a significant role in the column strength curves. Thus, considering a new pattern of residual stresses due to the welding of reinforcement is necessary. Also, they mentioned that the pattern and magnitude of residual stress are dependent on the welding sequence. Therefore, a favorable sequence of welding for obtaining a desired welding stress distribution should be considered. Wu and Grondin (2002) and Bhowmick and Grondin (2016) carried out an in-detailed parametric analysis on the behaviour of the reinforced steel columns by welding cover plates. In their studies, they investigated the effects of residual stress, initial out-of-straightness, column slenderness, reinforcing plates' placement and the grade of steel on the behaviour of columns reinforced while under load. They found that variation of the preload of the unreinforced column from 40% to 60% of its ultimate capacity, and initial residual stress, before welding the reinforcing plate, does not have a significant effect on the behaviour and ultimate resistance of the reinforced column. In addition, the effect of variation of the residual stress from 70% to 100% of the materials yield strength induced from welding the cover plate on the ultimate resistance of the column was small and negligible. In these studies, torsional buckling and simultaneous buckling about both axes were not considered. Vild and Bajer (2016) conducted experimental and numerical analysis on the lateral-torsional and local buckling failure of columns reinforced by welding cover plate while under load and

demonstrated that the effect of preload for these columns is insignificant on the capacity. In their study, the preload magnitude was limited to 50% of the base section's load resistance and authors believed that the deformation and residual stress due to welding of the cover plate is much higher than the stress due to preloading.

2.2. REINFORCING OF STEEL BEAMS WHILE UNDER LOAD

Liu and Gannon (2007) conducted an experimental test on 11 w-shaped beams under a four-point load to study the behaviour and capacity of flexural members reinforced while under load. Two reinforcing patterns with two span lengths (3000 and 1800 mm) under various preloading were considered in this investigation. The overall view of the test including a) strengthening pattern, b) position of strengthening plates and transverse stiffeners, c) schematic test setup, and d) welding sequence is shown in Figure 2.1. The average yield stress for beam components and reinforcing plates was 374 MPa and 346 MPa in their study, respectively.

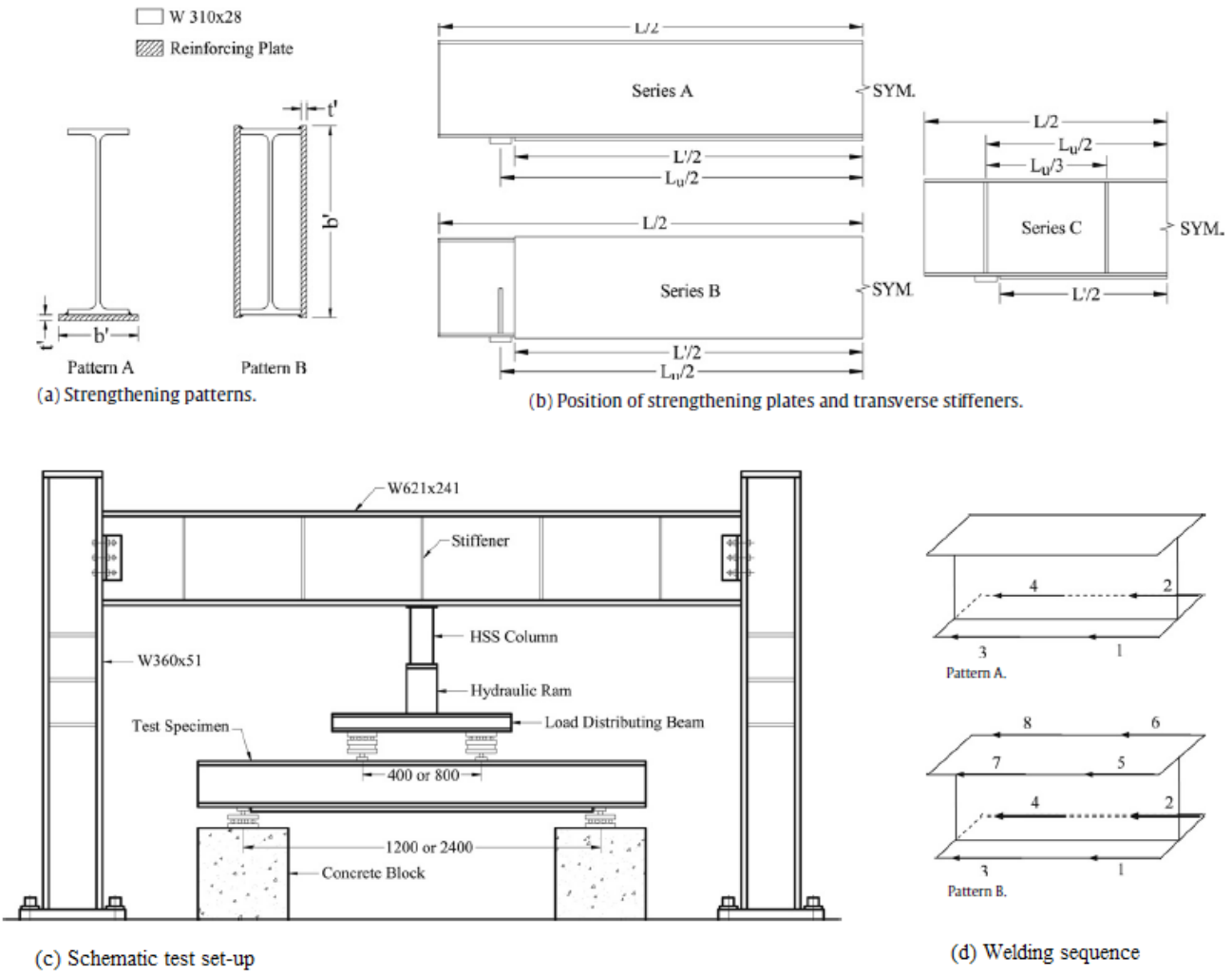

Figure 2.1: The overall view of the test; a) strengthening pattern, b) position of strengthening plates and transverse stiffeners, c) schematic test setup, d) welding sequence (Liu and Gannon 2007).

During the test, to reinforce the beam while under load, preloading was applied and held during the welding cover plate. Then, the applied load was increased until the failure of the beam. The failure criterion was increasing the deflection with a nearly constant level of loading or decreasing the load in the load-equilibrium path of the beam. In their study, the residual stress distribution was obtained by the sectioning method, described by Galambos (1998). Based on the result of Tall's investigation (1989) for columns, they assumed that the residual stress distribution and pattern for reinforced members are independent of the preload. Therefore, the residual stress distribution and magnitude due to the effects of hot rolling and welding the cover plate were measured for the reinforced beams without preloading.

The failure mode for Series A beams (with a length of 3000mm) was inelastic lateral-torsional buckling, in which lateral deflection of the top flange with twisting of the section about the longitudinal axes along with a yield line around the web area at the compression flange, was reported. The load versus mid-span top flange lateral deflection curves for all specimens and the deflection response for specimen A3 are shown in Figure 2.2 (a) and (b), respectively. It was seen that during the welding procedures a deflection occurred which was shown as a plateau in the diagrams corresponding to the preloading level. Furthermore, it was stated that the presence and variation of preload affect the magnitude of ultimate loads and the behaviour of the beams. Experimental results showed that for Series A specimens, there was a decrease in the load at which buckling occurs as the preload was increased. The buckling load of a specimen strengthened under the existing maximum stress of 0.33 Fy by welding a plate to the bottom flange is 15% less than that of a specimen strengthened under no load. It was believed that the additional deflection of the top flange during the welding (magnitude of the plateau) had a contribution on the decreasing of the buckling load.

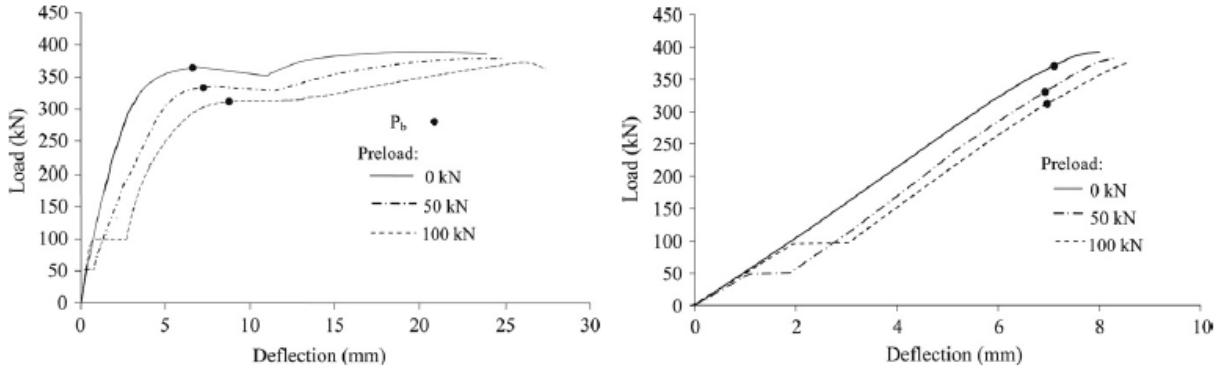

(a) Load vs.top flange lateral deflection

(b) Load vs.mid-span vertical deflection

Figure 2.2: Load vs. deflection response for Series A specimens (Liu and Gannon 2009).

The failure for the beams of Series B (with a length of 3000mm) started by yielding the cross-section. The load versus mid-span top flange lateral deflection curves for all specimens and the deflection response for specimen B3 are shown in Figure 2.3. It was noted that the variation of the preload does not have a significant effect on the ultimate bending resistance of the Series B beams. However, by increasing the preload, the stiffness and deflection changed, and more non-linearity was observed under a lower level of loading.

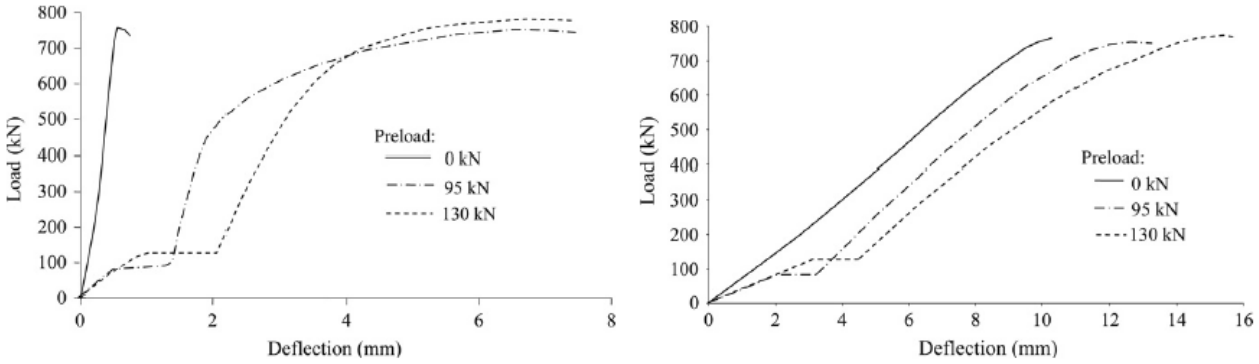

(a) Load vs.top flange lateral deflection (b) load vs. mid-span vertical deflection

Figure 2.3: Load vs. deflection response for Series B specimens (Liu and Gannon 2009).

In addition to Series A and B with the corresponding strengthening patterns A and B with a length of 3000 mm, the behaviour of Series C with the strengthening pattern A and a length of 1200 mm was also considered in their investigation. The failure of Series C was characterized by lateral instability of the compression flange between the loading points along with the yielding of the web in the end panels accompanied by large vertical deflection. In these series, increasing the preload level of 50% of the capacity of the bare beam resulted in the reduction of 13% of the resistance of the reinforced beam with no preload. It was believed that this reduction was related to residual stresses induced by the welding of transverse stiffeners for this series. The load versus lateral and vertical deflection diagrams for Series C are shown in Figure 2.4. Moreover, it was noted that these series had a smaller span length than series A and the effect of preload on the behaviour of these beams was marginal.

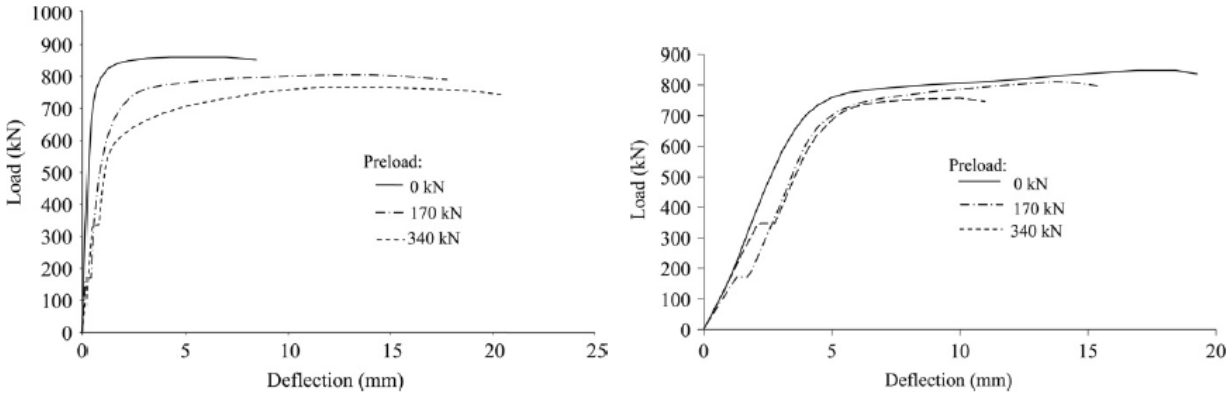

(a) Load vs.top flange lateral deflection (b) load vs. mid-span vertical deflection

Figure 2.4: Load vs. deflection response for Series C specimens (Liu and Gannon 2007).

Liu and Gannon (2009) extended their investigation to numerical parametric studies. They used ANSYS (2006) software for constructing their FE models in which the steel material of beam components and the reinforcing plate was considered elastic-perfectly plastic. Shell elements were used to model the beam cross-section, cover plate and weld. Solid brick elements were used to model the bearing plates at loading points and supports. Simple supports were used to model the boundary conditions. In their study, the source of imperfection for the reinforced beam was considered the combination of the geometric imperfection in the unreinforced beam from fabrication, deformations from preloading and deformations due to the welding of reinforcement. Furthermore, it was believed that the Canadian design standard does not have any specific guidelines for the initial imperfection of reinforced beams. Initial imperfection was incorporated into the FE model; by applying considered displacement to the nodes of the mid-span cross-section. Residual stress was incorporated into the FE model within two different steps. Residual stress due to hot-rolling was introduced to the unreinforced beam at the initial load-step by applying discrete and uniform stresses on the elements. Residual stress due to the welding of reinforcement was applied by introducing the temperature gradient in the longitudinal direction, after activating the cover plate in the beams reinforced while under load. For reinforced beams without preload, the combination of residual stresses was applied at the initial load step on elements. For the nonlinear analysis, a Newton-Raphson procedure was applied to follow the equilibrium path. In order to model the reinforcement procedures for beams strengthened while under load, the cover plate and welding elements were deactivated in the first load-step by the element birth and death feature of ANSYS. Then, hot rolling residual stress and initial imperfection were applied to the bare beam. Afterward, the preload was applied to the beam and a new nonlinear analysis was carried out. Then, all the deactivated elements were activated again with no strain history and residual stress due to welding was applied to the model. The final nonlinear analysis was performed to study the behaviour and ultimate capacity of the beam. The comparison of experimental and numerical load vs. deflection diagrams for their research is indicated in Figure 2.5.

Liu and Gannon (2009) believed that residual deformation of welding reinforcing plate (plateau), observed in the experimental tests on the beams reinforced while under load, mainly depends on the welding process and is complicated to simulate in the FE model. Therefore, the initial imperfection in A3 was adjusted in a way that the top flange deformation of the beam after preload becomes equal to the experimentally measured value.

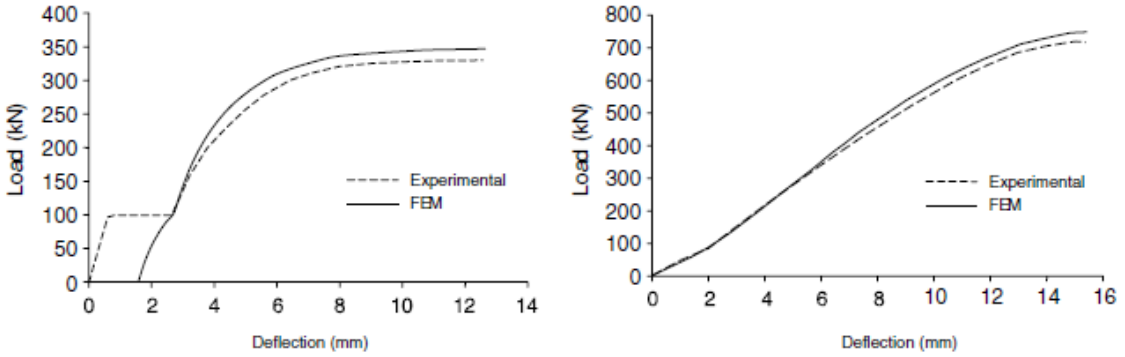

(a) Load vs.top flange lateral deflection for specimen A3 (b) Load vs. midspan vertical deflection for specimen B2

Figure 2.5: Comparison of experimental and numerical load vs. deflection diagrams (Liu and Gannon 2009).

The parametric study conducted by Liu and Gannon (2009) included the effects of preload magnitudes for beams with different lengths, initial imperfections of the unreinforced beam, plate length and lateral restraints at the loading point on the behaviour and ultimate resistance of the beams reinforced while under load. The reinforcing pattern considered in the study of Liu and Gannon (2009) is demonstrated in Figure 2.6.

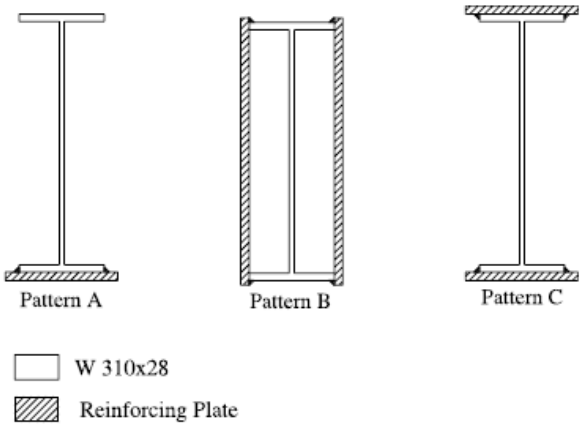

Figure 2.6: Reinforcing pattern considered in the parametric studies of Liu and Gannon (2009)

Load vs. lateral deflection diagram at different preload levels for beams with a length of 2400 mm and the reduction of the capacity vs. beam spans for patterns A and C, reported by Liu and Gannon (2009), are depicted in Figure 2.7 and Figure 2.8, respectively. Four levels of preload at 0%, 31%, 62%, and 93% of the unreinforced beam capacity with the beam length of 1200 mm, 1800 mm, 2400mm, 3000mm and 3600mm for all the strengthening patterns were considered to study the effects of preload

magnitude in beams with various length. Since the reduction of the capacity for reinforcing pattern B was insignificant, it was not shown in Figure 2.8.

Based on the study, it was noted that the effect of preload magnitude on the behaviour of beams reinforced while under load mainly depends on the failure mode of the steel beams. Dominant failure mode was lateral-torsional buckling for beams strengthened with patterns A and C in which variation of the preload level had a significant effect on the load-carrying behaviour of the reinforced beam. However, for the beams with reinforcing pattern B with failure mode of cross-section yielding it was negligible regardless of the beam span. Besides, it was mentioned that the reduction of capacity in pattern A was larger than pattern C. Reinforcing plate was added through welding in the bottom flange of the beams with pattern A making the cross-section to be mono-symmetric.

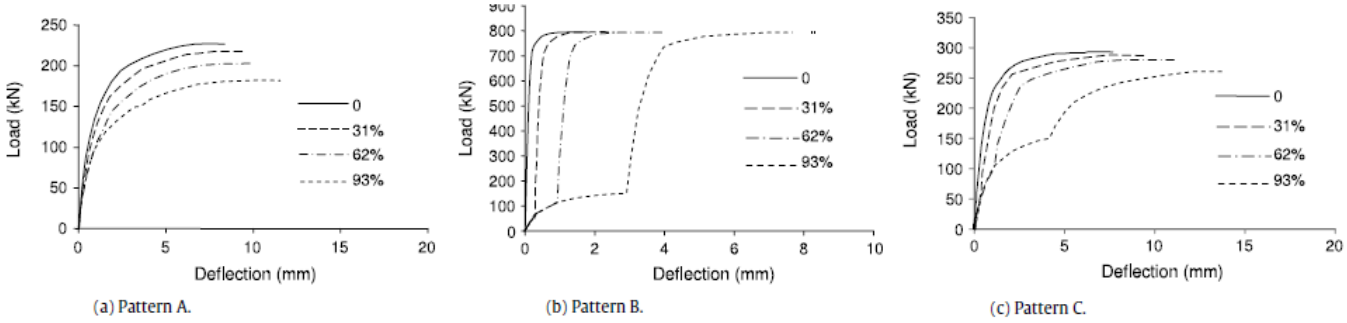

Figure 2.7: Load vs. lateral deflection diagram at different preload levels (Liu and Gannon 2009) (L=2400mm).

In the study of Liu and Gannon (2009), in order to consider the effect of initial imperfection on the behaviour of beams reinforced while under load, maximum initial imperfection magnitude of L/4000, L/1500, L/920, L/670, and L/500 were considered and applied on unreinforced beams with the span of 2400 mm and under preload of 62% of the capacity of the unreinforced beam. It was reported that the initial imperfection variation did not have any effect on the resistance of the beams with pattern B. However, increasing the magnitude of initial imperfection, decreased the capacities of the beams with patterns A and C. Load vs. lateral deflection curves for different initial imperfection magnitudes are shown in Figure 2.8.

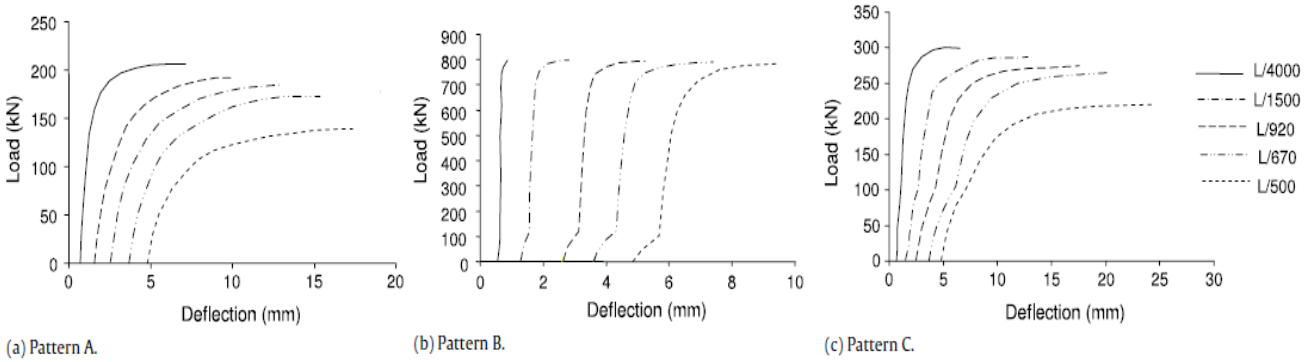

Figure 2.8: Load vs. lateral deflection curves for different initial imperfection magnitudes (Liu and Gannon 2009).

Another parameter considered in the study of Liu and Gannon (2009) was the effect of reinforcing plate length on the behaviour of the beams reinforced while under load. Three different lengths of 0.96L, 0.67L, and 0.33L for the beams with a span of 2400mm and preload of 100 kN were considered. It was reported that the reduction of the cover plate length led to the reduction of the capacity of the beams, mainly in the beams with pattern B. Reduction of the plate length in pattern B changed the failure mode from cross-section yielding to lateral-torsional buckling. Load vs. lateral deflection curves for different reinforcing-plate lengths are indicated in Figure 2.9.

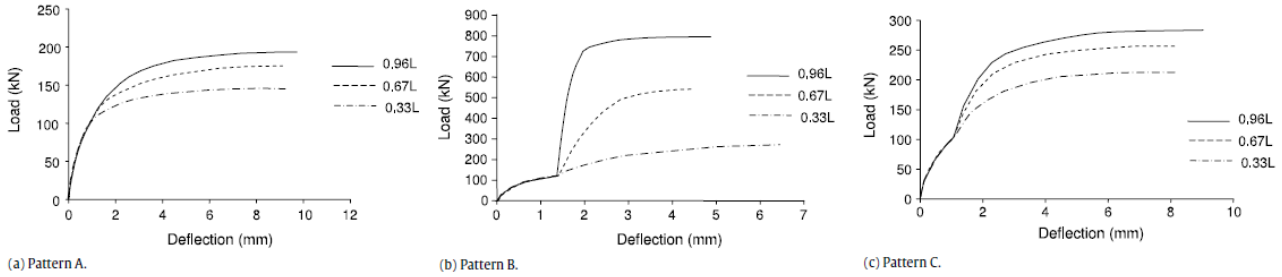

Figure 2.9: Load vs. lateral deflection curves for different reinforcing-plate lengths (Liu and Gannon 2009).

The last parameter studied by Liu and Gannon (2009) was the effect of lateral restraint at the loading points. They demonstrated that by increasing the lateral restraint, the failure mode for patterns A and C changed from lateral-torsional buckling to cross-section yielding. Therefore, their capacity increased significantly. However, increasing lateral restraint had an insignificant effect on the capacity of beams with pattern B.

Liang et al. (2015) conducted an experimental test on four simply supported steel beams under a three-point load to study the behaviour and capacity of beams with lateral-torsional buckling failure mode

reinforced while under load. The assigned name along with the geometrical dimension as well as the preload level for the beams considered by Liang et al. (2015) is demonstrated in Table 1. Also, the denotation of the beams section dimension symbols and test field is shown in Figure 2.10. The authors (2015) believed that for beams with lateral-torsional buckling, the initial bending of the top flange of the beams is the most crucial factor in the capacity of the beams. Therefore, the maximum distance from three section centers to the baseline connecting two end section centers was measured as the initial geometric imperfection. The material properties were obtained from the tension coupon test. Yield strengths for beam components and the reinforcing plate were 380.1 MPa and 398.5 MPa, respectively.

Table 2.1: Features of the considered beam by Liang et al. (2015)

Specimen no.	P_0 (kN)	L (mm)	L_u (mm)	H (mm)	b_f (mm)	t_w (mm)	t_f (mm)	L_s (mm)	b_s (mm)	t_s (mm)
Theoretical dimension		3200	3000	416	160	8	8	2720	130	6
BI-UR	–	3197.0	2999.5	415.5	159.5	7.92	7.91	–	–	–
BI-S1	0	3196.0	3000.0	415.3	159.5	7.92	7.94	2717.5	129.0	5.86
BI-S2	120	3192.0	3001.0	415.3	159.7	7.93	7.91	2718.0	128.8	5.92
BI-S3	240	3194.0	3000.5	414.8	159.0	7.92	7.90	2718.0	130.3	5.89

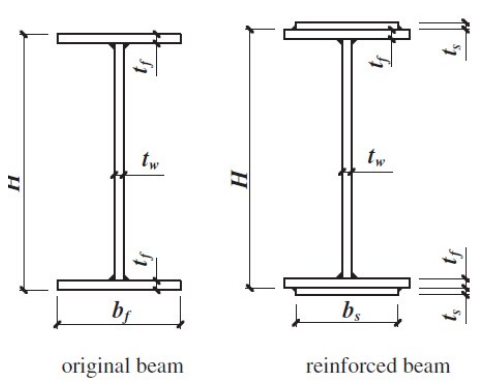

(a) Denotation of the specimen section dimension symbols.

(b) Test field.

Figure 2.10: (a) Denotation of the beams section dimension symbols, (b) Test field (Liang et al. 2015).

The loading procedure for the test of Liang et al. (2015) was similar to the loading procedure of the tests of Liu and Gannon (2007). The welding process was based on the Chinese design code, and it started from the ends to the middle of the beams. The division of the welding sections and welding sequence in each section are demonstrated in Figure 2.11.

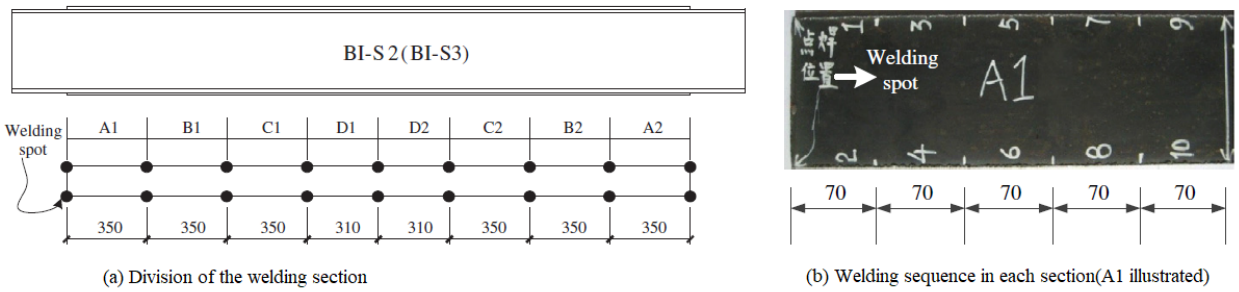

(a) Division of the welding section

(b) Welding sequence in each section(A1 illustrated)

Figure 2.11: (a) Division of the welding sections, (b) welding sequence in each section Liang et al. (2015).

Based on the reports of Yuan-qing et al. (2015), the failure mode of the beams was lateral-torsional buckling except for BI-S3, in which an unexpected local buckling failure happened.

The authors (Liang et al. 2015) demonstrated time-history curves for the vertical deflection (Figure 2.12) and lateral deflection (Figure 2.13) at the mid-span for BI-S3 to study the behaviour of the structural components during welding and cooling stages for beams reinforced while under load. Based on the vertical deflection diagram (Figure 2.12), it was noted that during the welding of the bottom flange, the vertical deflection increased. However, it decreased while welding the top flange. On the other hand, the vertical deflection increased during the cooling stage. Regarding the lateral deflection diagram (Figure 2.13), it was mentioned that for top and bottom flanges, welding near the mid-span creates more lateral displacements than welding near the ends of the beam. Also, lateral displacement would develop toward the direction of the welding.

The consideration of the strain changing for the web (Liang et al. 2015), before and after welding reinforcement, showed that web curvature increased significantly which was induced by the increasing web compression strain. The variation of web tension strain was negligible after welding the reinforcement. The distribution of web strain before and after welding is shown in Figure 2.14.

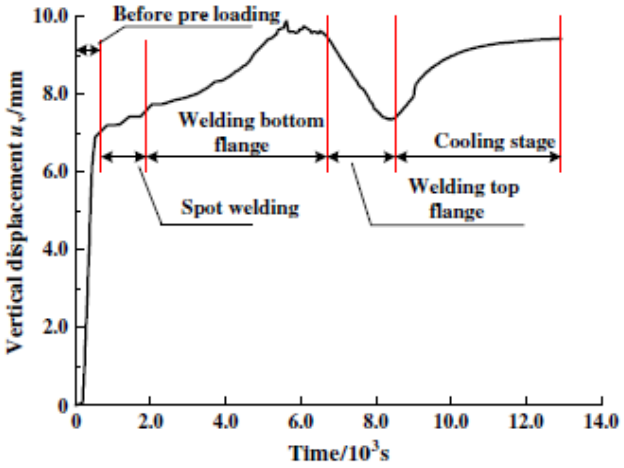

Figure 2.12: Time-history curves for the vertical deflection of the mid-span (BI-S3) (Liang et al. 2015).

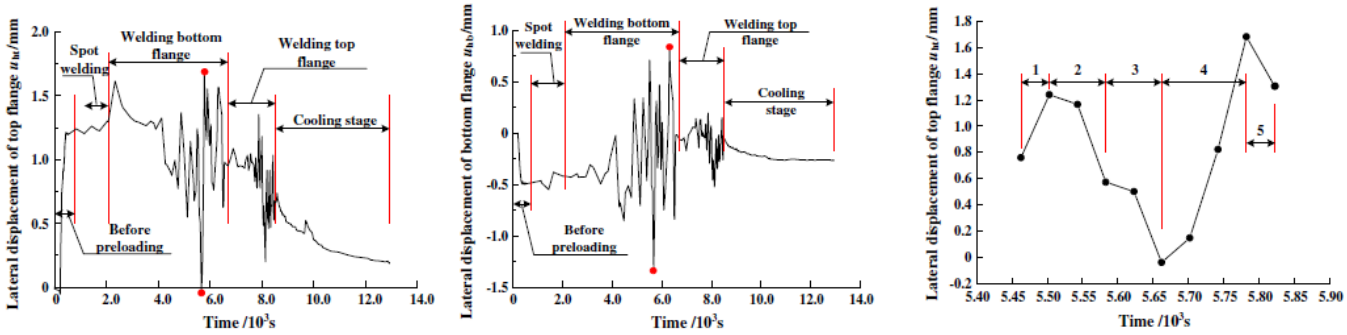

(a) Top flange (DI-1) (b) Bottom flange (DI-2) (a) Behavior of bottom flange when welding D1

Figure 2.13: Time-history curves for the lateral displacement of the mid-span (BI-S3) (Liang et al. 2015).

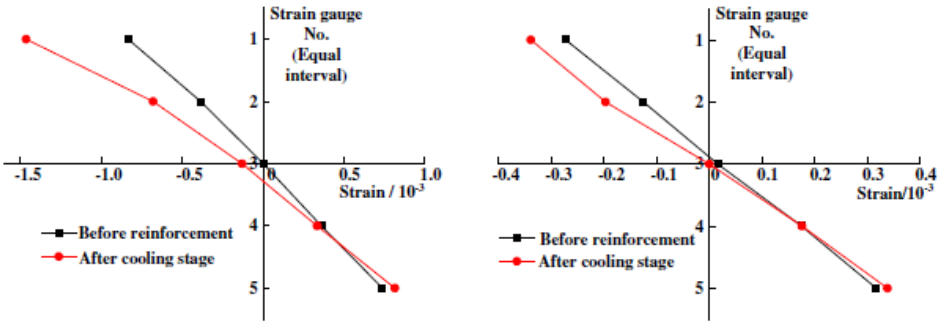

(a) BI-S2 (b) BI-S3

Figure 2.14: The distribution of web strain before and after welding (Liang et al. 2015).

Load versus displacement diagrams of the beams reported by Liang et al. (2015) is demonstrated in Figure 2.15. It was observed that reinforcing the beams by welding a cover plate at the top and bottom flange enhanced the stiffness of the beams regardless of the preloading level. In addition, the plateau

shown in the research of Liu and Gannon (2007) for the beams reinforced under load was also observed in their work (Liang et al. 2015). However, the development direction of the plateau for lateral displacements was opposite to the direction reported by Liu and Gannon (2007), which was related to the reinforcing pattern. The ultimate capacity decreased for BI-S2 (10.45%), with the flexural-torsional buckling failure, and increased for BI-S3 (3.92%), with the local buckling failure, in comparison to the capacity of the reinforced beam with no preload as a benchmark (capacity of the BI-S1). Thus, no clear and definable relationship was obtained between the preload and strength of the reinforced beam from the study of Liang et al. (2015).

Liang et al. (2015) tried to simulate the behaviours of their specimens with FE software, ANSYS (2006). They believed that the thermal input due to welding the reinforcing plate changes the material property of the steel and to obtain accurate simulation, it should be considered. Besides, the welding process to add a reinforcing cover plate was considered in the FE model. The pattern and magnitude of residual stress used by Liu and Gannon (2015) for the hot-rolled sections, were applied in their model. The experimentally measured geometric imperfection was implemented as initial geometric imperfection. The trilinear model was considered to model the material property of the beam components. Other assumptions and simulation procedures were similar to the procedures followed by Liu and Gannon (2009). The comparison of the constructed FE model and experimental results for lateral displacements reported by Liang et al. (2015) is depicted in Figure 2.16. The failure mode for all specimens including BI-S3 was flexural-torsional buckling in FE models and by increasing the preload level, the ultimate capacity was decreased. The observed plateau and its direction in load-displacement curves for beams reinforced under load were modeled through the constructed FE models. However, its magnitude was smaller than the real dimension of the plateau.

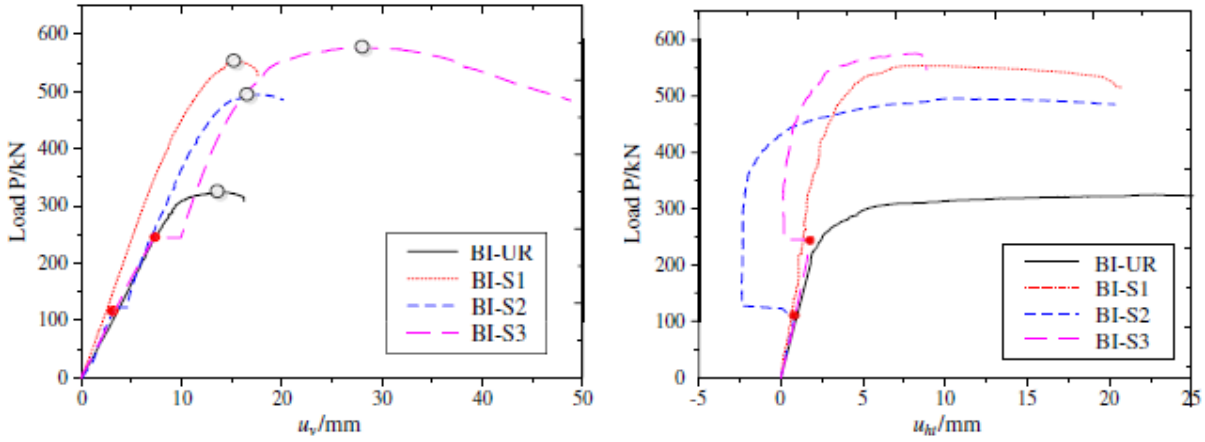

(a) Load vs. mid-span vertical deflection (b) Load vs. top flange lateral deflection

Figure 2.15: Load vs. displacement behaviour (Liang et al. 2015).

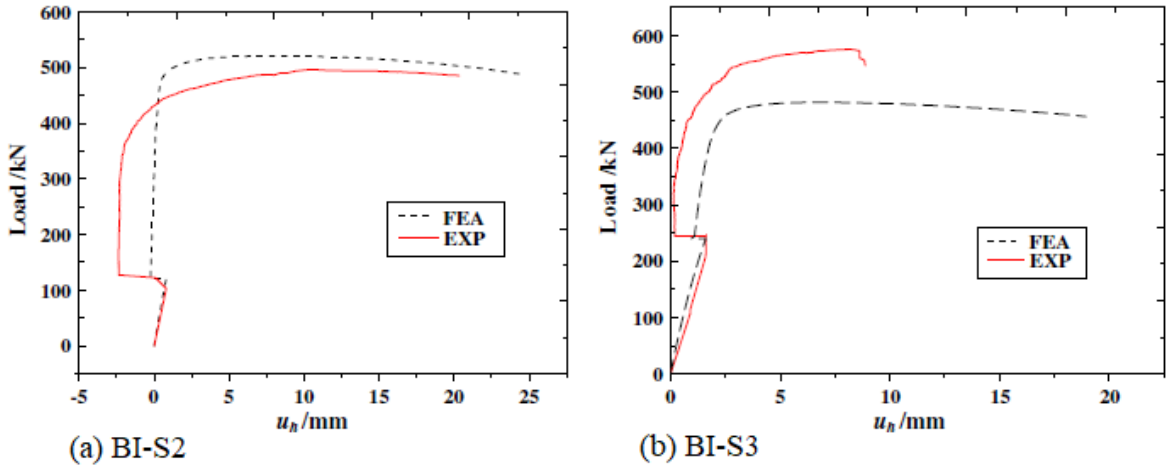

Figure 2.16: Comparison of the load vs. lateral deflection curves between FEA and the experiment (Liang et al. 2015).

Some researchers (Selvaraj and Madhavan 2018; Yossef 2015) tried to find an appropriate solution to strengthen steel beams while under load, mainly for beams with lateral-torsion buckling failure mode. For instance, Selvaraj and Madhavan (2018) used cold-framed steel channels to reinforce open hot-rolled steel channels. In this method, the mode of failure was changed, and lateral-torsional buckling was avoided by increasing the torsional rigidity of the section by changing the open section to the closed composite one. The integrity of the HRS–CFS section was constructed by adequate spot welding of the CFS section to the hot-rolled section at regular distances along the length of the beam to avoid residual stress and its effects. The schematic view of the proposed method for strengthening beams while in service by Selvaraj and Madhavan (2018) is shown in Figure 2.17. However, their solution is not robust, and it was mentioned that more research is required to study various parameters before arriving at an appropriate design procedure (Selvaraj and Madhavan 2019).

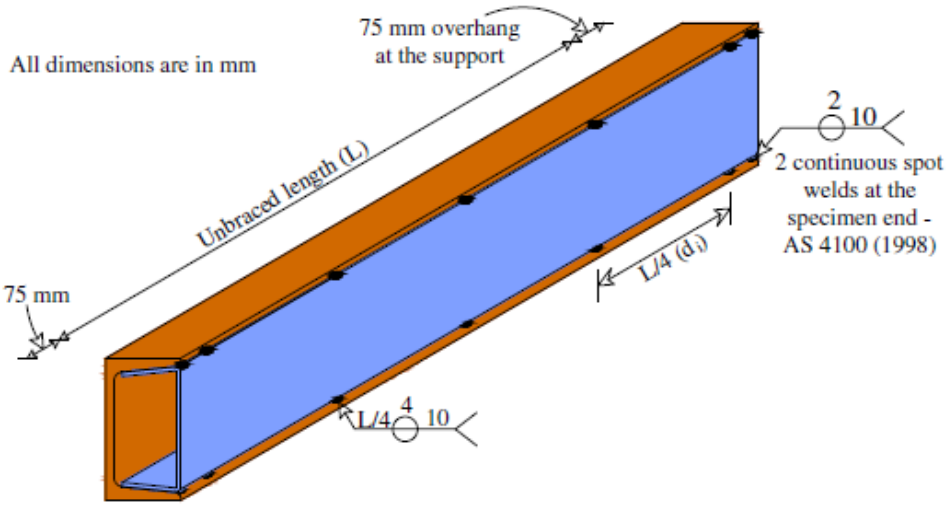

Figure 2.17: Schematic view of the retrofitted beam (Selvaraj and Madhavan 2018).

3. BEHAVIOUR OF STEEL I-BEAMS REINFORCED WHILE UNDER LOAD

3.1. ABSTRACT

Steel I-beams often require reinforcing while they are under load. A common method for strengthening steel beams is by welding steel cover plates to the bottom flanges of the existing members. Very limited research has been conducted on the behaviour of I-beams reinforced under load. This paper presents a finite element (FE) based study on steel I-beams welded with steel cover plates while under load. A series of simply supported steel I-beams reinforced with cover plates welded at the bottom flanges are analyzed. FE analysis shows that with increased preload, the capacity of the I-beam reinforced under load reduces when the failure mode of the beam is lateral-torsional buckling (LTB). On the other hand, the variation of the preload has an insignificant effect on the behaviour and ultimate strength of the reinforced beam when the reinforced beam fails in flexural yielding. Also, the effects of different parameters, such as residual stress patterns in the I-beam and cover plate, welding residual stress, type of welding patterns, the difference in steel grades between I-beam and reinforcing plate, on the behaviour of the steel I-beams reinforced while under load are investigated numerically. Finally, the flexural capacities of reinforced I-beams with welded cover plates obtained from FE analyses are compared with the capacities predicted by the American (AISC 360-16) and Canadian (CAN/CSA-S16-19) steel design standards. FE analysis shows that AISC 360-16, when the effect of loading height is considered, can reasonably predict the capacity of I-beam reinforced with welded cover plate at the bottom flange.

Keywords: Reinforced I-beam; preload level; finite element analysis; residual stress patterns

3.2. INTRODUCTION

Steel beams are often reinforced due to the change of the primary function of the structure or additional applied loads. Replacing the beams can be more expensive and time-consuming and can be avoided by reinforcing and increasing their capacity. On the other hand, beams that require strengthening often are in service, and complete relieving of their loads is not either possible or not economical. Thus, steel beams may need to be reinforced while under load. The main objective of reinforcing a steel beam is to increase the stiffness and strength of the reinforced beam or to change the structural behaviour and failure mode of the reinforced beam. When the bottom flange of the steel I-beam is easily accessible, the most economical option is to weld a cover plate to the bottom flange. The design procedure generally involves selecting a cover plate that can resist the additional factored moment applied in the beam. While

the current practice is simple, it is not clear how the reinforced beam will behave if locked-in stresses due to service loads are present during the reinforcement.

Very limited research is currently available on the behaviour of steel I-beams reinforced while they are subjected to load. Liu and Gannon (2009) first studied the behaviour of steel beams reinforced under load by conducting tests on steel I-beams reinforced with welded cover plates. Two different reinforcing patterns, one where a plate was welded to the bottom flange of the beam section along its length (pattern A) and the other where two plates were welded against tips of the flanges of the beam section along its length (pattern B), were considered and the specimens were tested for different preload levels. It was observed that increasing the preload resulted in a decrease in lateral-torsional buckling strength for beams with pattern A reinforcement (plate welded to the bottom flange) than the same specimen strengthened under no preload. It was also reported that the variation of the preload level has an insignificant effect on the ultimate resistance of beams with flexural yielding failure. Furthermore, Liu and Gannon (2007, 2009) also conducted parametric studies to investigate the effects of the preload magnitude, initial imperfection, length of the cover plate, and the span of the beam on the behaviour of reinforced steel beams. Similar to the experimental results, in their numerical study, a reduction of resistance of beams with lateral-torsional buckling failure by increasing preload was indicated for beams with type A reinforcement. Yuan-qing et al. (2015) conducted a detailed experimental investigation on the I-steel beams reinforced while under load by welding cover plates on the top and bottom flanges. In their research, the procedures of reinforcement, preloading, and welding of reinforcing plates and their effects were studied. Three reinforced I-beams with the preload level of 0%, 37%, and 74% of the unreinforced beam capacity were investigated. It was reported that for the beam with the 37% preload level, the failure was lateral-torsional buckling, and the ultimate capacity was reduced in comparison to the capacity of the reinforced beam without preloading. However, for the reinforced beam with the 74% preloading level, the ultimate capacity increased and the failure mode for this beam was flange local buckling. Thus, no clear and definable relationship was obtained between the preload and strength of the reinforced beam from the study of Yuan-qing et al. (2015).

Often there is a difference between the steel grades of the existing beam and the reinforcing cover plate. Beams in many existing structures are often of lower grade steel than the modern steel used for reinforcement. To the best of the authors' knowledge, no study is currently available on steel beams reinforced with cover plates of different grades. Also, the effect of different combinations of initial and welding residual stress on the strength and behaviour of beam reinforced under load is currently not

available. In this paper, the behaviour of simply supported steel I-beams reinforced with a welded cover plate at the bottom flange is studied by detailed FE analysis. In addition, the effects of preloading, initial and welding residual stress, initial geometric imperfection, cover plate thickness, loading pattern, welding type (continuous or intermittent welding), different cross-section classes for I-beams, and different steel grades of the beam components and reinforcing plate are studied. In the end, this paper also investigates the effectiveness of the flexural strength equations of AISC 360-16 (Specifications for Structural Steel Buildings, ANSI/AISC 360-16. American Institute of Steel Construction) and CAN/CSA-S16-19 (National Standard of Canada: Design of steel structures) for the design of I-shape beams reinforced with welded cover plate at the bottom flanges of the beams.

3.3. FINITE ELEMENT ANALYSIS OF REINFORCED STEEL I-BEAMS

A finite element model of a reinforced I-section steel beam was developed using the commercial finite element software Abaqus (Abaqus 2019. Simulia). Reinforcing was done by adding a cover plate to the bottom flange of a simply supported I-beam. This section provides details of the development of the FE model for reinforced steel I-beam.

3.3.1 Development of finite element model

The developed finite element model consists of four different parts: a base beam that is a build-up I-section, a reinforcing cover plate, an identical reinforcing plate with zero stiffness, and rigid beam connectors. The base beam, reinforcing plate, and identical reinforcing plate were modeled in Abaqus using shell element S4R. S4R is a 4-node doubly curved general-purpose shell element with reduced integration and it has 6 active degrees of freedom. Two-node rigid beam connectors were used to connect the base beam and the identical reinforcing plate. One end of each connecter was connected to the beam at the bottom flange tip weld location and the other one was connected to the identical reinforcing plate. The incorporated rigid beam connector element has 6 active degrees of freedom for each node and imposes kinematic constraints between the nodes. Usually, the beam is reinforced when there is some preloading in it. Therefore, the reinforcing plate will be active after the preload is applied in the FEM. Since the cover plate can not be modeled within the analysis step, a similar effect can be obtained by creating its elements in the model definition, removing them in the first loading step, and reactivating them, subsequently. However, during the reactivation, because of the preloading and related displacements, the new configuration of the beam will be different from the original one specified in the definition of the model. For the nodes of reinforcing plates to be in the correct position while reactivation,

these nodes were connected with the nodes of the identical reinforcing plate, called as a duplicate plate in this research, using tie interaction. The duplicate of the reinforcing plate is the same as the identical reinforcing plate with zero stiffness and it was not removed during the analysis. Material properties and thickness of the duplicate plate were assigned in a way that did not affect the solution of the reinforced beam, as well as did not cause numerical problems. In the developed FE model, to define contact between the bottom flange and the reinforcing cover plate, the distance between the reference surfaces (bottom flange of the I-beam and reinforcing plate) was kept zero and the thickness effects were provided by using appropriate shell offset in Abaqus. Surface-to-surface contact, hard contact in the normal direction with allowed separation after contact, and penalty in the tangential direction with a friction coefficient of 0.3 were incorporated between the bottom flange and the duplicate of the reinforcing plate.

The incorporated mesh in the finite element model was dense with 40 elements across the depth of the web and 12 elements throughout the width of the flanges. The mesh size in the longitudinal direction of the beam was based on keeping the aspect ratio of shell elements smaller than 2. This meshing size was obtained by conducting a mesh sensitivity analysis.

In this investigation, isotropic steel material with a multi-linear stress-strain curve for the base beam and reinforcing plate was used. For this material, the modulus of elasticity and poison ratio were 200, 000 MPa and 0.3, respectively. For the material model, tangent stiffness considered in the yield plateau region was 0.001E up to $\varepsilon_{sh} = 10\varepsilon_y$, where ε_{sh} is the strain-hardening strain and ε_y is the yield strain of the material, respectively. From this strain up to the strength of strain hardening, a constant strain-hardening modulus equal to 2% E was used (Kim 2010).

Initial residual stresses for the beam section were applied in the form of an initial stress field on the beam elements. These residual stresses were introduced as uniform stresses on each element of the beam section in the first step of the analysis. Initial residual stress of the reinforcing cover plate along with residual stresses induced from welding the cover plate to the beam section were introduced by applying a longitudinal temperature gradient. The initial temperature field of the structure was taken as zero and the expansion coefficient in the longitudinal direction for steel material was considered as 1.17×10^{-5} / ℃. This coefficient was taken as zero in transverse and through the thickness direction. Desired residual stresses were introduced by changing the temperature on each node using Eq. (3-1).

$$\sigma = -E.\alpha.\Delta T \qquad [3\text{-}1]$$

where σ is longitudinal residual stress, E is the elastic modulus of elasticity, α is the expansion coefficient and ΔT is the temperature gradient.

In this study, straight I-beams were mainly subjected to four-point loading. However, to study the effects of loading patterns on the behaviour of beams reinforced while under load, three-point and uniformly distributed loading were also considered. In the four-point loading case, equal concentrated loads were applied at one-third of the beam length. Also, transverse stiffeners were attached at the bearing and concentrated load locations. The considered failures were flexural yielding of flange, elastic and nonlinear lateral-torsional buckling. For the LTB failure, the beam was simply supported in-plane and out-of-plane, while lateral braces were provided in the load locations at the top and bottom flanges for the flexural yielding failure. To impose the simply supported boundary conditions, transverse and vertical displacements were restrained at both ends while longitudinal displacement was restrained at just one end of the beam. In addition, transverse displacement was restrained along both sides of transverse stiffener tips at the support locations. For this study, the flanges of the selected I-sections are compact and for the web, compact, non-compact, and slender webs were considered based on AISC 360-16. Therefore, just flange sweep was considered as the initial geometrical imperfection for the sections with compact flange and compact webs. For the cross-section with non-compact and slender webs, web out-of-flatness was incorporated in addition to flange sweep. For the beams reinforced while under load, there are three sources of imperfections: one is the fabrication and erection of the base beam (δi), the other one is the weld shrinkage deformation, induced from welding of reinforcing plate under load (δw), and the last one is $P-\delta$ deformations induced from the preloading of the base beam (δI).

Based on the American Welding Society (AWS. 2020. Structural welding code–steel) limitation/tolerance for the repairing of existing structures, $\delta i + \delta w$ should be smaller than $L_b/1000$ for the flange sweep regardless of the welding process and preloading level, in which L_b is the unbraced length of the beam. Therefore, a value of L_b /1000 was used as the geometrical imperfection and was applied at the mid-point of the unbraced length at the compression flange as a flange sweep in the first step of the loading. For noncompact and slender webs, an out-of-flatness value of d/400 was applied at the center of the depth of the web panels. Initial residual stresses of the beam were applied at the first loading step and the equilibrium of the residual stresses was ensured by going through an equilibrium step. Then, the concentrated loading pattern was applied through modified Risk analysis to follow the equilibrium path of the beam. To analyze the reinforced beams, the following steps were considered:

1. All components of the beam and reinforcing plates were modeled. To avoid interaction between the base beam and the reinforcing plate while applying initial residual stresses of the beam and preloading, all elements of the reinforcing plate were deactivated. Initial residual stresses of the beam along with the initial geometrical imperfection were incorporated into the beam.
2. For the beams reinforced while under-load, the considered preload was introduced. Four preloading levels, 0%, 20%, 40% and 60% of unreinforced beam strength, were considered in this study.
3. All elements of the reinforcing plate were reactivated in the strain-free mode. When stress/displacement elements are reactivated in a strain-free state, they become fully active immediately at the moment of reactivation (the start of the step at which they are reactivated) (Abaqus 2019). The reactivated elements are reset to an "annealed" state (zero stress, strain, plastic strain, etc.) at the start of the reactivation step (Abaqus 2019). Since these elements are reactivated in a virgin state (i.e., with zero stress), they exert zero nodal forces on the rest of the model. Thus, the current configuration at the start of the reactivation step is the new initial configuration for the reinforcing plate elements.
4. Surface-to-surface contact between the bottom flange and the duplicate of the cover plate was incorporated. In addition, initial residual stresses of the reinforcing plate were applied using a temperature gradient and equilibrated.
5. Residual stresses induced by welding the reinforcing plate to the beam were introduced by changing the temperature at the tips of the bottom flange and the corresponding locations of the reinforcing plate. The temperature in these locations was changed to reach 70% or 100% material yield strain and a self-equilibrating residual stress pattern developed in the cross-section of the reinforced beam.
6. The reinforced beam was further loaded until it reached failure.

Nonlinear static stress analysis was carried out for all steps 1 to 5. For loading step 6, the modified Risk method was incorporated. Details of the developed FE model along with the schematic view of the reinforced I-beam are presented in Figure 3.1.

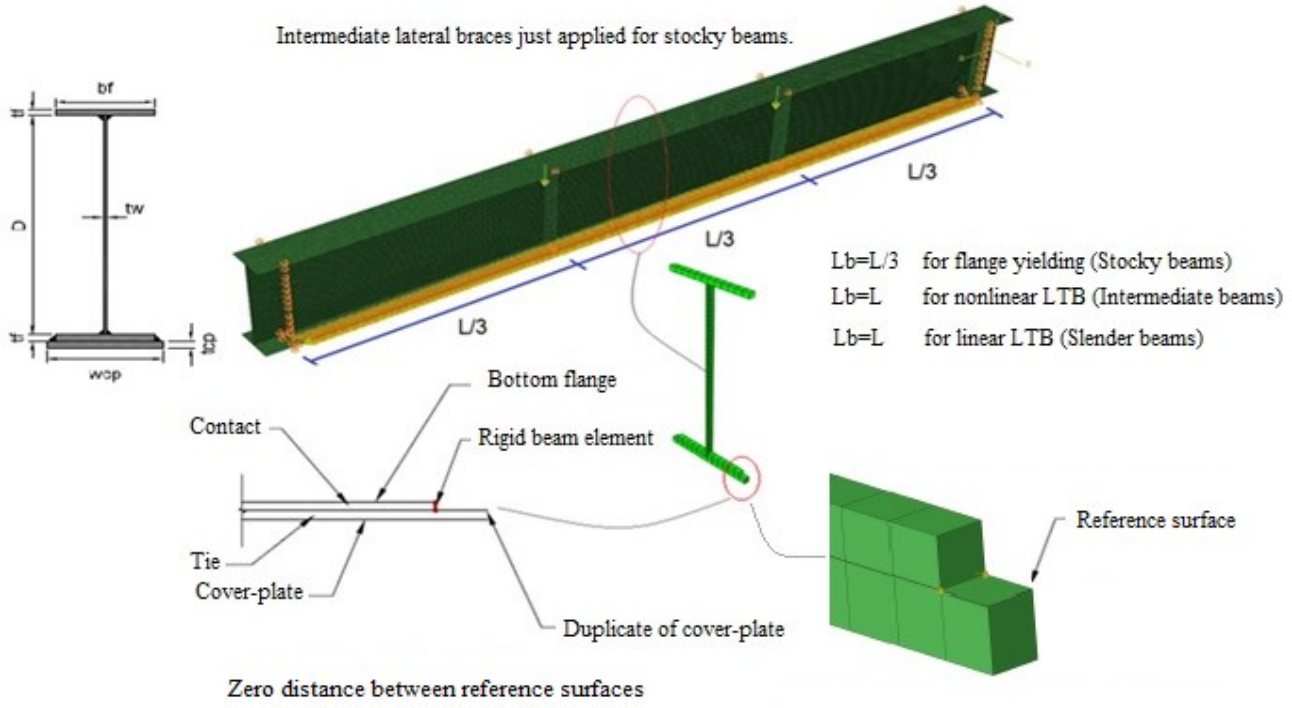

Figure 3.1: Details of the developed finite element model and schematic view of the reinforced I-beam for four-point loading case

3.3.2 Validation of finite element model

Liu and Gannon (2007, 2009) conducted a 4-point bending test on simply supported beams reinforced by welding a reinforcing plate at the bottom flange of the beam. The beam cross-section was W310×28 with an unbraced length of 2.4 m and the nominal dimension of the reinforcing plate was PL 2304×137×9.5. Three preload levels with magnitudes of 0 (without preload), 50 kN and 100 kN were considered and named as A1, A2, and A3 in their study. The yield stress, Fy, for the steel beam and the reinforcing plate was 374 MPa and 346 MPa, respectively. Initial residual stress distributions for the beam and combined residual stresses of hot rolling and welding for reinforced beams and the reinforcing plate were experimentally determined (Liu and Gannon (2007, 2009)). In their experimental work, the initial imperfection of the unreinforced beams was not reported. Liu and Gannon (2007, 2009) also developed a FE model and verified their tests. In their numerical study, it was stated that predicting the imperfection of the beams after welding the reinforcement is complicated since it is a function of various uncontrolled factors. Also, in their verification, the assembly of the plate, roller and ball bearing at the loading location was replaced by a 3D, 2-node nonlinear spring at the loading locations. More details regarding the spring element can be found in the work of Liu and Gannon (2007, 2009). In this paper, to

verify the overall simulating procedures, samples A1 (without preloading), A2 (with 50 kN preloading), and A3 (with 100 kN preloading) were modeled and load-top flange lateral deflection at the mid-span of these tests are compared with the experimental and finite element results of the Liu and Gannon (2007, 2009), as shown in Figure 3.2-a. Figure 3.2-b shows the typical failure modes of A-series, as observed during the test and FE analysis. An excellent agreement is observed in the failure pattern of A-series as both the tested specimen and the FE model showed lateral-torsional buckling failure mode. In Figure 2-b, the duplicate of the reinforcing plate was removed from the FE model for illustration of the stress distribution in the reinforcing plate. For the validation of the FE model, experimentally measured values for the residual stresses were used. In the experimental program of Liu and Gannon (2007, 2009), initial geometrical imperfections were not measured. Thus, similar to Liu and Gannon (2007, 2009), the initial imperfection in the numerical model was adjusted in such a way that top flange deflections after applying preload and welding reinforcement become approximately equal to the experimentally measured values. In the verification, bearing plates, available in the test setup at the loading and bearing locations, were modeled using C3D8R elements, an 8-node general-purpose linear brick element with reduced integration. The bearing plates were connected to the flanges using tie interaction. It can be observed from Figures 3.2-a and 3.2-b that the current FE model is capable of predicting the overall behaviour, buckling and ultimate capacities of the reinforced beams while under load. Furthermore, failure modes of the current FE models were nonlinear lateral torsion buckling, as observed during the tests.

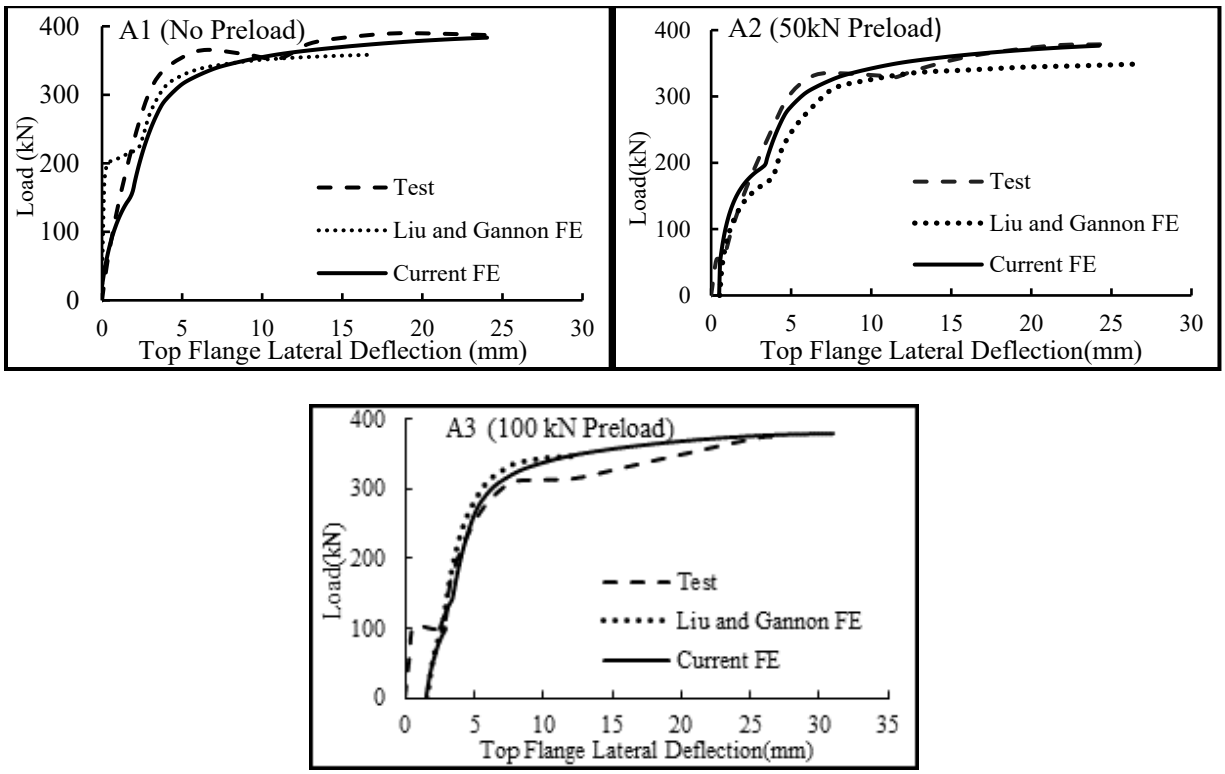

(a) Load-lateral deflection of top flange midpoint at the mid-span of specimensA1, A2 and A3

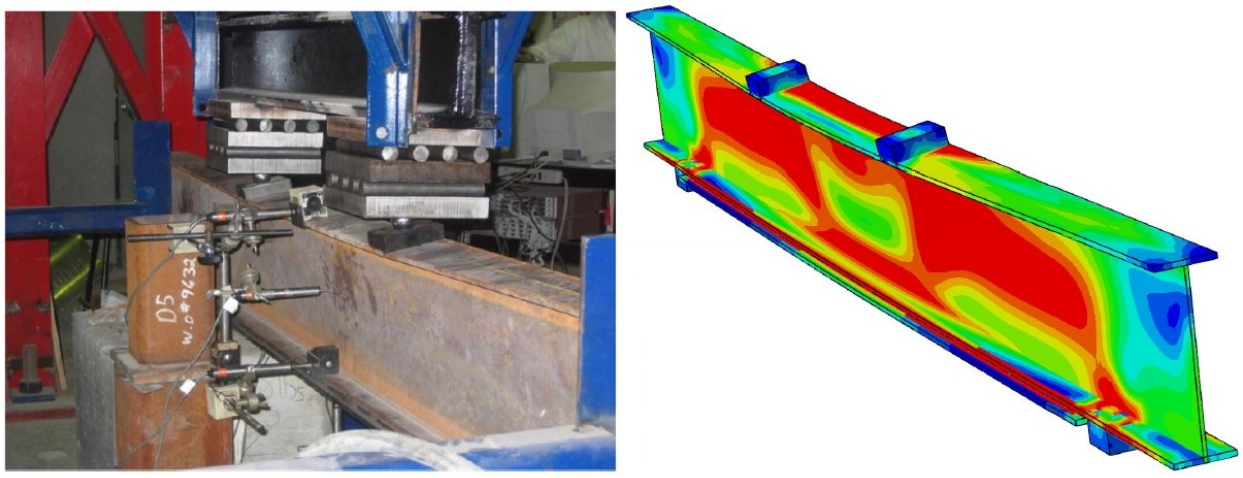

(b) Typical experimental and numerical failure modes for series A specimens (shell thickness in the FE model is rendered with scale factor:1)

Figure 3.2: Validation of FE model for A1, A2 and A3 specimens tested by Liu and Gannon (2007, 2009)

In the literature, no specific welding residual stress pattern is available for steel beams reinforced with a welded cover plate at the bottom flange. Experiments by Masubuchi (1980) and Tall (1961) showed that welding residual stress at the weld center can be as high as the yield strength (F_y) of the steel material at the weld location. Tall (1961) reported that in build-up sections, welding residual stresses will reach the yield point value only at and in the vicinity of the weld. Moreover, Tall (1961) indicated that the distance from weld location to reversal of stress varies between 18 mm and 35 mm. In this paper, in the verification of Liu and Gannon (2007, 2009) tests, the distance from the location of welding to the cover plate tip in the FE model is 17.5mm. Thus, in this study, welding residual stresses were achieved by applying 70% or 100% yielding strength of steel at the bottom flange tips and the corresponding location of the reinforcing plate. This is consistent with the study by Wu and Grondin (2002); Bhowmick and Grondin (2016) on steel columns reinforced with welded cover plates. The resulting residual stress pattern would be the combination of initial and welding residual stresses. To validate the accuracy of this method, it was incorporated into the numerical modeling of residual stresses of the sample A1, reinforced beam without preloading, and obtained residual stresses from this approach were compared with the experimentally measured ones. Figure 3.3 shows that the magnitude and distribution of the achieved residual stresses correlate very well with the experimentally measured pattern and can be used in numerical modeling.

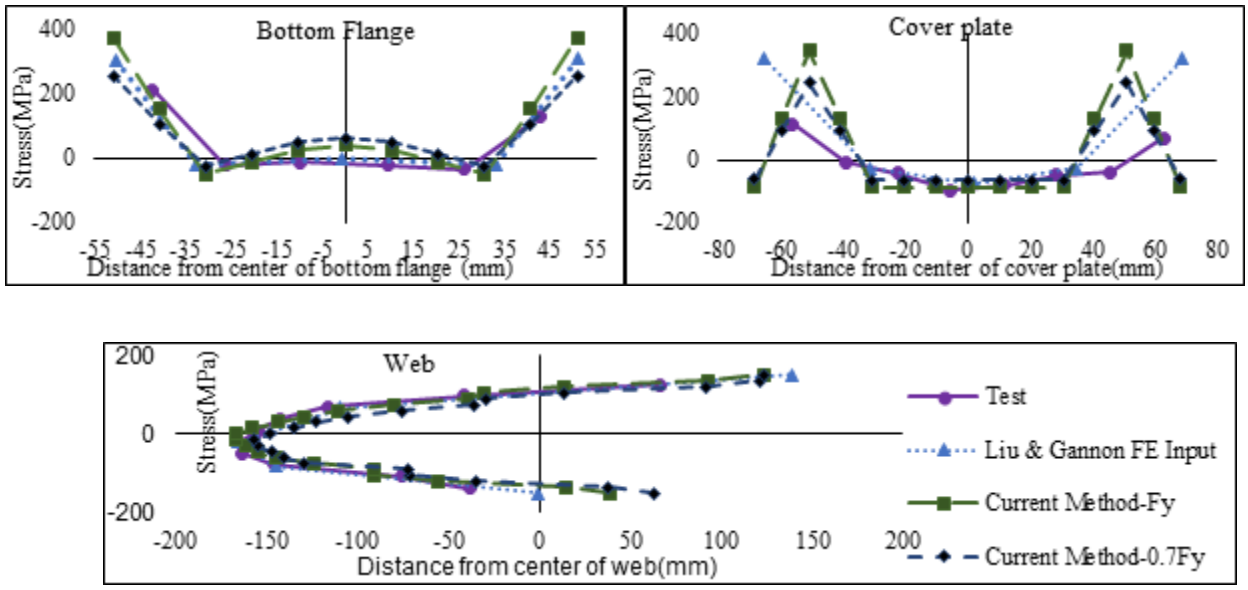

Figure 3.3: Validation of welding residual stress application in FEM

3.4. PARAMETRIC STUDIES

In total, 270 FE models were developed to conduct a parametric study to investigate the effects of important parameters, such as preload level, initial residual stress distributions and magnitudes, welding residual stress, initial geometrical imperfection, cover plate thickness, loading pattern, welding type (continuous or intermittent), material grade difference between the I-beam and the reinforcing plate, on the strength and behaviour of I-beam reinforced with a cover plate at the bottom flange. Three different base beam sections, as shown in Table 3.1, were considered in this study. For cross-section A, two different reinforcing plate sizes, 350 mm×25 mm ($w_{cp} \times t_{cp}$) and 350 mm×15 mm, were considered. Cross-section A with a reinforcing plate of 350 mm×25 mm is named as section A-1 and cross-section A with a reinforcing plate of 350 mm×15 mm is named as A-2 in this paper. For cross-section B, a reinforcing plate size of 350 mm×25 mm and for cross-section C, a reinforcing plate size of 550 mm×30 mm were considered. The parametric studies were conducted for the beams with three different unbraced lengths with the expected failure modes; cross-section yielding (Stocky), inelastic LTB (Intermediate) and elastic LTB (Slender), respectively (Figure 3.1). The geometrical properties of the cross-sections along with the flange and web classifications based on AISC 360-16 and CAN/CSA-S16-19 and considered unbraced lengths are presented in Table 3.1. In the parametric studies, unless otherwise stated, the initial residual stress was 'Best-Fit' pattern (Shown in Figure 3.5), 100% yielding strength as welding residual stress, previously discussed values as geometrical imperfection, 4-point loading as loading pattern, continuous welding as welding type and homogeneous cross-section with the yield strength (F_y) of 345 MPa and ultimate strength (F_u) 450 MPa were used.

Table 3.1: Geometrical properties of the cross-sections, classifications, and unbraced lengths

Base beam cross-sections	Top Flange $(b_f \times t_f)$ mm x mm	Bottom Flange $(b_f \times t_f)$ mm x mm	Web $D \times t_w$ mm x mm	AISC		CSA		Unbraced span length, L_b (mm)		
				Compression Flange	Web	Compression Flange	Web	Stocky	Intermediate	Slender
A (Doubly symmetric)	300 × 20	300 × 20	760 × 11	Compact	Compact	1	2	2000	6000	9000
B (Singly symmetric)	200 × 11	300 × 20	760 × 11	Compact	Non-compact	2	2	1000	3000	6000
C (Doubly symmetric)	450 × 25	450 × 25	2000 × 16	Compact	Slender	2	4	2500	7500	16500

3.4.1 Effect of preload magnitude

In order to study the effect of preloading on the behaviour of beams reinforced while under-load, four levels of preloading; 0% (CP-NPL), 20% (CP-20%Preload), 40% (CP-40%Preload), 60% (CP-60%Preload), of the unreinforced beam capacity were considered. Moment-top flange lateral deflection diagrams at the mid-span of the beams under considered preloading levels are depicted in Figure 3.4. These diagrams are for stocky, intermediate and slender beams for the cross-section A-1. As shown in Figure. 3.4, adding a cover plate to the bottom flange increases the stiffness and ultimate capacities of I-beams regardless of the preloading level. Furthermore, it can be seen that preloading variation does not have a significant effect on the behaviour and ultimate capacity of stocky beams with yielding failure mode. The presence of preloading was also found to have a very small effect on the behaviour of the beams with nonlinear LTB failure modes. For the beam with nonlinear LTB failure mode, the reduction in the ultimate capacity of the reinforced beam was smaller than 5% for a preload level of up to 60% of the strength of the unreinforced beam. For the beams with elastic LTB, the presence of preloading had a significant effect on the buckling behaviour of the reinforced beam, and it reduced the buckling capacity.

However, post-buckling capacity compensated the reduction, and the beam with preloading was able to reach its full capacity, but at a very large deflection.

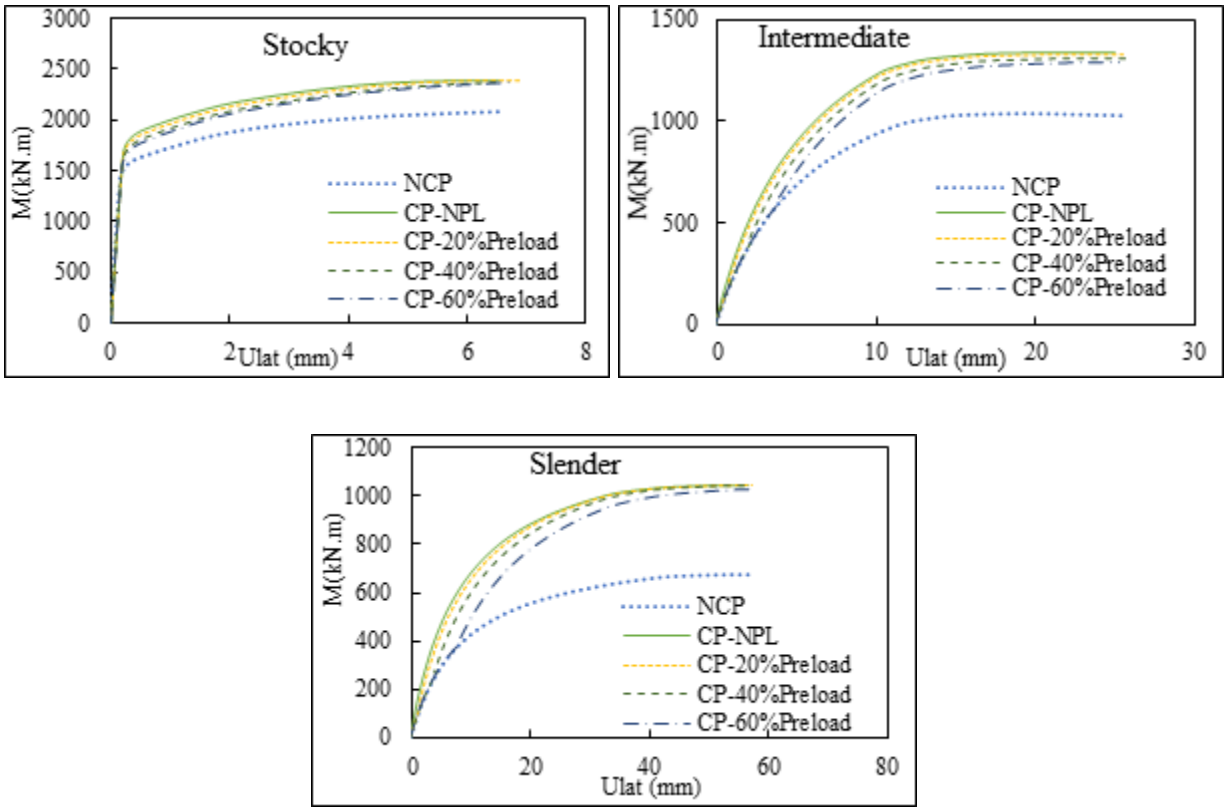

Figure 3.4: Moment- top flange lateral deflection at the mid-span under various preload levels for cross-section A-1

3.4.2 Effect of initial residual stress

In order to study the effects of initial residual stress on the beams reinforced under load, four commonly used patterns, Best-Fit Parel (Kim, (2010)), ECCS (2000), Chacon (Chacon et al. (2012)), Flame-Cut (Chernenko and Kennedy (1991)), and recently proposed modified Dwight and Moxham (1969) pattern (abbreviated as Modified D&M) proposed by Unsworth et al. (2021), for the welded I-section and one residual stress pattern for the reinforcing cover plate (Wu and Grondin (2002)) were considered, as shown in Figure 3.5.

The ultimate capacities for different initial residual stress patterns of the beams without preloading for cross-section A-1 are listed in Table 3.2.

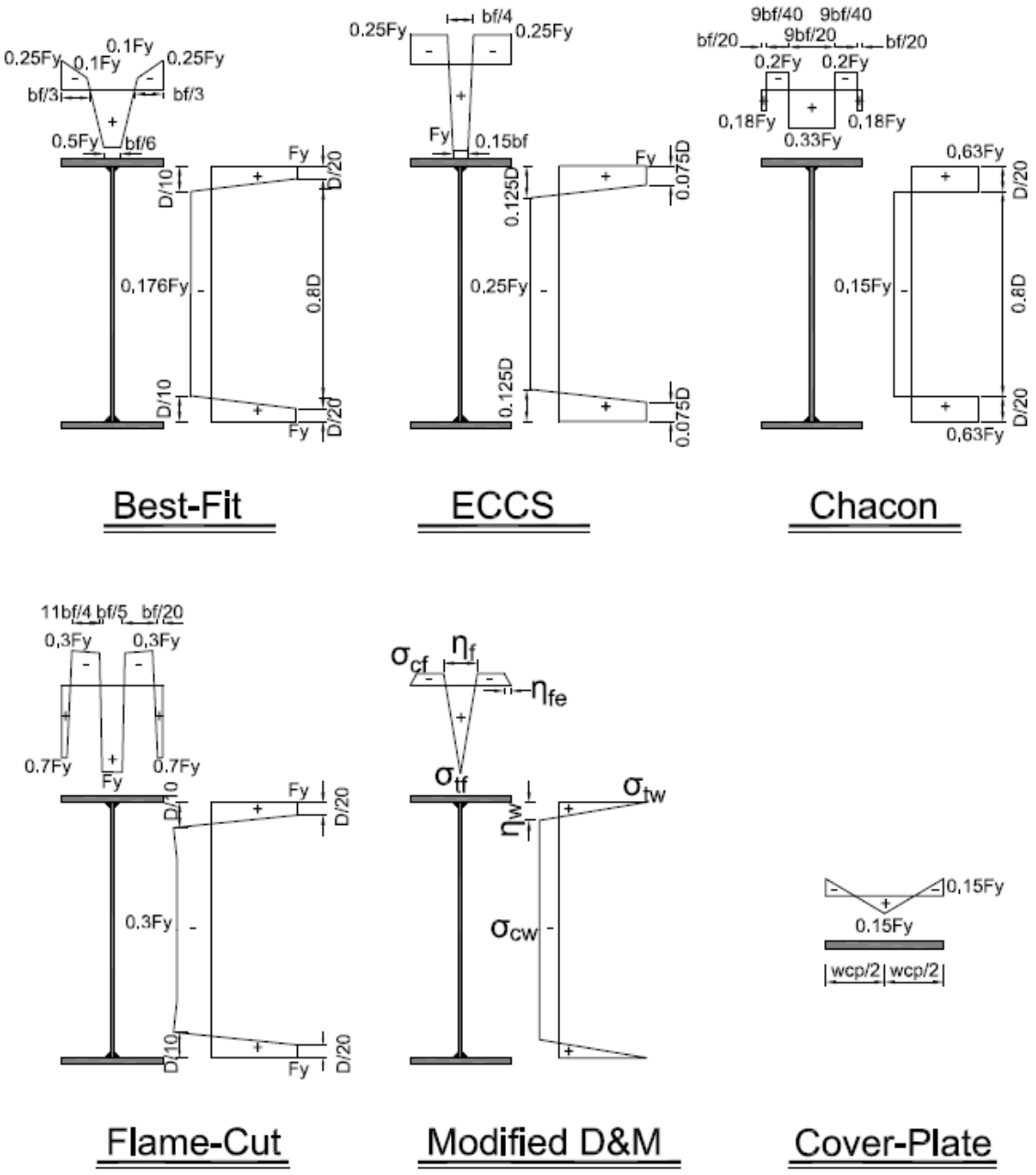

Figure 3.5: Initial residual stress patterns for I-beam and cover plate

Based on the results presented in Table 3.2, reinforcing I-beams by adding cover plates increases the ultimate capacities of I-beams when there is no preload. The average capacity increase is 12.66%, 28.98%, and 52.81% for stocky, intermediate and slender beams, respectively. It is observed that adding a cover plate significantly increases the capacity of I-beams, especially for slender sections. In the stocky beams, the maximum amount of capacity increase is 14.31%, which happens in the beam with Chacon initial residual stress. Furthermore, the minimum amount of capacity increase, which is 10.4%, in these

beams happens for the 'ECCS' initial residual stress. For intermediate beams, the maximum capacity increase is 30.85% which happens for the flame cut initial residual stress. In addition, for intermediate beams, the minimum capacity increase is 27.5%, which is for Chacon's initial residual stress. For the stocky beams, the capacity increase for all types of initial residual stress is very close.

Table 3.2: Ultimate capacities for the initial residual stresses of reinforced beams without preloading for cross-section A-1

I-Beams	Patterns	Capacity (kN·m)		Capacity increase (%)
		Unreinforced	Reinforced	
Stocky (2m unbraced beam)	Best Fit, Fy	2112.66	2393.46	13.3
	Flame Cut, Fy	2137.5	2372.94	11.01
	ECCS, Fy	2100.42	2318.76	10.4
	Chacon, Fy	2125.31	2429.46	14.31
	Modified D&M	2120.24	2422.75	14.27
Intermediate (6m unbraced beam)	Best Fit, Fy	1035.44	1338.32	29.29
	Flame Cut, Fy	1085	1419.74	30.85
	ECCS, Fy	991.44	1288.04	29.61
	Chacon, Fy	1075.5	1371.24	27.5
	Modified D&M	1090.66	1392.44	27.67
Slender (9m unbraced beam)	Best Fit, Fy	675.95	1042.57	54.24
	Flame Cut, Fy	715.64	1070.55	49.6
	ECCS, Fy	670	1031.06	53.9
	Chacon, Fy	694.31	1065.12	53.41
	Modified D&M	702.99	1074.87	52.9

The effect of the initial residual stress pattern on the ultimate capacity reduction of the beams reinforced while under load is presented in Figure 3.6. In this Figure, parameter β is the ratio of the beam ultimate capacity under considered preloading level to the beam ultimate capacity without preloading.

For the beams, the selected cross-section was A-1, and the varying parameters were the initial residual stress patterns and preloading level. As observed from Figure 3.6, initial residual stress plays a negligible role in the capacity reduction of stocky and slender beams since the reduction of capacity is negligible or equal for the considered patterns. However, for intermediate beams, the capacity reduction is different for different initial residual stress patterns and the capacity decreases with increased preload level. As shown in Figure 3.6, in intermediate beams, the capacity is reduced up to 5% for the beams with 60% of preloading. It is also observed that the minimum capacity reduction is for the 'Chacon' initial residual stress pattern and the maximum capacity reduction is for the 'ECCS' initial residual stress pattern.

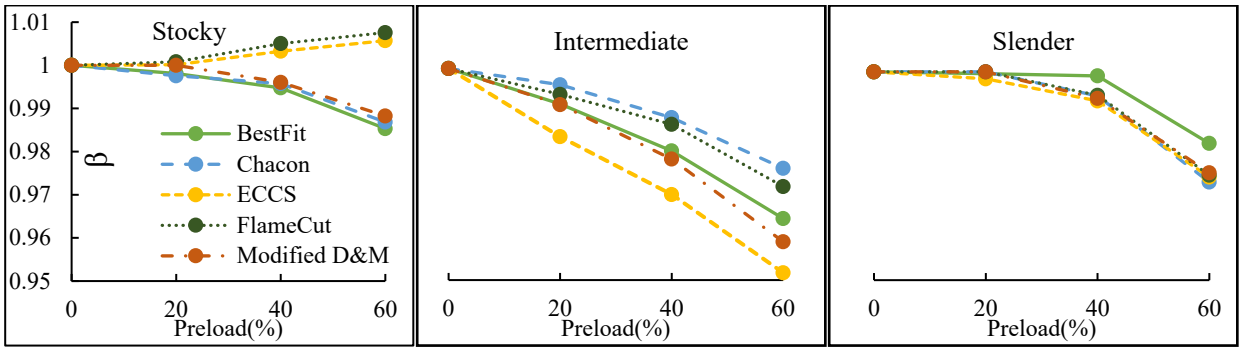

Figure 3.6: Effect of the initial residual stress on the capacity reduction of the beams reinforced under load for cross-section A-1

3.4.3 Effect of welding residual stress

Welding residual stress of two different magnitudes, 100% and 70% of yielding strength of steel material, at the location of welding were considered to study the effects of residual stresses induced from welding the cover plate to the bottom flange of I-beams. For investigating the effect of welding residual stress, cross-section A-1 was considered. It was observed that the differences in the capacities for the two different welding residual stresses were negligibly small. The ultimate capacities of the intermediate beams without preloading and with the two selected welding residual stresses are listed in Table 3.3.

Table 3.3: Capacities for the welding residual stresses of intermediate reinforced beams without preloading

Beams	Patterns	Capacity (kN·m)		Capacity increase (%)
		Unreinforced	Reinforced	
Intermediate (6m unbraced beam)	Best Fit, Fy	1035.44	1338.32	29.29
	Best Fit, 0.7Fy	1035.44	1338.12	29.23

For the welding residual stresses, the capacity reduction for the beams was approximately equal when the preload was applied. The effect of welding residual stress on the capacity reduction of the intermediate beams reinforced while under load is presented in Figure 3.7. Therefore, welding residual stress does not have a significant effect on the capacity reduction of the reinforced beams while under load.

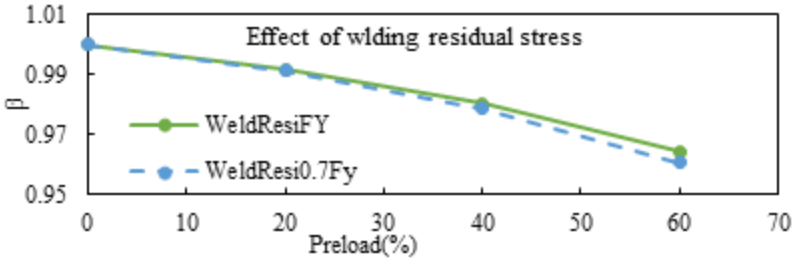

Figure 3.7: Effect of the welding residual stress on the capacity reduction of the intermediate beams reinforced while under load

3.4.4 Effect of initial geometric imperfection

The effect of initial geometric imperfection on the capacity of the I-beams reinforced while under load was studied using cross-section A-1 for the stocky, intermediate and slender beams. Four different magnitudes of flange sweep L/2000, L/1500, L/1000 and L/500 as the initial imperfection were studied. For each imperfection magnitude the beams were under 0, 20%, 40% and 60% of preloading. The aim of this study was to examine the capacity reduction sensitivity for the geometrical imperfection of the I-beams reinforced while under load. The capacity reduction diagrams for the beams are shown in Figure 3.8. It is observed that the moment capacity reduces with increased preload level and the capacity

reduction is higher when the imperfection magnitude is higher. However, the capacity reduction is negligible for the stocky beams, regardless of the preload level. In the intermediate and slender beams, the reduction of the capacity is meaningful and with increased preload level, the capacity reduces more. It is also observed from Figure 3.8 that the capacity reduction for the imperfection magnitude up to L/1000 (AWS limitation) and preload level up to 60% is small for the intermediate and slender beams.

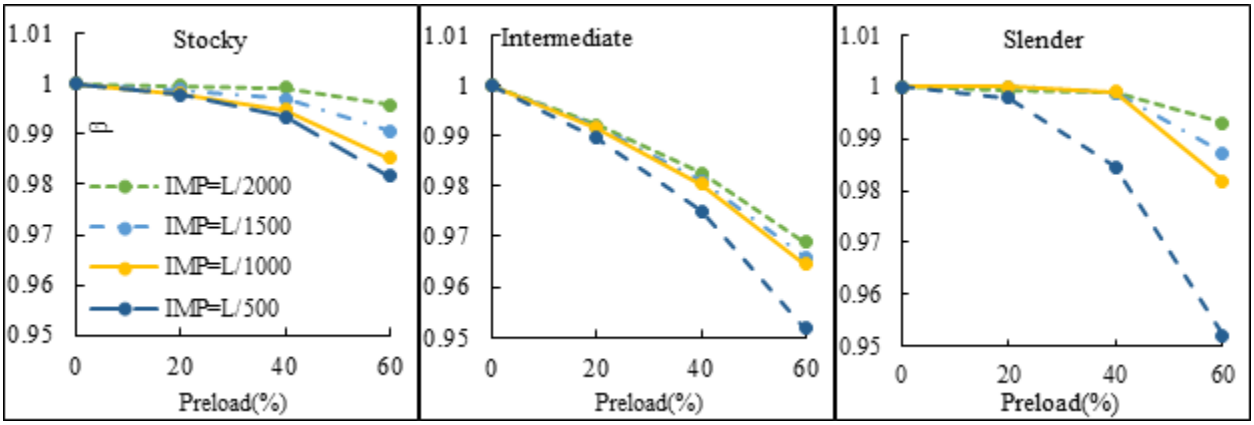

Figure 3.8: Effect of the initial imperfection on the capacity reduction of the beams reinforced under preload

3.4.5 Effect of cover plate thickness

To examine the effect of cover plate thickness on the behaviour of I-beams reinforced while under load, the beams with cross-sections A-1 and A-2 were used. The reinforcing plate size was 350 mm×25 mm and 350 mm×15 mm for A-1 and A-2, respectively. Four different preload levels were considered when reinforcing the cover plates. Moment-top flange lateral deflection diagrams at the mid-span of the intermediate beams with cross-section A-2 are depicted in Figure 3.9 for different preload levels. As shown in Figure 3.9, in general, the behaviour of the I-beams with different reinforcing plate thicknesses is similar.

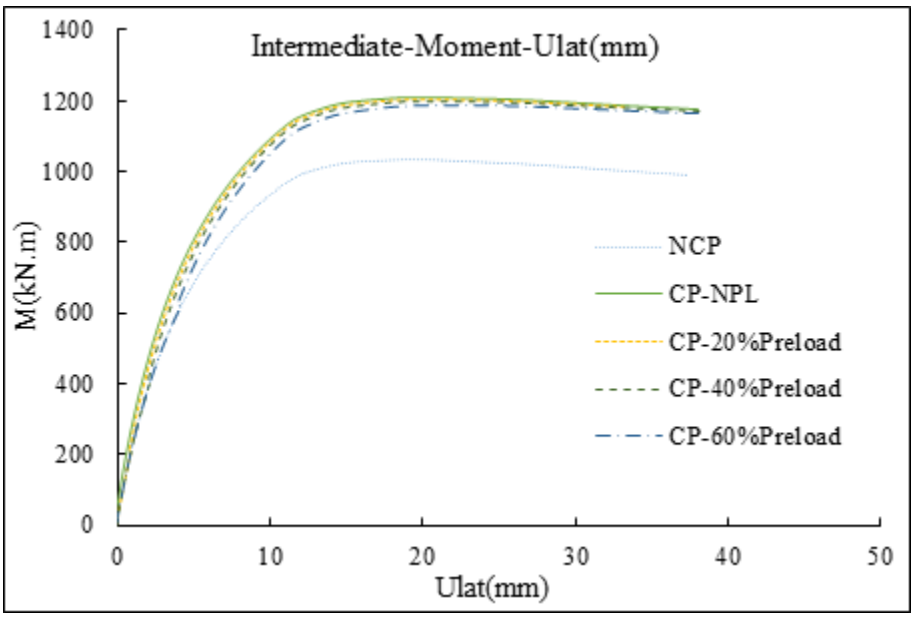

Figure 3.9: Moment- top flange lateral deflection of the intermediate beams with cross-section A-2 at mid-span under various preload levels

A comparison of the capacity increases due to welding of the cover plate of two different thicknesses, 25 mm (specimen A-1) and 15mm (specimen A-2), without any preloading is presented in Table 3.4. The difference of capacity increase for the reinforcing plate with the thickness of 15 mm and 25 mm is 1.14%, 12.4%, and 25.65% for stocky, intermediate, and slender beams, respectively. The failure of the stocky beam when reinforced with a welded cover plate at the bottom flange was observed as compression flange yielding. This is consistent with the limit state mentioned in section F4 of AISC 360-16 for singly symmetric I-shaped members. Based on the calculation of the yield moment in the compression flange, it was observed that increasing the thickness of the cover plate from 15 mm to 25 mm resulted in a very small increase in the capacity of the reinforced steel beam. This is consistent with the FE analysis results obtained for the stocky beams. However, for the intermediate and slender beams, an increase in cover plate thickness increases the capacity of the beams.

Table 3.4: Capacity increase due to welding of cover plate of different thicknesses without any preloading

Beams	Capacity (kN·m)			Capacity increase (%) (25 mm)	Capacity increase (%) (15 mm)
	Unreinforced	Reinforced (25 mm)	Reinforced (15 mm)		
Stocky	2112.66	2393.46	2369.62	13.3	12.16
Intermediate	1035.44	1338.32	1209.946	29.25	16.85
Slender	675.95	1042.57	869.2	54.24	28.59

The effect of cover plate thickness on the capacity reduction of the reinforced beams under different preload levels is demonstrated in Figure 3.10. For stocky beams, the reduction of the capacity for both thicknesses is negligible, less than 2%, for different preload levels. It can be observed that in intermediate and slender beams, the capacity reduces more in the beams with the thicker reinforcing plate when the preload level is increased.

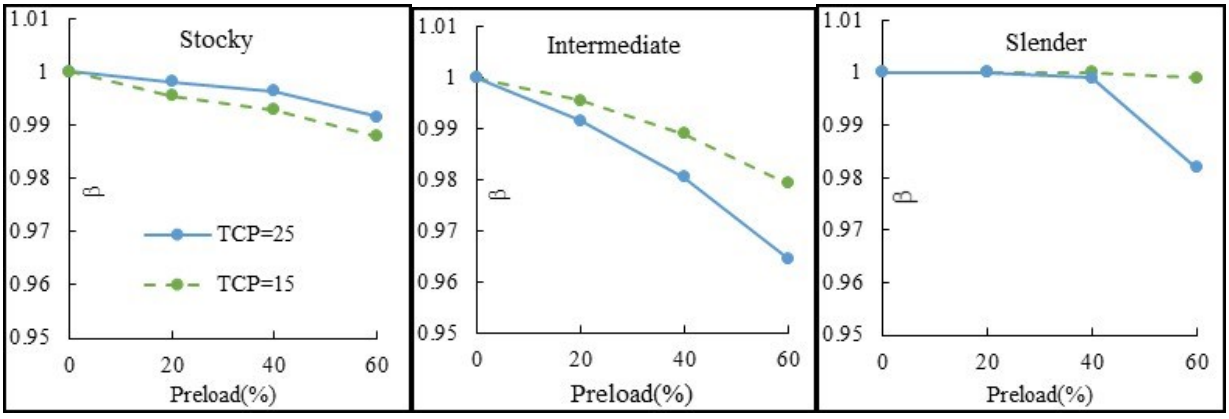

Figure 3.10: Effect of the cover plate thickness on the capacity reduction of the beams reinforced while under load

3.4.6 Effect of loading pattern

To study the effect of the loading pattern on the behaviour of the I-beams reinforced while under load, three different loading patterns, 3-point, 4-point, and uniformly distributed loading, were considered and applied at the top flange of I-beams with cross-section A-1 under different preloading levels. The considered loading patterns are shown in Figure 3.11. It should be noted that in the case of uniformly distributed loading, intermediate transverse stiffeners were not included in the web of the beams.

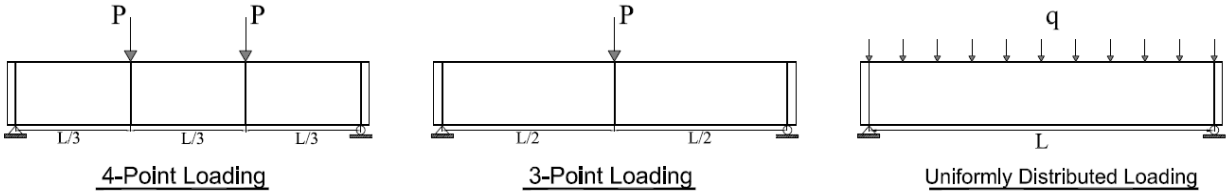

Figure 3.11: Studied loading patterns on the behaviour of reinforced I-beams under preloading

Moment-top flange lateral deflection diagrams at the mid-span of the intermediate beams for uniformly distributed loading are shown in Figure 3.12. It can be seen that the overall behaviour of the beams under various preload levels is similar.

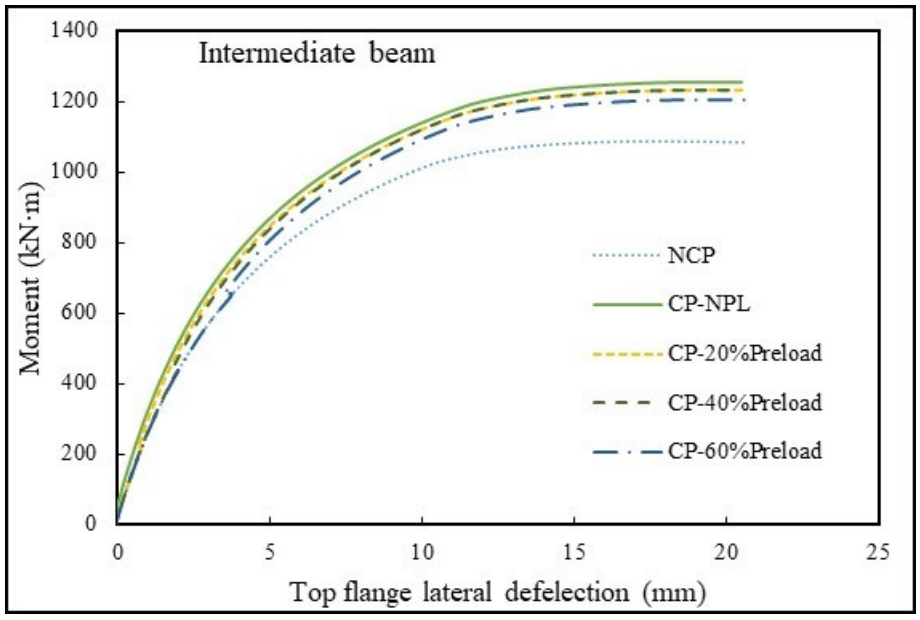

Figure 3.12: Moment-top flange lateral deflection diagrams for intermediate beams under a uniformly distributed loading pattern

The capacities of A-1 I-section reinforced with welded cover plate, without the presence of preloading, and subjected to three different loading patterns are presented in Table 3.5. It can be observed that the value of capacity increase is different for the beams with different loading patterns. The difference between 3-point and 4-point loading is negligible for the intermediate and slender beams and is 5.91% for stocky beams. In comparison to 3-point and 4-point loadings, the capacity increase of the intermediate and slender beams for uniformly distributed loading is small. In these beams, the increase is 15.45% and 34.16% for uniformly distributed loading, while the average capacity increase is 29.6% and 53.15% for 3-point and 4-point loadings, respectively.

Table 3.5: Capacity increase of 3-point, 4-point and uniform loading patterns without the presence of preloading in I-beams reinforced with welded cover plate

Beams	Capacity (kN·m)						Capacity increase (%)		
	Unreinforced (3-point loading)	Unreinforced (4-point loading)	Unreinforced (Uniform loading)	Reinforced (3-point loading)	Reinforced (Four-point Loading)	Reinforced (Uniform Loading)	3-point loading	4-point loading	Uniform loading
Stocky	2235.382	2112.66	2142.72	2400.42	2393.46	2364.88	7.38	13.29	10.37
Intermediate	1186.61	1035.44	1086.83	1542.026	1338.32	1254.74	29.95	29.25	15.45
Slender	785.0139	675.95	716.802	1193.72	1042.57	961.675	52.06	54.24	34.16

Furthermore, for the selected loading patterns, the capacity reduction of the beams reinforced while under load is presented in Figure 3.13. It can be seen that the loading pattern does not have a significant effect on the capacity reduction for the stocky beams. For the intermediate and slender beams, the capacity reduction is more for the uniformly distributed loading pattern without intermediate stiffeners in the web, mainly in the slender beams under preload levels of 40% and 60%. However, for all loading patterns, the reduction of capacity is under 5% up to the preloading level of 60%.

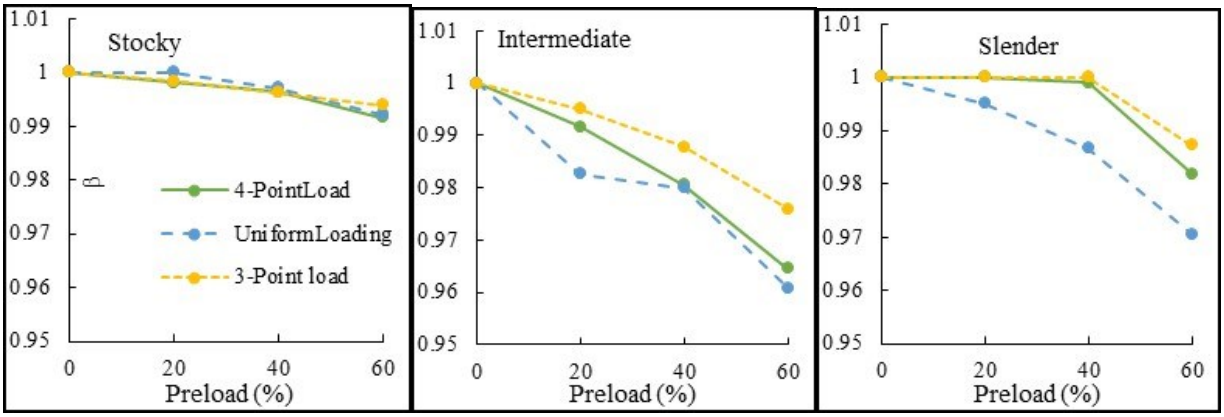

Figure 3.13: Effect of the loading pattern on the capacity reduction of the beams reinforced while under load

3.4.7 Effect of welding type- continuous and intermittent welding

In literature to control the potential unfavorable effects of continuous welding such as welding residual deformations and stresses, and welding thermal input, the use of intermittent welding for adding a reinforcing plate to the beam is recommended (Tide 1990). To examine the performance of intermittent welding in comparison to continuous welding, the behaviour of beams reinforced by adding a cover plate using intermittent welding was studied and compared with the ones with continuous welding. For this reason, in-line intermittent fillet welds were used to add the reinforcing cover plate with a thickness of 25 mm to the cross-section A (A-1). In-line intermittent weld features such as the size, length of each segment and longitudinal spacing of each weld segment were designed for the stocky, intermediate and slender beams based on the existing shear flow and AISC/CSA code requirements. No weld was considered across the end of the cover plate. Therefore, the welds connecting the termination of the reinforcing cover plate to the beams were continuous welds along both edges of the reinforcing plate in a length equal to two times of the cover plate width, i.e., $2w = 700\ mm$. This length of the weld was developed from the ends of the reinforcing cover plate for each beam. From the end of this weld to the concentrated load location, weld length segments of 60 mm for stocky beams and 40 mm for intermediate and slender beams with a spacing of 300 mm between each segment were used, respectively. Between the concentrated forces, the length of the weld segments was 40 mm and the space between each segment was 300 mm for the beams. In terms of FE modeling, a method similar to continuous welding was used. i.e., zero-length rigid beam connectors used at weld locations to connect the bottom flange to the duplicate of the reinforcing plate. 100% steel yielding strength was taken as the weld residual stress at the welding segments. Moment-lateral deflection diagrams of the intermediate beams reinforced by

adding a cover plate with in-line intermittent welding under different preloading levels are shown in Figure 3.14. Based on these diagrams, the overall behaviour of I-beams reinforced by adding a cover plate using a continuous and intermittent welding type is similar.

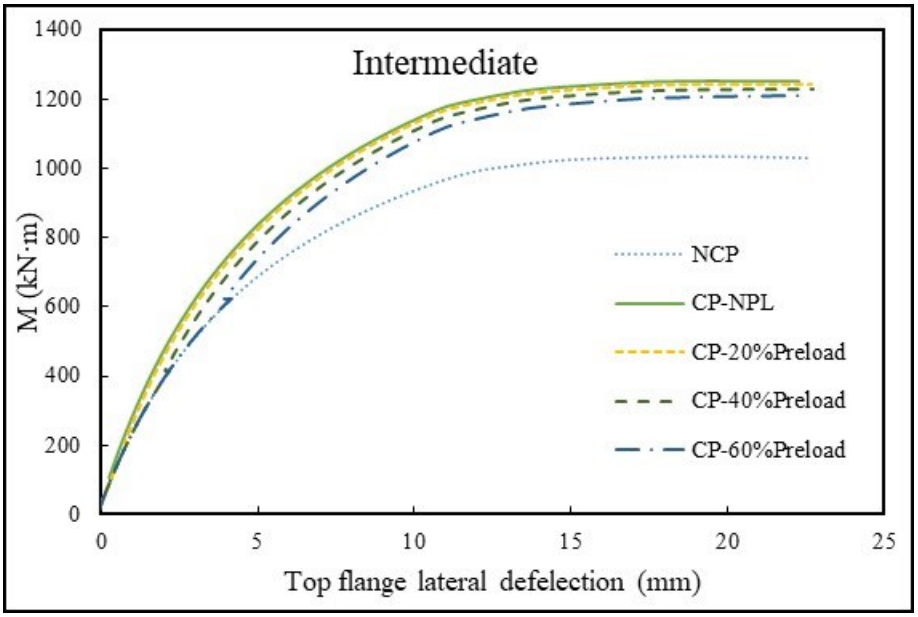

Figure 3.14: Moment- top flange lateral deflection at the mid-span of intermediate beams reinforced by a cover plate using in-line intermittent welding

The comparison of the capacity increase by adding a cover plate with continuous and in-line intermittent welding without any preloading is presented in Table 3.6. Based on the table, the capacity increase for stocky beams is similar for continuous and intermittent welding. However, the capacity enhances more in continuous welding comparing with intermittent welding in intermediate and slender beams. The capacity increase difference in the intermediate beams reaches 8.17%. The difference of the capacity increases is the maximum in the slender beams and reaches 19.68%.

Table 3.6: Difference in strength of reinforced beam for continuous and in-line intermittent welding without any preloading

Beams	Weld Type	Capacity; Unreinforced (kN·m)	Capacity; Reinforced (kN·m)	Capacity increase (%)
Stocky	Intermittent	2112.66	2391	13.17
	Continuous	2112.66	2393.46	13.3
Intermediate	Intermittent	1035.44	1253.72	21.08
	Continuous	1035.44	1338.32	29.25
Slender	Intermittent	675.95	909.57	34.56
	Continuous	675.95	1042.57	52.24

For continuous and intermittent welding, the capacity reduction of the beams reinforced while under load is presented in Figure 3.15. It can be seen that capacity reduction for intermittent and continuous welding is almost similar for all types of beams; stocky, intermediate, and slender beams.

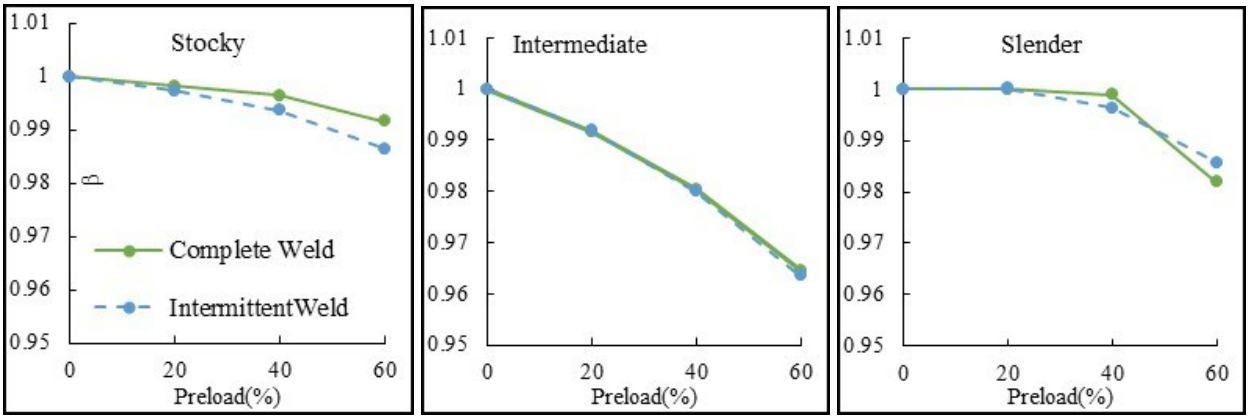

Figure 3.15: Effect of the welding type; continuous or intermittent welding, on the capacity reduction of the beams reinforced while under load

3.4.8 Effect of type of cross-section of I-beam

To study the cross-section effects on the behaviour of I-beams reinforced by welded cover plate while under load, homogeneous cross-sections A-1, B, and C with a yield strength of 345 MPa were used. In cross-section C, to avoid shear failure, transverse stiffeners were added between the load and bearing locations as intermediate stiffeners. Also, it should be noted that in these sections the ratio of reinforcing plate area to bottom flange area was almost equal. Cross-section A-1 has a compact compression flange and web. Cross-section B has a singly symmetric base beam, and its compression flange and web are compact and non-compact, respectively. For section B, the size of the compression flange was changed in comparison to cross-section A-1. Cross-section C has a compact compression flange, and a slender web with 2m depth. To illustrate the behaviour of these different sections, moment-lateral deflection diagrams of the intermediate and slender beams with cross-sections B and C are depicted in Figure 3.16. It is observed that the overall behaviour of different I-beams (different cross-sections) reinforced with welded cover plates under different preload levels is similar.

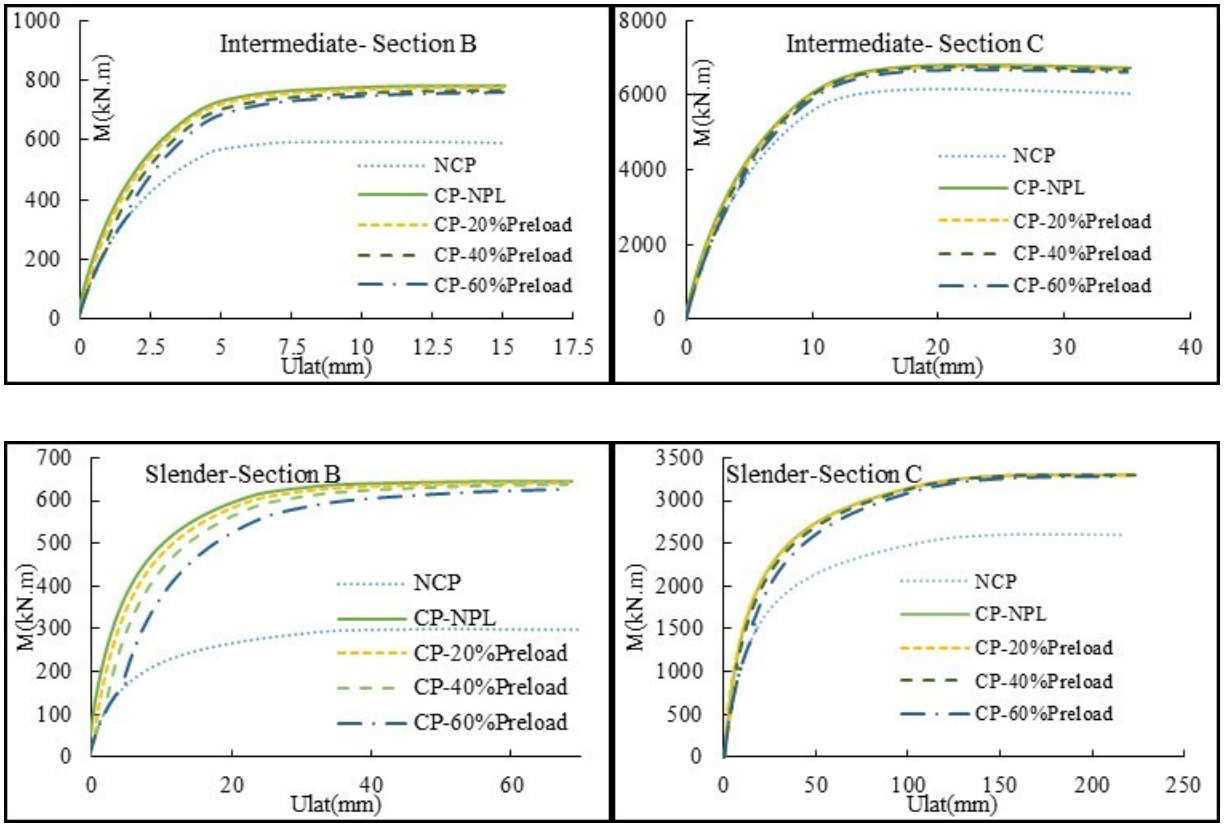

Figure 3.16: Moment- top flange lateral deflection at mid-span of intermediate and slender beams reinforced by welded cover plate for homogeneous cross-sections B and C

Furthermore, the capacity reduction diagrams for different levels of preloading for the reinforced beams with selected cross-sections are presented in Figure 3.17. It can be seen that for cross-section C the reduction of capacity is negligible regardless of the failure type. For cross-sections A-1 and B, the capacity reduction in intermediate beams is almost equal. Among all the considered cross-sections, section B has the largest capacity reduction in the case of intermediate span length (beams with linear and nonlinear LTB failures).

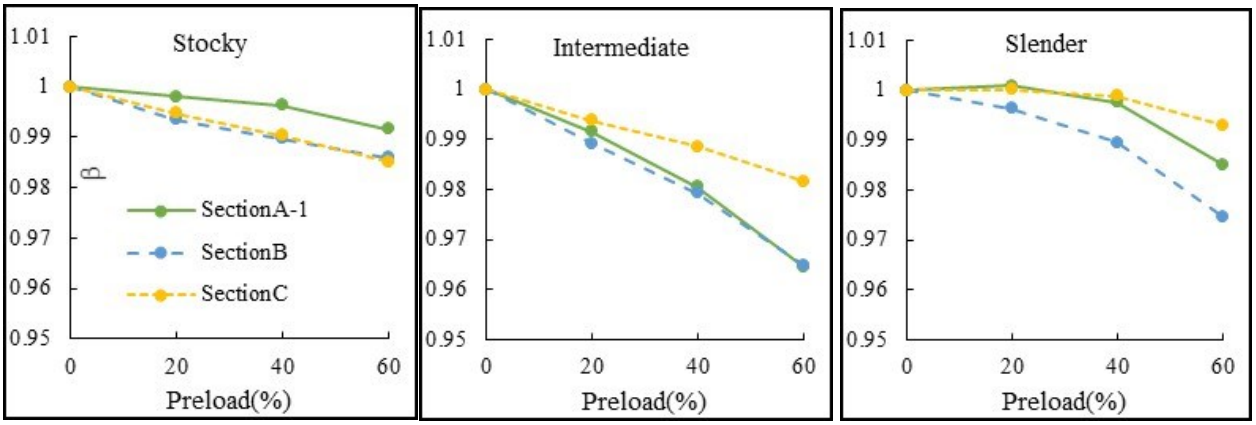

Figure 3.17: Effect of cross-section class on the capacity reduction of the beams reinforced while under load

3.4.9 Hybrid Sections

Two types of hybrid cross-sections were considered in this study. In the first one, named as hybrid type I in this paper, the flanges and web of the unreinforced sections were from the same steel material and the reinforcing plate was from a higher steel grade. In the second one, the unreinforced steel beam itself was also considered as a hybrid material. In these sections, the web, flanges and reinforcing plate had different steel grades and were named as hybrid type II in this study.

3.4.9.1 Effect of difference in steel grade between I-beam and cover plate (Hybrid type I)

In order to study the effect of the difference in steel grade between the base I-section and cover plate on the behaviour of reinforced I-beams, two different steel grades were considered for the I- section. As presented in Table 3.7, the unreinforced I-beam is made of ASTM A36 steel material with a yield strength (F_y) of 250 MPa and ultimate strength (F_u) 400 MPa and previously considered ASTM A572 grade 50 with a yield strength of 345 MPa and ultimate strength of 450 MPa. Also, for this study two different cross-sections, A-1 and C, were considered. For the reinforcing plate, F_y and F_u were 345 MPa

and 450 MPa, respectively. From FE analyses, it was observed that the overall behaviour of hybrid (Type I) and homogeneous beams reinforced while under load were similar. Table 3.7 compares the capacities of hybrid type I beams and homogeneous reinforced beams when there is no preloading.

Table 3.7: Capacities of hybrid type I and homogeneous reinforced beams with no preloading

Beams	Cross-section	F_y (MPa) Base I-beam		F_y (MPa) Cover plate	Capacity Unreinforced (kN·m)	Capacity Reinforced (kN·m)	Increase (%)
Stocky	A-1	Hybrid type I	250	345	1552.66	1839.97	18.5
		Homogeneous	345	345	2112.66	2393.46	13.3
	C	Hybrid type I	250	345	8485.25	9211.23	8.56
		Homogeneous	345	345	11038.3	11742.48	6.38
Intermediate	A-1	Hybrid type I	250	345	860.87	1134.62	31.8
		Homogeneous	345	345	1035.44	1338.32	29.25
	C	Hybrid type I	250	345	5105.22	5843.92	14.47
		Homogeneous	345	345	6181.97	6831.25	10.5
Slender	A-1	Hybrid type I	250	345	605.84	927.73	53.13
		Homogeneous	345	345	675.95	1042.57	54.24
	C	Hybrid type I	250	345	2355.92	3048.83	29.41
		Homogeneous	345	345	2597.30	3296.94	26.94

For cross-section A-1 with compact flanges and web, the capacity increases for the hybrid type I and homogeneous stocky beams are 18.5% and 13.3%, respectively. Also, the increase of capacities for hybrid type I and homogeneous intermediate beams is 31.8% and 29.25%, respectively. Furthermore, for the hybrid slender beams, the capacity increase is 53.13% while for homogeneous slender beams, it is 54.24%. Moreover, for cross-section C with compact flanges and slender web, the capacity increases for the hybrid type I and homogeneous sections are 8.56% and 6.38% for stocky beams, 14.47% and 10.5% for intermediate beams, and 29.41% and 26.94% for slender beams. It can be concluded that using higher strength material for the cover plate will not have a significant effect on the capacity increase of the reinforced section.

For cross-section A-1, moment-top flange lateral deflections of the intermediate hybrid beams under various preload levels are shown in Figure 3.18. Figure 3.18 (a) also presents moment-lateral deflection results of two more cases: (1) when there is no cover plate (NCP) and (2) when there is no preload during the reinforcement (CP-NPL). Figure 3.18 (b) compares capacity reduction for hybrid and homogeneous intermediate beams. It was observed that for the intermediate beams, the reduction of the ultimate capacity is close for both hybrid (type I) and homogeneous steel beams and the capacity reduction is under 5% for the intermediate beams.

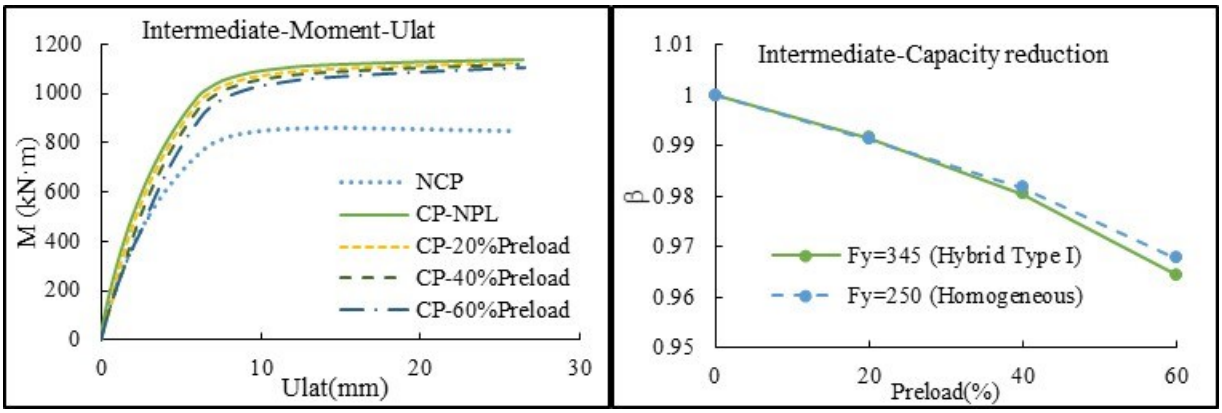

(a) (b)

Figure 3.18: a) Moment-lateral deflection. b) Reduction of capacity for intermediate hybrid beams (Cross-section A-1)

3.4.9.2 Effect of difference in steel grade between flanges, web and cover plate (Hybrid type II)

To study the effect of the difference in steel grade between flanges, web and cover plate (Hybrid type II) on the behaviour of steel beams reinforced under preload, I-beams with cross-sections A-1 and C were considered. In these beams, the yield strength of the web, flanges and reinforcing plate were 250MPa, 345MPa and 483MPa, respectively. Table 3.8 provides the capacities of the selected hybrid reinforced sections when there was no preload during the reinforcement. Comparing the results of this table and the results obtained for the homogeneous section in Table 3.7, it is observed that the rate of capacity increase is almost equal for both cases.

Table 3.8: Capacities of reinforced beams with hybrid type II without preloading

Beams	Cross-section	F_y Web (MPa)	F_y Flange (MPa)	F_y Cover plate (MPa)	Capacity Unreinforced (kN·m)	Capacity Reinforced (kN·m)	Increase (%)
Stocky	A-1	250	345	483	1999.27	2295.2	14.8
	C	250	345	483	10511.05	11200.31	6.56
Intermediate	A-1	250	345	483	1030.39	1352.08	31.22
	C	250	345	483	6205.11	6983.49	12.54
Slender	A-1	250	345	483	668.21	1050.23	57.17
	C	250	345	483	2555.59	3340.03	30.69

To illustrate the behaviour of beams reinforced while under load with hybrid base beams (Hybrid type II), moment-lateral deflections of intermediate beams, as well as comparison of capacity reduction diagram for these sections and homogeneous ones under various levels of preloading for section A-1, are presented in Figure 3.19. As observed from Figure 3.19, the overall behaviour of the Hybrid II type beams is similar to the homogeneous ones.

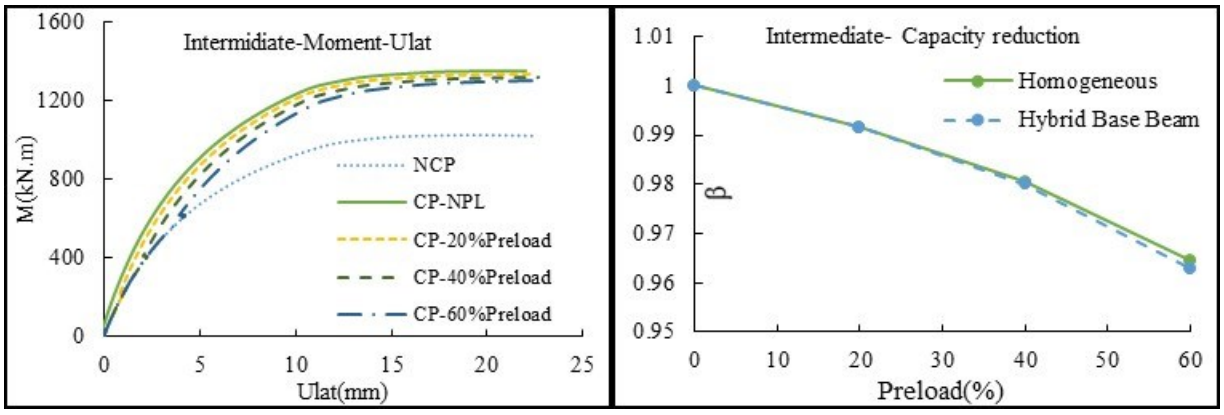

(a) (b)

Figure 3.19: a) Moment-lateral deflection. b) Reduction of capacity for intermediate beams with different steel grades between flanges, web and cover plate (Hybrid type II)

3.5. EVALUATION OF AISC AND CSA STRENGTH EQUATIONS FOR STEEL I-BEAM REINFORCED WITH WELDED COVER PLATE

Many steel beams in existing structures, including steel buildings, are often of lower grade steel than the more modern steel used for reinforcement, and this can complicate the design and analysis of the reinforced steel beam. While some design engineers believe that using a higher grade reinforcing plate will result in a capacity increase, a common engineering practice is to ignore the effects of hybrid material and just use the code capacity curves for homogeneous cross-sections with a minimum yield strength (Fy) of the hybrid section. This section investigates the effectiveness of the common design practice of using code capacity equations with the lower yield strength of the hybrid sections. The ultimate capacities of the selected reinforced I-beams obtained from FE analyses were compared with the predicted capacities by AISC 360-16 and CSA S16-19. In the FE models, the loads were applied at the top of the flanges and the reinforcing plates were welded only at the bottom flanges. Thus, reinforced cross-sections were singly symmetric with loads at the top flanges. This loading position with respect to the shear center of the cross-section can have a destabilizing effect on the lateral-torsional buckling of singly symmetric cross-sections (Helwig et al. 1997). To examine this destabilizing effect, the codes' capacities were obtained with and without taking load positions into account. To consider the loading position effect, Eq. (3-2) and Eq. (3-3) recommended by Helwig et al. (1997) were used. In these equations, $C_b^*$and ω_3^*, used in AISC and CSA, respectively, for laterally unsupported singly symmetric beam, are LTB modification factors for non-uniform moment distribution accounting for the loading position, $\mathrm{C_b}$and ω_3 are LTB modification factors for non-uniform moment distribution when the load is applied at the shear center of the cross-section. Also, $h_0$is the distance between flange centroids and y is the distance between the loading point and the mid-height of the section; y is equal to $-h_0/2$ for top flange loading.

$$C_b^* = 1.4^{(2y/h_0)}(C_b) \text{ for AISC} \quad [3\text{-}2]$$

$$\omega_3^* = 1.4^{(2y/h_0)}(\omega_3) \text{ for CSA} \quad [3\text{-}3]$$

In Figure 3.20, flexural capacities obtained from FE analyses for homogeneous reinforced beams with the preload levels of 0%, 20%, 40% and 60% are compared with the two north American standards (AISC and CSA). Figure 3.20 (a) shows the capacity comparison for section A-1 with 4-point and

uniform loading. In this figure for the beams with 4-point loading, four different initial imperfection magnitudes (L/2000, L/1500, L/1000 and L/500), five different initial residual stresses (Best-Fit Prawel, ECCS, Chacon, Flame-Cut and modified Dwight and Moxham), two different welding residual stresses (100% and 70% of yielding strength of steel material) and two different welding types (continuous and intermittent) were considered. For the uniform loading condition of Figure 3.20 (a) and Figure 3.20 (b-e), the initial imperfection magnitude was L/1000, initial residual stresses were Best-Fit Prawel, welding residual stresses were 100% yielding strength of the steel material, and the welding type was continuous. In these diagrams, the flexural capacities of the codes are nominal moment resistance. Based on the results, the capacities predicted by AISC 360-16 are close to the FE capacities with slight overestimation for homogeneous cross-sections with compact and non-compact webs (cross-sections A-1, A-2, and B) in stocky beams. AISC limits the nominal moment resistance to $\mathrm{M_n = R_{pc}M_{yc}}$ while CSA limits the capacity to $\mathrm{M_n = M_p}$ for singly symmetric cross-sections with compact/non-compact webs in AISC and class 1 or 2 sections in CSA. For homogeneous cross-section C in the stocky range, the predicted capacities based on AISC, and CSA are close and both overpredict the flexural capacities of the reinforced beams. AISC limits the capacity to $\mathrm{M_n = R_{pg}M_{yc}}$ for singly symmetric I-beams with slender webs in the stocky range. CSA does not provide any specific equation for singly symmetric sections with web class 4. In this study, the equations for class 3 webs are used, instead. For the stocky range, the capacity limit is $\mathrm{M_n = M_{yc}}$ in CSA for class 3 sections. In these equations, $\mathrm{R_{pc}}$is the factor of web plastification, $\mathrm{M_{yc}}$is the compression flange yield moment, $\mathrm{M_p}$is the plastic bending moment and $\mathrm{R_{pg}}$ is the reduction factor for bending strength. For the homogeneous intermediate beams, AISC (with both factors C_b^* and $\mathrm{C_b}$) and CSA (with both ω_3^* and ω_3 factors) overpredict the flexural capacities of the selected reinforced beams. However, flexural capacities predicted by AISC with factor C_b^* are found close to the FE simulation results with slight overestimation. Also, it can be seen that for the elastic beams, AISC and CSA by accounting the effect of the load position ($C_b^*$and ω_3^*) can predict the capacity of the reinforced beam with reasonable accuracy.

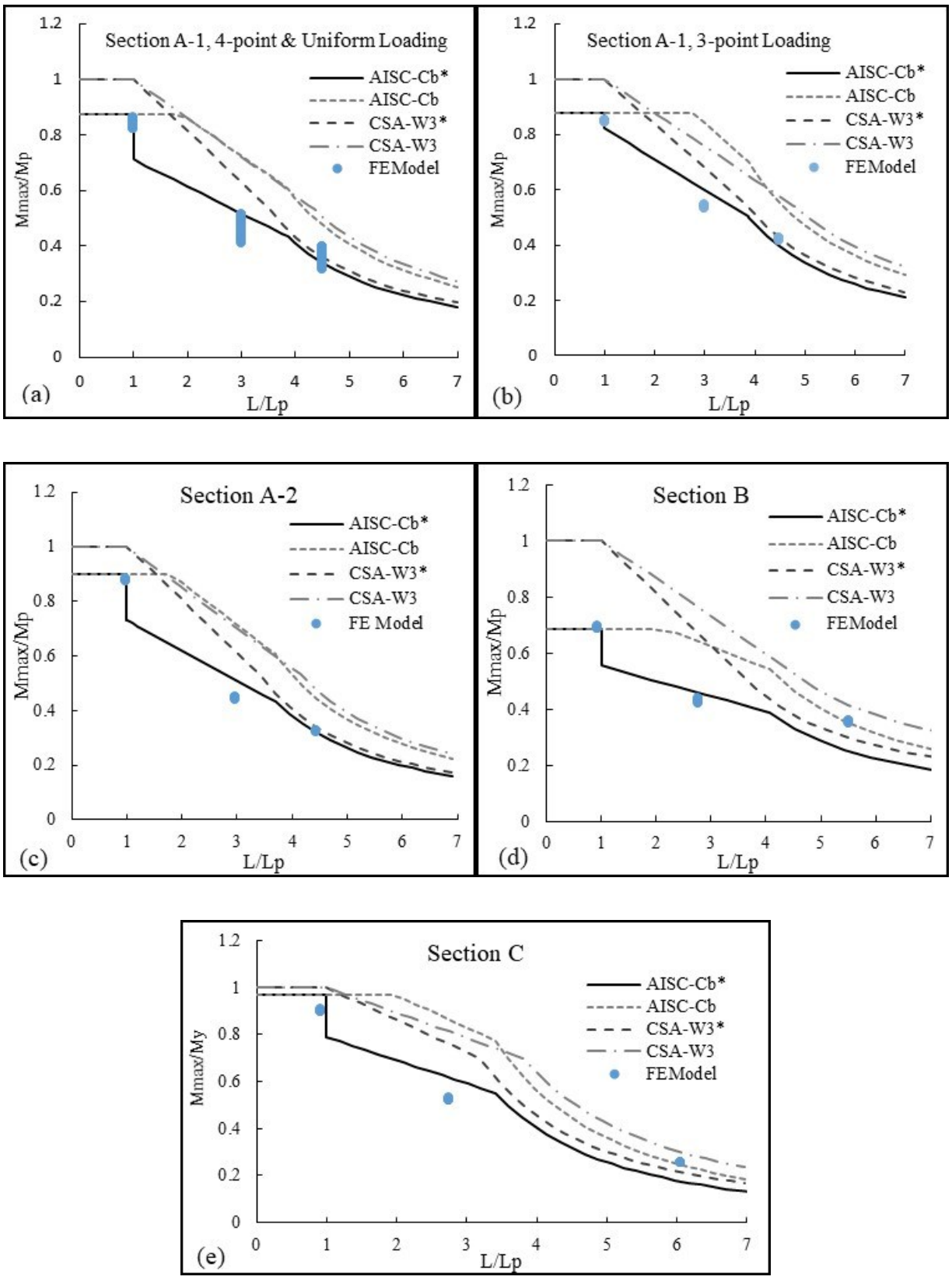

Figure 3.20: Flexural capacity comparison for AISC, CSA and FE simulation for homogeneous sections

In addition, flexural capacities obtained from AISC, CSA and FE simulations for hybrid sections are compared in Figure 3.21. In these hybrid sections, the varying preload levels were 0%, 20%, 40% and 60%, the initial imperfection magnitude was L/1000, the initial residual stresses were Best-Fit Prawel, welding residual stresses were 100% of yielding strength of steel material and continuous welding type was used to connect the reinforcing plate to the beam. In both AISC and CSA codes, the capacities are based on the specified minimum yield stress (F_y) used within the cross-section and the codes do not account for the potential favorable/unfavorable effects of the components of the cross-section with different strength steel. As mentioned earlier, two types of hybrid sections are considered in this study. In the first one, just the reinforcing cover plate is from a higher steel grade (Type I). While in the second one, the base beam itself is a hybrid section with a higher steel grade for flanges (Type II). As it can be observed from the diagrams, predicted capacities by AISC with C_b^* are close for the first case and neglecting the potential favorable effects of the higher grade of reinforcing plate is a reasonable assumption. In hybrid type II, the flexural capacities obtained from FE analyses are higher than the capacities predicted by AISC with C_b^* for stocky and intermediate reinforced beams. Thus, neglecting the positive effects of higher steel grade is a conservative assumption for these beams, mainly for stocky ones.

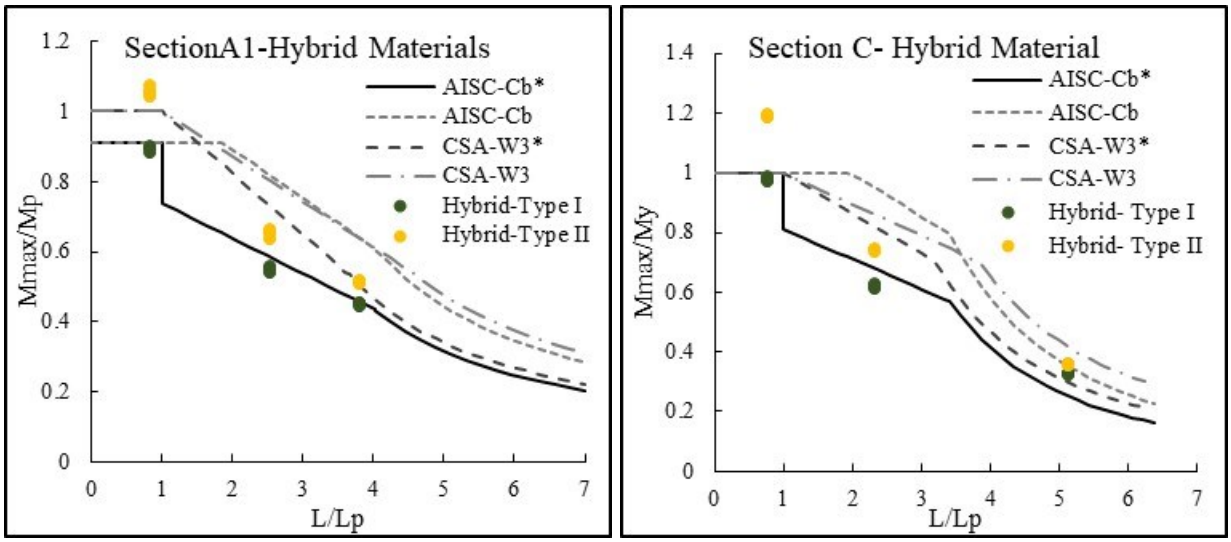

Figure 3.21: Flexural capacity comparing AISC, CSA and FE simulation for hybrid sections

3.6. CONCLUSIONS

A numerical study was conducted to investigate the effects of preloading, initial and welding residual stress, initial geometric imperfection, cover plate thickness, loading pattern, welding type; continuous or intermittent, different cross-section classes and steel grades of the beam components and reinforcing plate on the behaviour of steel I-beams reinforced by welding a cover plate to the bottom flange. The following results are drawn from this investigation.

- Preload did not have a significant effect on the behaviour and ultimate capacities of reinforced I-beams with flexural yielding failure modes. However, preload had some effect on the behaviour of beams with linear and nonlinear LTB failure modes. For the nonlinear LTB, the ultimate capacities decreased when the preload magnitude was increased; however, the reduction was smaller than 5% for a preload level of up to 60% of the strength of the unreinforced beam. For the beams with linear LTB, the presence of preload changed the buckling behaviour of the reinforced beams and reduced the buckling capacity.

- Initial residual stress has a negligible effect on the capacity reduction of I-beams with flexural yielding and linear LTB failures. However, the capacity reduction was different for different initial residual stress patterns and the difference increased with an increase in the preload level in the I-beams with nonlinear LTB failure. It was observed that the minimum capacity reduction was for the 'Chacon' initial residual stress pattern and the maximum capacity reduction (up to 5% for beams with 60% preloading) was for the 'ECCS' initial residual stress pattern.

- Variation of the maximum welding residual stress from 70% up to 100% yielding strength of the material did not change the capacity and behaviour of I-beams reinforced while under load.

- For the beams with different geometrical imperfection magnitudes, the flexural capacity was reduced when the preload level was increased. This was clear for the slender and intermediate beams with higher imperfection magnitude. However, the capacity reduction was small for beams with an imperfection magnitude of L/1000 (AWS limitation) and a preload level up to 60% of the capacity of the base beam. Also, the capacity reduction was negligible for the stocky beams, regardless of the preload level.
- In general, the behaviour of the reinforced I-beams with different reinforcing plate thicknesses was similar. The thickness of the cover plate did not affect the capacity increase in the stocky beams (with no preload). However, for the intermediate and slender beams, increasing the cover

plate thickness affected the capacity increase. In intermediate and slender beams, the capacity reduction under preloading was more significant in the beams with thicker reinforcing plates, mainly in the intermediate ones.

- The overall behaviour of the beams with different loading patterns and preload levels was similar. When no preload was present, the capacity increase of the reinforced beam was different for beams with different loading patterns. When reinforced under preload, the loading pattern did not have a significant effect on the capacity reduction for the stocky beams. For the intermediate and slender beams, the capacity reduction was more for the uniformly distributed loading pattern without any intermediate stiffener in the web, mainly in the slender beams under preload levels of 40% and 60%. However, for all loading patterns, the capacity reduction of reinforced beams was under 5%, up to a preload level of 60% of the capacity of the base beams.
- From this study, it was observed that the overall behaviour of I-beams reinforced with cover plates using continuous and intermittent welding was similar. For the stocky beams, the capacity increase was similar for I-beams reinforced with intermittent and continuous welding. However, for the intermediate and slender beams with no preload, cover plates welded with continuous welding, in comparison to the intermittent welding, provided higher capacities. For the beams reinforced under preload, capacity reduction for intermittent and continuous welding was almost similar.
- For the different considered cross-sections, the rate of buckling and ultimate capacity reduction for the beams reinforced under load was different. This difference was more noticeable in the intermediate and slender beams.

- For the homogeneous base (I-) beams, using higher strength material for welded cover plate did not have a significant effect on the capacity increase. For the hybrid base (I-) beams, using high strength reinforcing plate did not have any noticeable effect on the capacity increase of I-beams with no preload. Also, steel grade did not have any significant effect on the capacity reduction of the beams reinforced while under load.

- The capacities predicted by AISC were close to the FE capacities with slight overestimation for homogeneous cross-sections with compact and non-compact webs in stocky beams, while CSA S16-19 significantly overestimated the capacities for these beams. For the homogeneous intermediate beams, AISC without considering the effect of loading position and CSA with and without considering the effect of loading height into account significantly overpredicted the

flexural capacities. Predicated capacities for AISC with modification factor of loading position were close to FE results with slight overestimation. For the elastic beams, AISC and CSA, considering the effect of loading height, could predict the capacity with reasonable accuracy. In addition, using the minimum yield strength of the cross-section components to find the capacities of reinforced I-beams with higher steel grades just for the reinforcing plate was shown to be a reasonable assumption. This assumption gave a conservative capacity prediction for stocky and somewhat intermediate reinforced beams with cross-sections having different steel grades for web, flanges, and reinforcing plate.

4. REINFORCING PRELOADED STEEL I-BEAMS BY CONSIDERING WELDING HEAT EFFECTS AND GEOMETRIC IMPERFECTIONS

4.1. ABSTRACT

Steel I-beams are often strengthened by welding steel cover plates to the bottom flanges of the beams. However, very limited studies have been conducted on the effect of welding heat on the behaviour of I-beams reinforced while under load. This paper presents a finite element (FE) based study on the behaviour of preloaded steel I-beams reinforced with welded cover plates at the bottom flanges of beams considering welding procedure simulation. FE analysis was conducted to study the effects of welding heat, welding sequence and weld length on the residual welding deformation and behaviour of steel I-beams reinforced while under load. Study shows that an appropriate welding sequence and weld length can reduce the residual lateral deformations induced from welding a reinforcing plate to the bottom flange of the preloaded I-beam and thus control the unfavorable welding effects. Based on the study, a welding segment length of L/9, where L is the length of the beam, is recommended for practical applications. In addition, the effects of initial geometric imperfection and preload level on the welding residual deformation and the behaviour of the reinforced beams are studied numerically. FE analysis shows that the direction and magnitude of initial geometrical imperfection can change the value and direction of the residual deformation resulting from welding. Furthermore, it is observed that preloading does not have any significant effect on the behaviour and ultimate capacity of the I-beam reinforced at a preload level up to 50% of the strength of the unreinforced beam.

Keywords: Reinforced I-girder; preload level; finite element analysis; weld simulation; initial imperfection

4.2. INTRODUCTION

Steel I-beams are primary load-carrying members in highway bridges. These beams often need to be strengthened to meet new or additional load requirements in the structure. Flexural members such as steel I-beams that require strengthening often are in service for a certain period and thus a complete relief of loads is not either possible or not economically viable. Thus, the I-girders may need to be strengthened while under load. Strengthening of a steel beam can increase the stiffness and ultimate capacity of the original beam. In addition, it sometimes prevents the undesirable failure mode, such as lateral-torsional buckling failure, of the steel beam. When the steel girder is in service, only the bottom

flange of the steel I-beam is fully accessible for reinforcement. The reinforcement can be done by welding a cover plate to the bottom flange of the original beam. Research on the behaviour of steel I-beams reinforced while under load is very limited. The first study conducted on the behaviour of steel beams reinforced under load was by Liu and Gannon (2009). Liu and Gannon (2009) tested steel I-beams reinforced with welded cover plates for different preload levels. Two different reinforcing patterns, pattern A where a plate was welded to the bottom flange of the beam, and pattern B where two plates were welded against the tips of the flanges of the beam section, were considered. Liu and Gannon (2009) concluded that an increased preload would decrease the lateral-torsional buckling strength of I-beams welded with cover plates at the bottom flanges (pattern A reinforcement) than the same specimen strengthened under no preload. Also, it was observed that a change in the preload level did not have any significant effect on the ultimate strength of beams with flexural yielding failure. Furthermore, a deflection plateau was observed at the preload level in the vertical and lateral directions during the welding process in the load-deflection diagrams of the reinforced beams. It was reported that the magnitude of the plateau increased with an increase in the preload level. In the vertical direction, the plateau was downward, whereas the plateau was in an unfavorable direction for the lateral direction caused by the welding as the lateral deflection of the compression flange of the beam increased. It was believed that the additional lateral deflection at the top flange location contributed to the reduction of lateral-torsional buckling load for increased preload level. In the research of Liu and Gannon (2009), initial geometric imperfections were not measured experimentally. While the welding sequence was provided in the report, weld length and welding features, such as the input heat of the weld, were not reported. Yuan-qing et al. (2015) conducted an experimental study on the behaviour of steel I-beams reinforced with welded cover plates both at the top and bottom flanges. The detailed study considered the welding procedure and the effect of different preload levels. Three reinforced I-beams with the preload level of 0%, 37%, and 74% of the strength of the unreinforced beam were tested. For the beam with the 37% preload, the failure was reported as lateral-torsional buckling, and the ultimate capacity was smaller in comparison to the capacity of the reinforced beam with no preload. However, for the reinforced beam with the 74% preloading level, the ultimate capacity increased and the failure mode for this beam was flange local buckling. Thus, no clear and direct relationship was obtained between the preload and the strength of the reinforced beam from the study of Yuan-qing et al. (2015). In addition, in the research of Yuan-qing et al. (2015), a plateau was observed in the vertical and lateral directions while welding the reinforcing plate under load. Based on the report of Yuan-qing et al. (2015), the plateau in the vertical direction was increasing the deflection (downward) similar to the specimens of Liu and

Gannon (2009). However, for the lateral deflections, the plateau was in a favorable direction, and the lateral deformation was reduced, unlike the specimens of Liu and Gannon (2009). Also, the value of the plateau in the lateral direction was not sensitive to the preload level and the plateau for the specimen with preload level of 37% was greater than the specimen with a 74% preloading level, based on the reported diagrams by Yuan-qing et al. (2015). Mohammadzadeh and Bhowmick (2022) conducted a numerical study to investigate the effects of preloading, initial and welding residual stresses, and steel grade on the behaviour of simply supported steel I-beams reinforced by welding a cover plate to the bottom flange. It was observed that the preloading had an insignificant effect on the behaviour and strength of beams with flexural yielding failure mode. However, preloading had some effect on the behaviour of beams with linear and nonlinear LTB failure modes. Also, it was reported that for the nonlinear LTB, the buckling and ultimate capacities decreased when the preload magnitude was increased. The reduction of ultimate capacities was smaller than 5% for a preload of up to 60% strength of the unreinforced beam. In addition, it was observed that initial and welding residual stresses did not change the capacity and behaviour of I-beams reinforced while under load.

Thus, welding a cover plate to the bottom flange of the I-beam can be a potential solution for strengthening steel I-beams. However, the local heating induced by welding can cause transient and permanent deflections in the beams. Also, this intense heat might change the behaviour and reduce the capacity of the beams reinforced by welding a cover plate temporarily or permanently. Currently, structural engineers select a cover plate in such a way that the reinforced beam has adequate flexural strength. While the current practice is simple, it is not clear how the welding and intense local heat of welding, affects the behaviour of reinforced beams with locked-in stresses due to service loads present during the welding process. Thus, the main objective of this study is to investigate the effect of welding heat input, welding sequences, and weld length on the residual deformation (plateau) due to welding, behaviour, and ultimate capacity of the I-beams when reinforced by welding a cover plate. To the best of the authors' knowledge, no study is currently available that considers the welding effect on the steel beams reinforced with cover plates. In this paper, detailed FE analyses are conducted to study the effect of welding on the behaviour of simply supported steel I-beams reinforced by welding a cover plate at the bottom flange. Also, the effect of initial geometric imperfection value and direction, as well as preloading level on the welding residual deformation (plateau), behaviour and capacity reduction of reinforced beams by considering welding procedures are studied.

4.3. FINITE ELEMENT ANALYSIS OF REINFORCED STEEL STEEL I-BEAMS

A 3D-finite element model of a reinforced steel I-section beam was developed using the commercial finite element software Abaqus (2020) and Qustomweld (2020), (an Abaqus-based plugin). Reinforcing was carried out by welding a cover plate to the bottom flange of the simply supported I-beam. Reinforcement was done for the I-beams while under load and a sequential nonlinear thermal-mechanical analysis was carried out. This section presents details of the developed FE model for reinforced steel I-beam.

4.3.1 Development of finite element model

This study investigates the effect of welding and heat on the behaviour of steel I-beam reinforced with a welded cover plate at the bottom flange while under load. To simulate the welding procedures, a sequentially coupled-thermal analysis was carried out for welding and considered welding sequences. A nonlinear thermal analysis as a heat transfer analysis was conducted for welding and considered welding sequences. Then, the thermal profile of the analysis was recorded as the thermal history and applied as thermal load input to the nonlinear stress analysis. There is wide use of this analysis procedure for weld simulations, such as in the studies conducted by Nguyen et al. (2019), Peric et al. (2014), and Lourenco et al. (2014). A three-dimensional FE model was developed for heat transfer and stress analysis. The numerical model used for the stress analysis consists of a base steel I-beam and reinforcing cover plate. The FE model implemented for heat-transfer analysis includes weld elements in addition to the base beam and the reinforcing plate. The same mesh size and coordinates were used for the heat transfer and stress analysis. The developed finite element model in this study was designed to have different mesh sizes: very refine near the weld location to consider the strong temperature and stress variations and rather coarser mesh size at far distances from the weld location. Mesh size across the flange and reinforcing plate width at a distance of 25 mm from the weld location was 5 mm. The typical mesh size was 10 mm along the length of the base beam and reinforcing plate. Four elements were assigned through the bottom flange thickness, and three elements through the reinforcing plate thickness, while two elements were used to discretize the web and top flange thicknesses. The size of the mesh in the remaining part of the model was based on keeping the aspect ratio of the 3D elements smaller than 3. The configuration of the mesh for the FE model included about 190000 elements and 270000 nodes for the studied beams in this paper.

In this paper, the material properties of the base beam, reinforcing steel plate, and weld elements were the same and were thermal dependent. The properties of the considered steel material for the thermal analysis are presented in Table 4.1 (extracted from Yuan-qing et al. 2015, Nguyen et al. 2019). Furthermore, thermal dependant mechanical properties of used isotropic, elastic-plastic steel are listed in Table 4.2 (Yuan-qing et al. 2015, Nguyen et al. 2019). It should be noted that Poisson's ratio was considered thermal independent with a value of 0.3 in the mechanical analysis (Yuan-qing et al. 2015).

Table 4.1: Thermal temperature-dependent property of the steel material (Yuan-qing et al. 2015, Nguyen et al. 2019)

Temperature (°C)	Density (kg/m^3)	Thermal conductivity (W/ (m K))	Specific heat (J/(kg K))
20	7900	53.3	439.8
100	7880	50.7	487.6
200	7830	47.3	529.8
300	7790	44.1	564.7
400	7750	40.7	605.9
500	7660	37.4	650
600	7560	34	650
800	7370	27.3	650
1600	7320	27.3	650

Table 4.2: Mechanical temperature-dependent property of the steel material (Yuan-qing et al. 2015, Nguyen et al. 2019)

Temperature (°C)	Yield stress (MPa) at plastic strain=0	Yield stress (MPa) at plastic strain= 0.1	Modulus of elasticity (MPa)	Thermal expansion coefficient ($1/10^5$°C)
20	345	422	205000	1.2
100	329	405	203535	-
200	308	384	202070	-
300	272	338	199204	-
400	236	291	164809	-
500	181	225	101752	-
600	126	160.5	60191	-
700	67	93	45100	-
800	63	86	30095	1.31
900	43	56	20780	-
1000	14	23	11465	-
1600	13	22	11465	1.43

4.3.2 Thermal analysis

Qustomweld, an Abaqus-based plugin (2020), was implemented to do the heat transfer analysis for the weld simulation. In the plugin, deposition welds were used to apply the prescribed temperature (called a torch) at the weld location. Deposition weld was defined as a single bead, and torch placement was based on the considered welding sequences. The prescribed temperature was defined based on the welding parameters and Goldak's double ellipsoidal heat source model (1984). Abaqus element DC3D8, an 8-node linear heat transfer brick element, was used to model the base beam, reinforcing plate, and weld elements for heat transfer analysis. The ambient temperature was considered as 20°C. Heat transfer analysis included film condition on beads with the film coefficient of 0.025 mJ/s/mm^2/c and radiation condition on beads with the emissivity coefficient of 0.9. The weld size and welding speed were considered as 10 mm and 10 mm/s, respectively. Welding and Goldak heat source parameters, as presented in earlier research by Lourenco et al. (2014), were adapted for the considered weld size. A linear interpolation was used, and it was made sure that the resultant weld temperature was higher than the steel melting temperature (1,450°C). In the developed FE model, fillet welds were used, and weld elements were thermally coupled to the base beam from one leg and to the reinforcing plate from the other leg using tie interaction. Thus, the base beam and reinforcing plate had the same value of temperature as weld elements. Cooling time after the last weld placement was assigned based on the temperature of the structure to reach the ambient temperature, approximately. Details of the developed FE model for heat transfer analysis along with the thermal profile sample for welding of reinforcing plate to the bottom flange are presented in Figure 4.1.

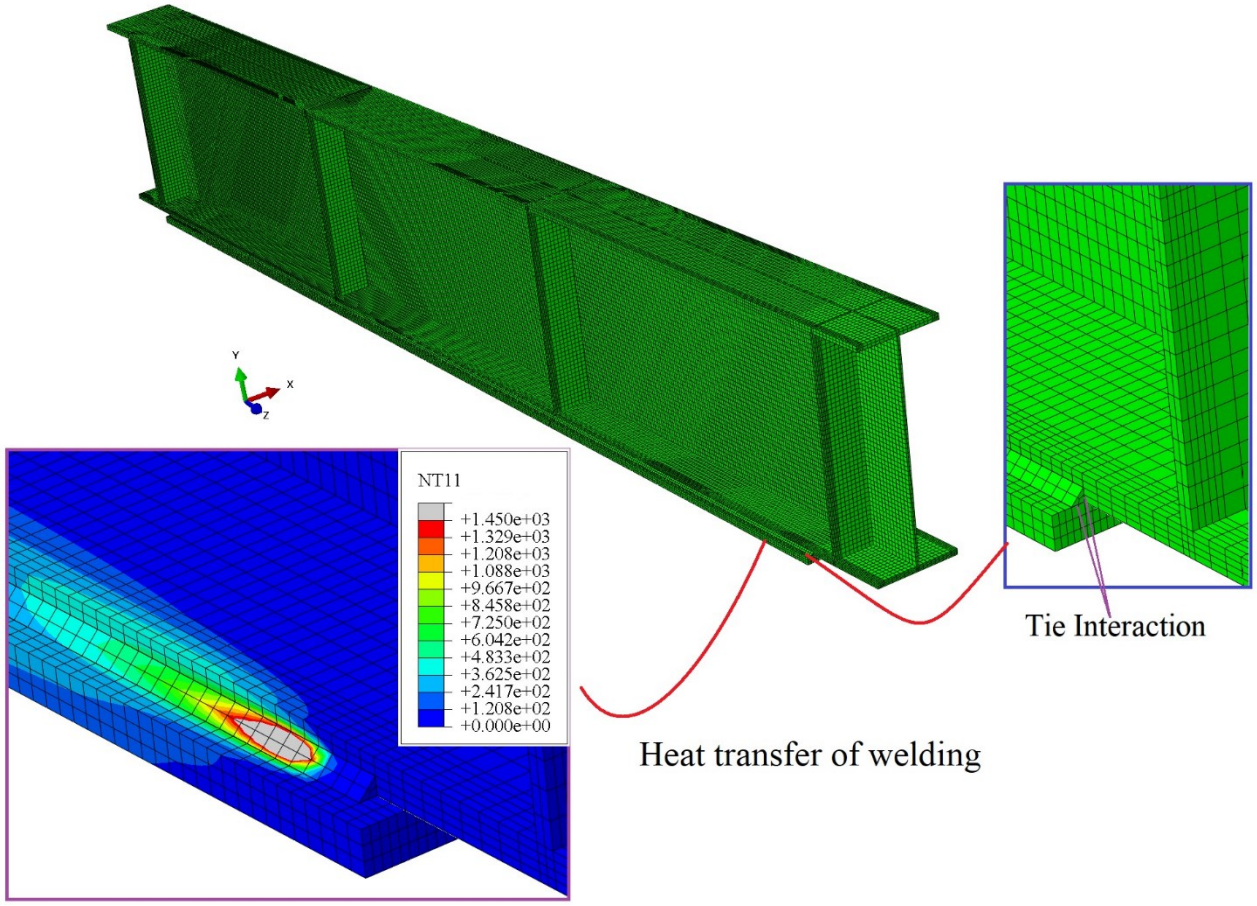

Figure 4.1: Details of the developed finite element model for thermal analysis

4.3.3 Mechanical analysis

After completing the thermal analysis, a mechanical analysis was carried out to study the effect of welding on the steel I-beams reinforced while under load. In the developed finite element model for the stress/strain analysis, weld elements that were used to apply the temperature were removed. Abaqus element C3D8, 8-node linear brick, a general-purpose element, was used to model the beam components and the reinforcing plate. In the mechanical analysis, nodes of the reinforcing plate at the weld location were constrained to have the same displacement as nodes of the bottom flange tips (weld locations) using tie interaction. Between the bottom flange and reinforcing plate, surface-to-surface contact was assigned in which penalty in the tangential direction and hard contact in the normal direction were applied. Initial residual stresses were introduced in the form of an initial stress field on the element of the base beam and reinforcing plate. These stresses were applied as uniform stress on each element in the first step of the analysis. For the base beam, Best-Fit Parel (Kim 2010) pattern; and for the reinforcing plate, an initial

residual stress pattern used by Bhowmick and Grondin (2016), were incorporated as the initial residual stresses in the finite element models.

The reinforcing plate was removed at the first stage of the analysis and activated after applying the preload level. In this paper, the numerical test specimens were analyzed under four-point loading conditions where equal point loads were applied at one-third of the base beam length. Furthermore, transverse stiffeners were used at the point load and bearing locations. The studied failures were cross-section yielding and lateral-torsional buckling. The considered steel I-beam was simply supported out-of-plane and in-plane for lateral-torsional buckling. For cross-section yielding failure mode, lateral braces were used in the load locations at the tension and compression flanges. To apply simply-supported boundary conditions, vertical and transverse displacements were restrained across the width of bearing stiffeners at the ends of the beam. Also, in one of the base beam ends, longitudinal displacement was restrained. Furthermore, at the bearing stiffener tips, transverse displacement was restrained along both sides. In this paper, the flange and web of the selected base beam are compact sections based on AISC 360-16 (2016). For the initial geometrical imperfection, flange sweep was considered. Based on the studies conducted by Subramanian and White (2017), using one-half of the American Welding Society (2020) limitation/tolerance as initial geometrical imperfection in FE modeling results in more accurate numerical capacity prediction when compared with the experimental results. Therefore, a value of $L_b/2000$ (L_b is the unbraced length) was taken as the geometrical imperfection induced from the erection and fabrication of the base beam and was applied in the initial loading step at the mid-point of the unbraced length at the compression flange. Initially, the base beam was analyzed to obtain the ultimate capacity, preloading values, and equilibrium path of the unreinforced beam by applying initial residual stresses and imperfection and conducting a nonlinear modified Risk method. Mechanical analysis for the reinforced steel beams is more complicated and the following steps were considered for the analysis:

1. Both geometrical imperfection and initial residual stresses of the base beam and reinforcing plate were applied. Besides, elements of the reinforcing plate were deactivated.
2. The considered preloading level was applied for the beams reinforced by welding a steel cover plate at the bottom flange. In this study, three preloading levels, 0%, 25%, and 50%, of base beam strength, were utilized.
3. Reinforcing plate elements were reactivated. By reactivation of the reinforcing plate, initial residual stresses of the plate defined at the first step were applied. Also, surface-to-surface contact between the reinforcing plate and bottom flange was introduced.

4. Recorded thermal history obtained from the heat transfer analysis was applied as the welding procedure to the mechanical analysis. Thermal analysis was based on the considered welding sequence and subsequent cooling.
5. In the final step, loading increased in the reinforced beam to obtain the equilibrium path and ultimate capacity of the reinforced beam.

For all steps except step number 6, nonlinear static stress analysis was conducted. For loading step 6, the modified Risk method was used. Details of the developed FE model for the mechanical analysis of the reinforced steel I-beam are presented in Figure 4.2.

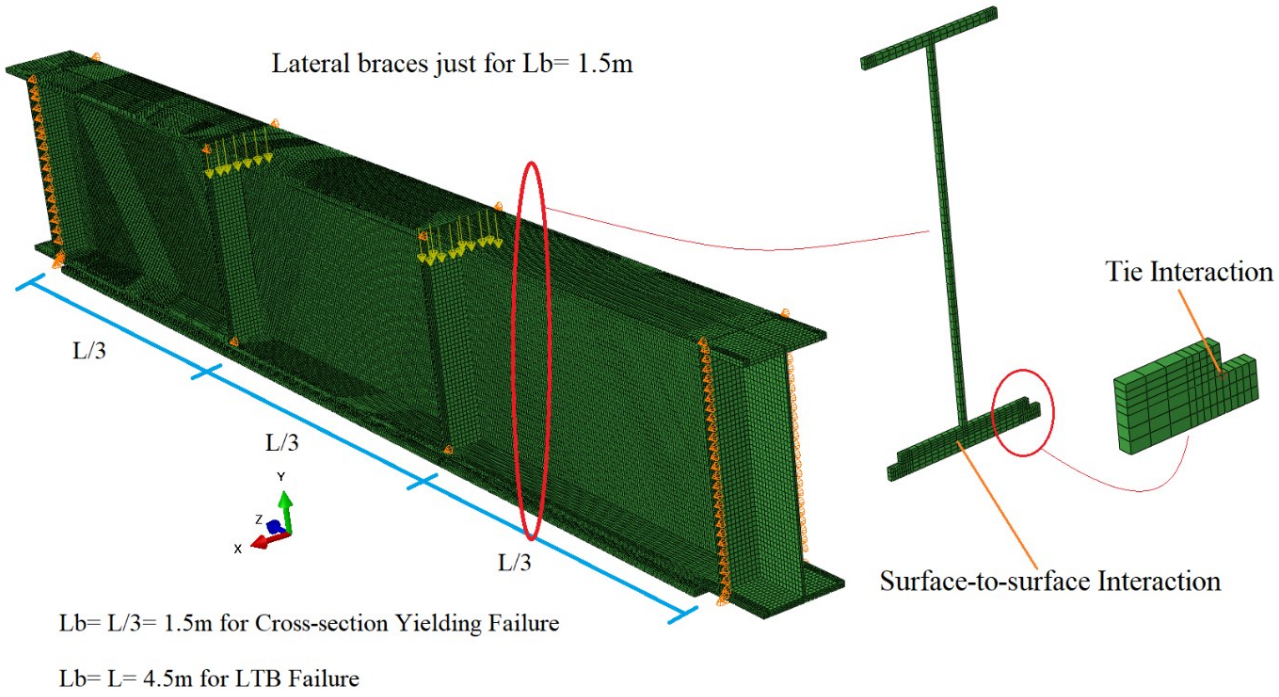

Figure 4.2: Details of the developed FE model for the mechanical analysis of the reinforced steel I-beam

4.3.4 Validation of finite element model

Yuan-qing et al. (2015) carried out a 3-point bending experimental test on simply supported beams reinforced by adding a cover plate at the tension and compression flanges through welding. The cross-section of the beam was a build-up I-section with a nominal; flange size of 160×8 mm ($b_f \times t_f$) and web size 400×8 mm ($D \times t_w$) with a total length of 3200 mm and unbraced length of 3000 mm. Also,

the nominal reinforcing plate dimension was PL 2720×130×6 mm. Three different reinforced beams with the preload level of 0%, 37%, and 74% of the base beam capacity were studied. These beams were named BI-S1, BI-S2, and BI-S3, respectively. The yield stress, Fy, for the component of the steel I-beam and cover plates was 380.1 MPa and 398.5 MPa, respectively. Initial geometrical imperfection and welding sequences were reported in their experimental research. However, initial residual stresses for the base beam and reinforcing plate, accurate temperature-dependent properties of the used steel material and input heat properties were not reported in the experimental work. Yuan-qing et al. (2015) also developed a FE model using shell elements for the base beam, reinforcing plate, and weld elements, and tried to model welding procedures by doing thermal and mechanical analysis. In this paper, overall simulating procedures were verified using the test specimen BI-S2 with preload magnitude of 120 kN. It should be noted that in the FE modeling for specimen BI-S2, experimentally measured values for the initial geometrical imperfection were implemented. Furthermore, the Goldak heat source was implemented as the heat function for the welding of 4 mm of weld size. Welding speed was assumed to be constant during welding and calculated as an average speed, based on the welding length and welding time extracted from Yuan-qing et al. (2015). Figure 4.3 compares the load-vertical deflection of the current FE modeling procedure with the experimental and finite element results of Yuan-qing et al. (2015). It can be observed that the current FE model can reasonably predict the ultimate capacity, plateau deflection induced from welding, and overall behaviour of reinforced beams while under load. Moreover, as observed during the tests, the failure mode of the current FE model was lateral torsion buckling.

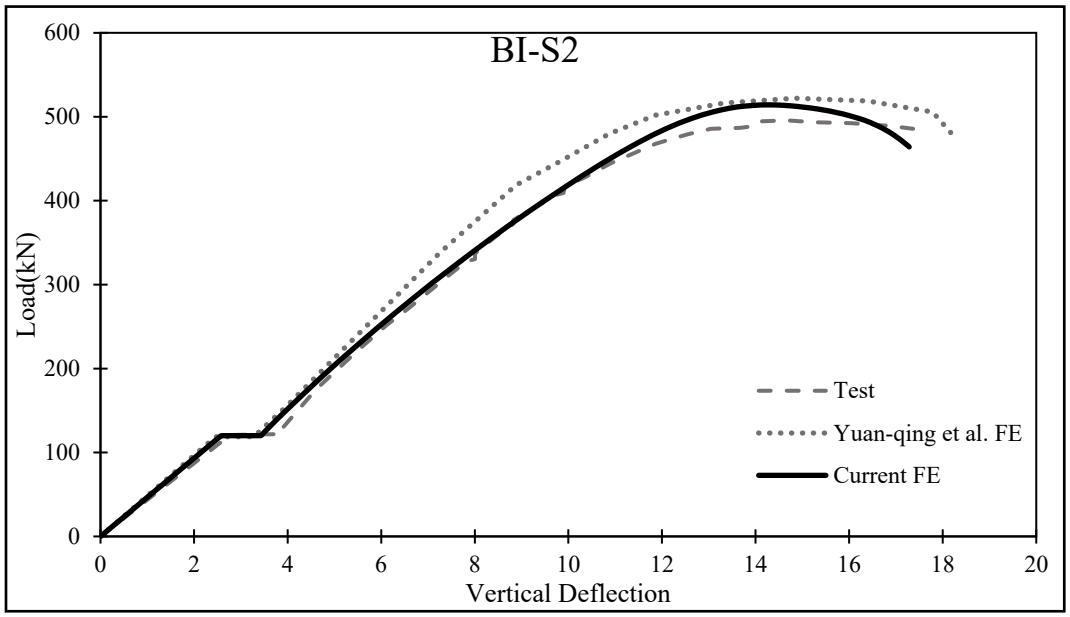

Figure 4.3: Load-vertical deflection of FE model for BI-S2 specimen tested by Yuan-qing et al. (2015)

4.4. PARAMETRIC STUDIES

A parametric study was conducted to investigate the effects of important parameters such as welding sequence, heat and deformation induced from welding, preload levels, and initial imperfection on the behaviour and strength of the simply supported steel I-beam reinforced by welding a cover plate at the bottom flange while under load. For the parametric study, welding procedures were simulated by doing thermal and mechanical analysis. Parametric studies were conducted on a doubly symmetric built-up steel I-section with a flange size of 300 mm×25 mm ($b_f \times t_f$) and web size of 760 mm×11mm ($D \times t_w$). Based on AISC 360-16 (2016) and AASHTO (2020) unreinforced cross-section has compact flanges and web. A steel plate with a size of 350 mm×25 mm ($w_{cp} \times t_{cp}$) was considered as the reinforcing plate in this research. For welding the reinforcing plate to the bottom flange of the beam, three different welding sequences were considered. Also, the parametric studies were carried out on the beams with two unbraced lengths with expected failures of cross-section and lateral-torsional buckling failure modes. Unbraced length of the beam for LTB was 4.5 m, while the unbraced length was 1.5 m for the cross-section yielding.

4.4.1 Effect of welding sequence

To test the effect of welding sequence on the behaviour of the steel I-beams reinforced while under load, three different welding sequences were considered in this study and presented in Figure 4.4. In sequence 1, welding started from one side and continued to reach the end of the reinforcing plate at the same side parallel to the longitudinal direction. Welding was done by side changing and continued to the end of the reinforcing plate. Finally, the reinforced beam cooled gradually with the assigned cooling time (Figure 4.4-1). In sequence 2, the welding operation started from one longitudinal edge, continued with the shown length (almost L/6), and then welding went on from the other longitudinal edge (parallel edge) of the cover plate, and this procedure continued till the end of welding. Welding sequence 2 is the recommended welding sequence in the literature and it is believed that residual stress of this welding sequence is favorable for the structures reinforced while under load (Liu and Gannon 2009, Marzouk and Mohan 1990) (Figure 4.4-2). In sequence 3, welding started from one longitudinal edge and then went on from the parallel edge with the same welding length similar to the welding sequence 2. The other step of welding continued from the opposite end of the beam and this order was kept on reaching the middle length of the beam, as shown in Figure 4.4-3. Moment-compression flange lateral and vertical deflections at the mid-span of the beams for the considered welding sequences are depicted in Figure 4.5. While studying the effect of welding sequence, the considered preload level was 50% of the unreinforced beam

capacity, and initial imperfection (flange sweep) of $L_b/2000$, and the failure mode was lateral-torsional buckling with the unbraced length of 4.5 m. Based on the results shown in Figure 4.5, the behaviour of the beams reinforced by different welding sequences is similar. Also, the deformation induced by the welding of the reinforcing plate to the bottom flange of the base beams was similar to the plateau observed in the experimental results in the lateral and vertical directions. Table 4.3 compares the ultimate capacities of reinforced beams along with the values of deformations induced from welding (plateau values) in the vertical and lateral direction for the studied welding sequences. Based on Table 4.3, maximum capacity is obtained for welding sequence 1 with the value of 1614.3 kN·m, and the least capacity is obtained for welding sequence 2 with the value of 1606.87 kN·m. However, the difference in capacity in the considered welding sequences is very negligible. Maximum lateral deflection induced from welding is for welding sequence 1 with the value of 0.27 mm and it is in the favorable direction, which reduces the lateral deflection, and it can be the reason for having the maximum capacity for this welding sequence. The least lateral deflection is for welding sequence 2 with the value of 0.019 mm. Although welding sequence 1 has the maximum bending moment capacity and the welding lateral deformation is in the favorable direction, in practice, it is not a desirable welding sequence, as it will be shown later that the lateral deformation can be in the favorable/unfavorable direction depending on the direction of the initial geometrical imperfection. A welding sequence that provides the least weld deformation (welding sequence 2) is desirable and reliable. This issue is discussed in detail in section 5.4.2, and it is shown that the direction of the initial geometrical imperfection can change the welding residual deformation in the lateral direction for the beam with welding sequence 1. In addition, for the reinforced beams under studied welding sequences, the vertical deflection induced from welding is almost equal and in the downward direction. Therefore, the welding sequence does not have a significant effect on the welding vertical residual deformation for steel I-beams reinforced while under load.

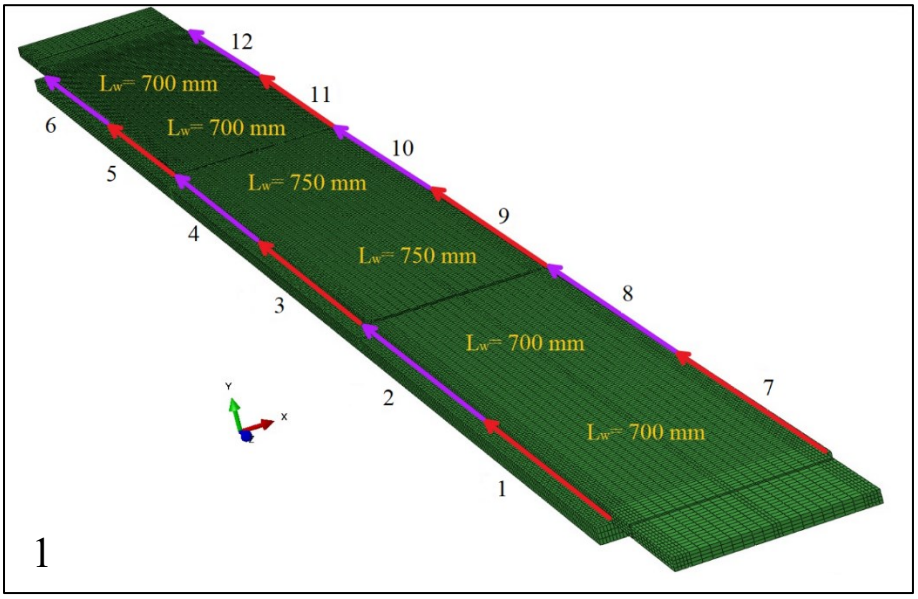
12
11
10
9
8
7
6
5
4
3
2
1
Lw= 700 mm
Lw= 700 mm
Lw= 750 mm
Lw= 750 mm
Lw= 700 mm
Lw= 700 mm
Y
X
1

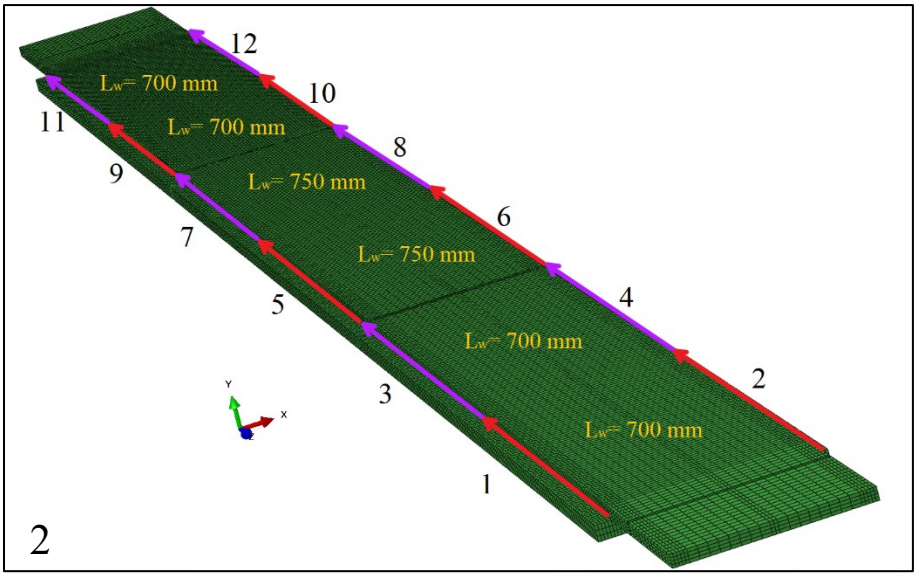
12
11
10
9
8
7
6
5
4
3
2
1
Lw= 700 mm
Lw= 700 mm
Lw= 750 mm
Lw= 750 mm
Lw= 700 mm
Lw= 700 mm
Y
X
2

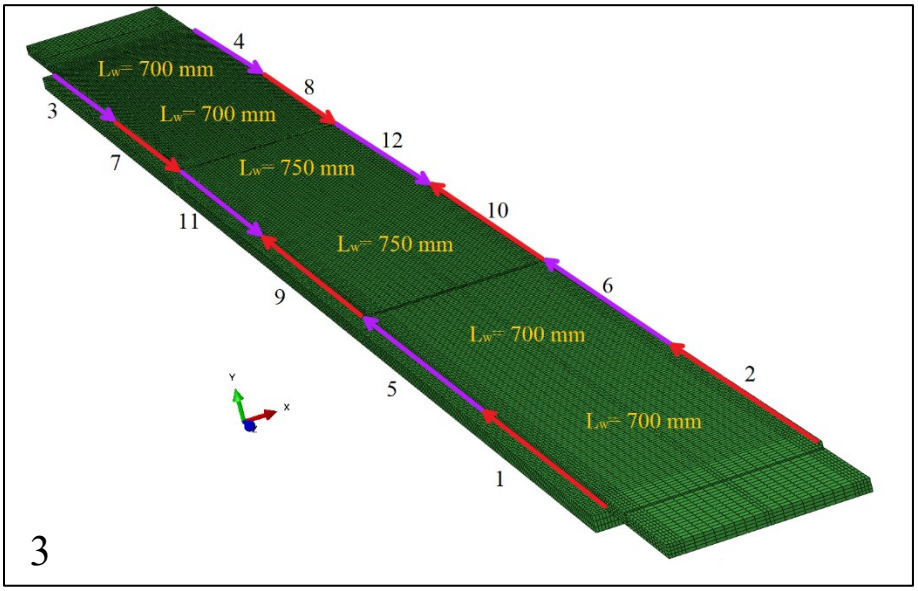

Figure 4.4: Sequences for welding the reinforcing plate to the bottom flange of steel I-beam

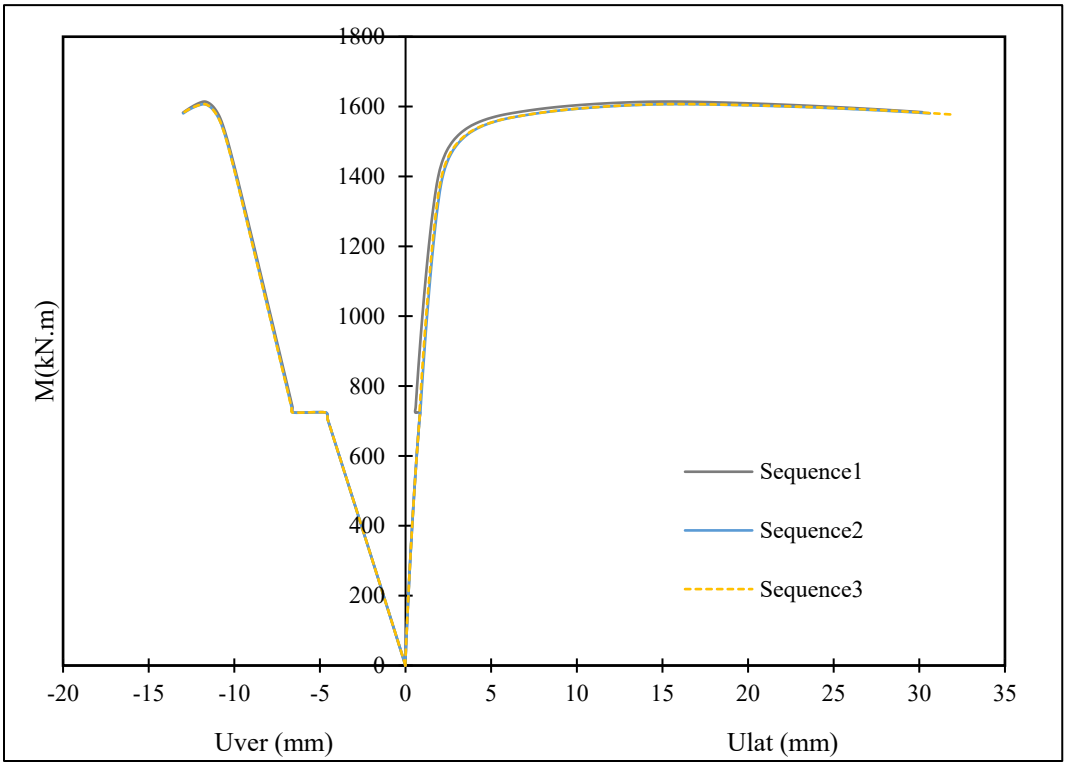

Figure 4.5: Moment- compression flange lateral and vertical deflections at the mid-span of the beams for the considered welding sequences

Table 4.3: Comparison of the ultimate capacity and welding deformations of the reinforced beams under 50% of preloading level for different welding sequences

Welding Sequence	Ultimate capacity (kN·m)	Weld deformation (plateau) (mm)	
		Lateral	Vertical
Sequence 1	1614.30	0.27	1.85
Sequence 2	1606.87	0.019	1.91
Sequence 3	1607.10	0.031	1.92

4.4.2 Effect of initial imperfection

To study the effect of initial imperfection on the magnitude and direction of the welding residual deformation (plateau in the load-deformation diagrams) in the beams reinforced by welding a cover plate at the bottom flange, the reinforced beams with welding sequences 1 and 2 under preload level of 50% of the base beam strength and with an unbraced length of 4.5 m were considered. For the beam reinforced by welding a cover plate with welding sequences 1 and 2, the base beam was considered to have four different initial geometrical imperfections with the values $\pm L_b/2000$ and $\pm L_b/1000$ with respect to the positive X direction shown in Figure 4.2. Moment-top flange lateral and vertical deflections at the mid-span of the beams for the welding sequence 1 and 2 with the considered geometrical imperfections are depicted in Figure 4.6. It should be mentioned that lateral deformations in these diagrams are absolute values without considering their directions (i.e., absolute values regardless of positive or negative X-direction). Furthermore, Table 4.4 presents the ultimate capacities and values of lateral and vertical deformations induced by welding of the reinforcing plates, while the I-beam is under load, for different geometrical imperfections and welding sequences. Comparing the diagrams of Figure 4.6 and the welding lateral deformations of Table 4.4 for welding sequences 1 and 2 show that the direction and magnitude of the welding lateral deformation are sensitive to the welding sequence and the value/direction of initial geometric imperfection. For example, the welding-induced lateral deformation

values are favorable (reduce lateral deformation of preloading) when the initial imperfections are in the positive direction (in the positive X-direction as shown in Figure 4.2) while they are unfavorable (increasing lateral deformation of preloading) for the opposite direction of the initial imperfection for welding sequence 1. However, the direction of the welding lateral deformation is insensitive to the initial imperfection direction/magnitude for welding sequence 2. As seen in Table 4.4, for welding sequence 2, welding lateral deformation is in the unfavorable direction for both positive and negative imperfection directions. In addition, by comparing the residual lateral deformation induced by welding for the considered welding sequences, it can be observed that the value and the variation of the lateral deformations are greater for welding sequence 1. For instance, the maximum lateral deformation in the favorable direction is 0.27 mm for an initial imperfection of $+L_b/2000$, whereas in the unfavorable direction it reaches 0.56 mm for an initial imperfection of $-L_b/1000$. For welding sequence 2, residual lateral deformations are in the unfavorable direction, but they are small and have less variation. By comparing the ultimate capacities in Table 4.4, it can be observed that the ultimate capacity of the reinforced beam varies significantly for welding sequence 1 than that for welding sequence 2 for the same value of initial imperfection but in different directions. For instance, the ultimate capacity of the reinforced beam with the initial imperfection of $+L_b/2000$ is 1614.3 kN·m, whereas the ultimate capacity decreases to 1591.57 kN·m with the imperfection value of $-L_b/2000$. The difference in the capacity between the two imperfections is 22.73 kN.m when welding sequence 1 was used. This difference for welding sequence 2 with the same initial imperfection values is 12.06 kN·m, which is smaller than the difference for welding sequence 1. Therefore, it can be concluded that from a practical point of view, welding sequence 2 is preferable because of small lateral residual deformations, low variation in the ultimate capacity of the beam, and independence with respect to the direction and value of initial geometrical imperfection.

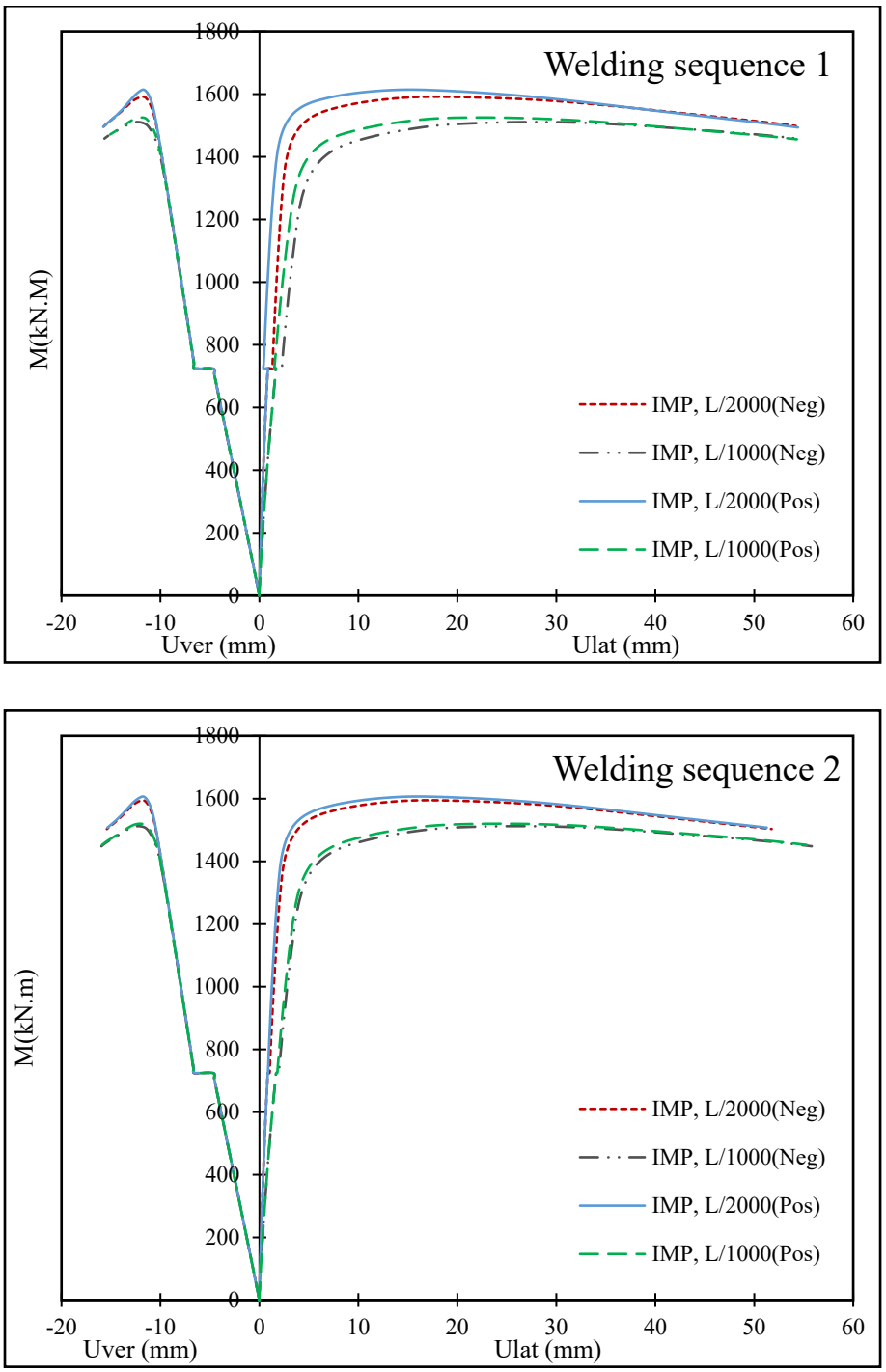

Figure 4.6: Moment- compression flange lateral and vertical deflections at the mid-span of the reinforced beams under 50% of preloading for the welding sequences 1&2 with different initial geometrical imperfections

Table 4.4: Comparison of the ultimate capacity and welding deformations of the reinforced beams under 50% of preloading level for different initial geometrical imperfections and welding sequences.

Welding Sequence	IMP	Ultimate capacity (kN.m)	Weld deformation (plateau) (mm)	
			Lateral (Favorable/Unfavorable)	Vertical
Sequence 1	L/2000 (Pos)	1614.30	0.27 (Favorable)	1.85
Sequence 1	L/2000 (Neg)	1591.57	0.47 (Unfavorable)	1.85
Sequence 1	L/1000 (Pos)	1525.27	0.17 (Favorable)	1.85
Sequence 1	L/1000 (Neg)	1510.89	0.56 (Unfavorable)	1.85
Sequence 2	L/2000 (Pos)	1606.87	0.019 (Unfavorable)	1.91
Sequence 2	L/2000 (Neg)	1594.81	0.178 (Unfavorable)	1.91
Sequence 2	L/1000 (Pos)	1519.92	0.117 (Unfavorable)	1.91
Sequence 2	L/1000 (Neg)	1512.21	0.275 (Unfavorable)	1.90

4.4.3 Effect of preload magnitude

To study the effect of preloading on the behaviour of the reinforced steel I-beams and the direction and magnitude of the welding residual deformations (plateau in load-deformation diagrams), beams with an unbraced length of 4.5 m and 1.5m were considered. As it was noted, the expected failure of the beam with 4.5 m unbraced length was nonlinear lateral-torsional buckling while cross-section yielding failure was the expected failure mode for the beam with 1.5 m unbraced length. To study the preloading effect, three different preloading levels, 0% (CP-NPL), 25% (CP-25%Preload), and 50% (CP-50%Preload) of the unreinforced beam capacity, were considered. To weld the reinforcing plate to the bottom flange of the base beam, welding sequence 2 was used. Moment-lateral and vertical deflections for the beams with the unbraced length of 1.5 m and 4.5 m are depicted in Figure 4.7 for the studied preloading levels. In Figure 4.7, in addition to the beams reinforced while under load, moment-deflection diagrams for the base beams are also presented and identified (NCP). Based on the diagrams in Figure 4.7, reinforcement increases the ultimate load and stiffness of the reinforced steel I-beams while under load. Using welding sequence 2, the difference in lateral residual deformation induced by welding the reinforcing plate to the bottom flange under different preload levels is negligible and moment-lateral deformation relations for the reinforced beams under different preload levels are very similar. There is a uniform vertical deformation, which can be seen in the moment-vertical deformation plots in Figure 4.7, during the welding of the reinforcing plate. However, the overall behaviour and ultimate capacities of the I-beams reinforced by welding a cover plate at the bottom flange are similar and preloading has an insignificant effect on the ultimate capacities of the reinforced beams. Table 4.5 presents the ultimate capacities of unreinforced and reinforced beams along with the welding residual lateral and vertical deformations for the reinforced beams under different preloading levels. As observed in Table 4.5, only the vertical deformation is sensitive to the preloading level. The vertical welding residual deformation of the reinforced beam with an unbraced length of 1.5 m and preload level of 25% is 0.98 mm, whereas it is 2.05 mm for the reinforced beam with the same unbraced length but with a 50% preload level. For the reinforced beam with an unbraced length of 4.5m, the vertical deformation for a preload level of 25% of the strength of the base beam is 1.26 mm. This deformation is 1.91 mm for the preload level of 50% of the strength of the base beam. Therefore, vertical deformation (plateau) induced from welding of a cover plate to the bottom flange of a simply supported I-beam increases with an increase in the preload level.

Table 4.5: Comparison of the ultimate capacity and welding deformations of the reinforced beams for different preloading levels.

Base beam Unbraced Length	Preload level	Ultimate capacity (kN·m)		Weld deformation (plateau) (mm)	
		Unreinforced	Reinforced	Lateral	Vertical
1.5 m (cross-section yielding failure)	0%	2142.95	2445.93	0	0
	25%	2142.95	2446.75	0	0.98
	50%	2142.95	2447.60	0	2.05
4.5 m with LTB (failure)	0%	1426.71	1613.67	0	0
	25%	1426.71	1610.3	0.04	1.26
	50%	1426.71	1606.87	0.019	1.91

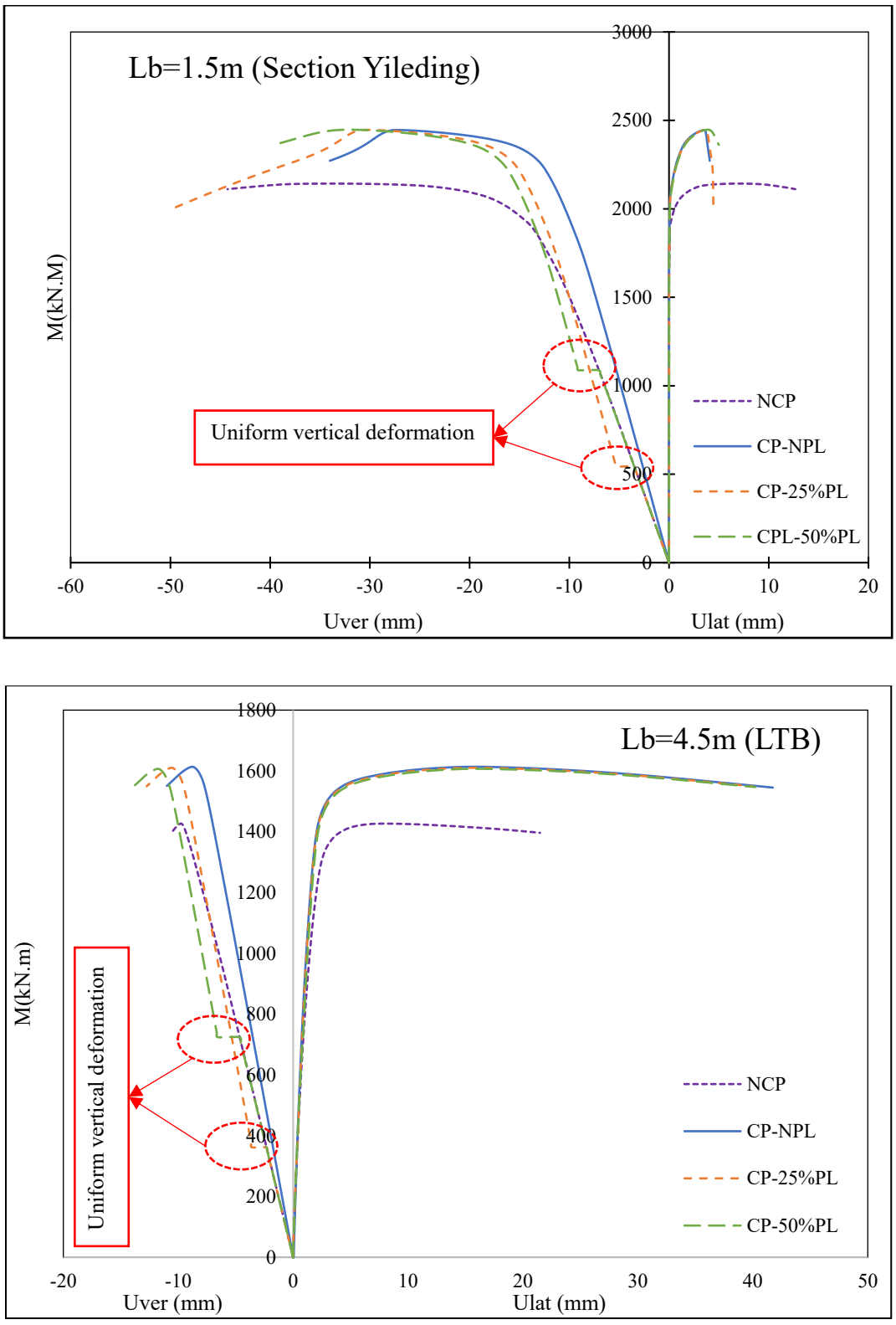

Figure 4.7: Moment- lateral and vertical deflections for reinforced beams under different preloading levels with cross-section and LTB failures

4.4.4 Effect of weld length

Four different divisions of weld partitions were considered to study the effect of welding length on the magnitude of the welding residual deformations (plateau) and behaviour of the steel I-beams reinforced while under load. The studied welding partitions were based on welding sequence 2 of this paper and are shown in Figure 4.8. There are 3, 6, 9 and 15 segments for the welding of reinforcing plate to the bottom flange of the beam in the longitudinal direction for each side, respectively. The selected weld segments' lengths are shown in Figure 4.8 (welding segments' lengths are about L/3, L/6, L/9, and L/15). While studying the effect of welding length, the initial geometrical imperfection was considered as $-L_b/2000$ with respect to the positive X direction. The objective of selecting the initial imperfection in the opposite direction with respect to the positive X ($-L_b/2000$) was because this initial imperfection produced higher welding residual deformation in the lateral direction in comparison to the welding residual deformation obtained for an initial imperfection of $+L_b/2000$ (as presented in Table 4.4). Therefore, to investigate the effectiveness of the reduced weld length in controlling the welding residual deformation, an initial imperfection of $-L_b/2000$ was considered.

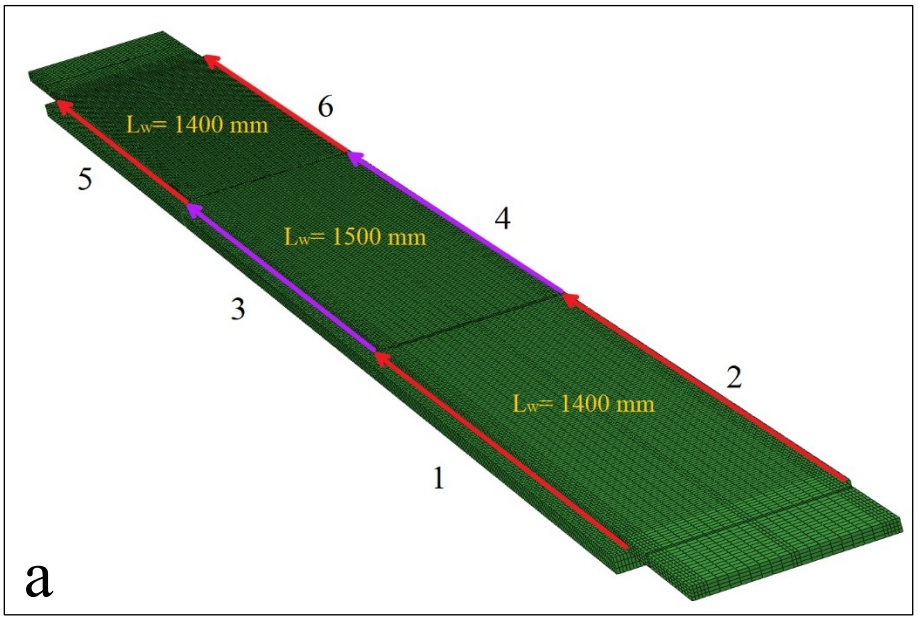

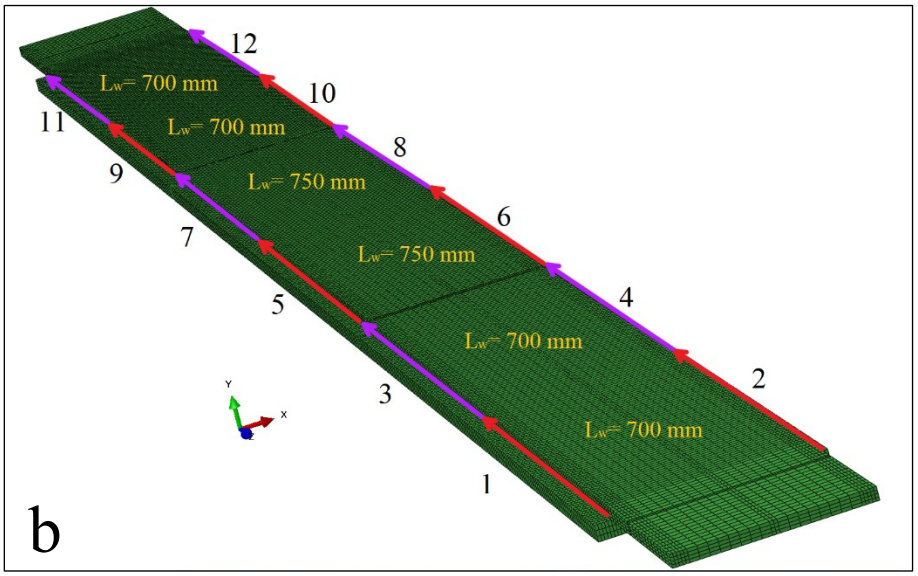
12
10
11
8
9
6
7
4
5
2
3
1
Lw= 700 mm
Lw= 700 mm
Lw= 750 mm
Lw= 750 mm
Lw= 700 mm
Lw= 700 mm
b

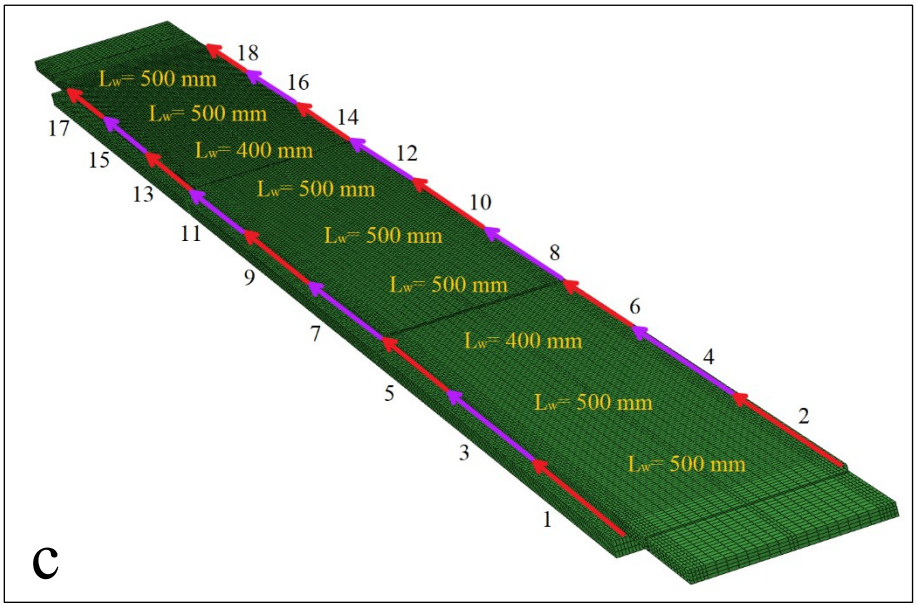
18
16
17
14
15
12
13
10
11
8
9
6
7
4
5
2
3
1
Lw= 500 mm
Lw= 500 mm
Lw= 400 mm
Lw= 500 mm
Lw= 500 mm
Lw= 500 mm
Lw= 400 mm
Lw= 500 mm
Lw= 500 mm
c

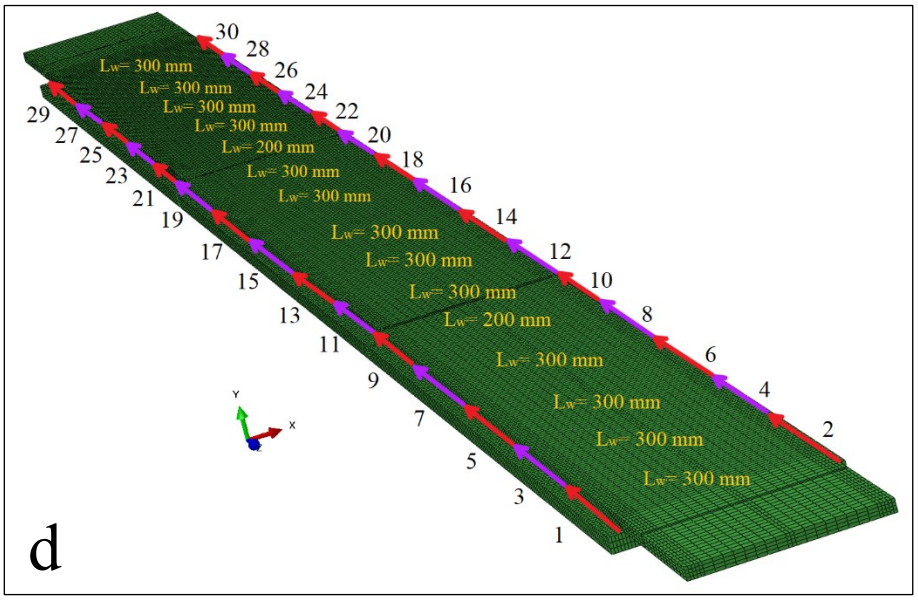

Figure 4.8: Welding partitions for adding the reinforcing plate to the bottom flange of the steel I-beam

Based on the results, it was observed that using shorter welding segments can reduce the welding residual deformation in the lateral direction for the welding sequence 2. However, vertical residual deformation induced by the welding is not sensitive to the welding segment length for welding sequence 2. Also, the ultimate capacity of the reinforced beam increased when the welding segment length was reduced. Figure 4.9 shows the moment-top flange lateral and vertical deflections at the mid-span of the reinforced beams under 50% of preloading for welding sequence 2 with different studied welding segment lengths. Furthermore, Table 4.6 compares the ultimate capacity and welding deformations of the reinforced beams under 50% of the preloading level for the welding lengths. As observed from Table 4.6, lateral welding residual deformation (plateau) was 0.184 mm for weld segment lengths of L/3, and it was reduced to 0.068 mm for the weld segments of L/15. Moreover, the moment capacity of the reinforced beam increased from 1588.71 kN·m to 1601.12 kN·m when the weld segment length was reduced from L/3 to L/15. Table 4.6 also shows that the difference in moment capacity between weld segments L/9 and L/15 is very small and as a practical welding segment length, a length of L/9 can be used. The capacity for the welding segment length of L/9 is 1598.66 kN·m.

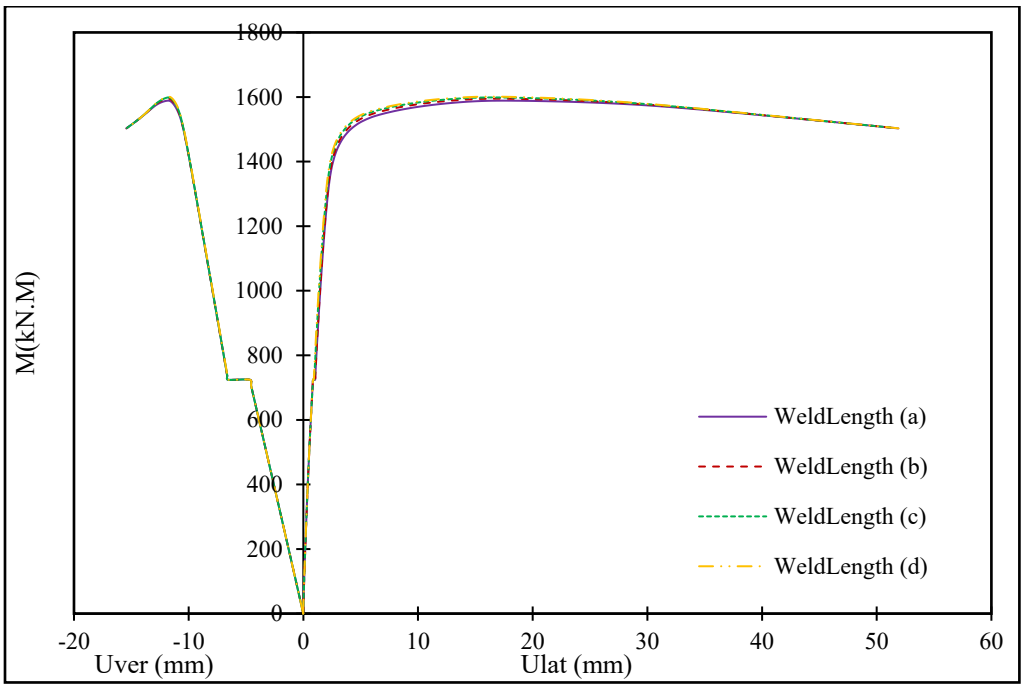

Figure 4.9: Moment- compression flange lateral and vertical deflections at the mid-span of the reinforced beams under 50% of preloading for sequence 2 with different welding lengths

Table 4.6: Comparison of the ultimate capacity and welding deformations of the reinforced beams under 50% of preloading level with different welding segment lengths

Weld Segment length	Ultimate capacity (kN·m)	Weld deformation (plateau) (mm)	
		Lateral	Vertical
a	1588.71	0.184	-1.9
b	1594.81	0.178	-1.9
c	1598.66	0.102	-1.9
d	1601.12	0.068	-1.88

4.5. Conclusions

A finite element study was carried out to investigate the effects of local but intense welding heat, welding sequence, and welding length on the behaviour of reinforced steel I-beams by welding procedure simulation. Also, the effects of initial geometrical imperfection and preloading were studied numerically on the welding residual deformation and behaviour of the reinforced beams while under load by welding a cover plate to the bottom flange of the I-beam. The following conclusions were obtained from this paper:

- There was deformation induced due to the welding of reinforcing plate to the bottom flange of the base beams similar to the plateau observed in the experimental results in the lateral and vertical directions. The value and direction of residual out-of-plane deformation were dependent on the welding sequence. However, in-plane welding residual deformation was equal for all considered welding sequences. Also, it was shown that the conventional welding sequence recommended in the literature had the least welding residual deformation in the lateral direction. Therefore, using this welding sequence will lead to a reliable behaviour of the reinforced steel beam mainly for the beams which might have lateral-torsional buckling failure.
- For a specific welding sequence, the direction and value of welding lateral deformation changed for different initial geometric imperfection values and directions of the reinforced steel beams. However, welding-induced vertical deformation was not sensitive to the initial geometric imperfection. Also, the conventionally recommended welding sequence (welding sequence 2 in this study) was a preferable welding sequence for the reinforced steel I-beams because of the small variation of lateral residual deformations, low variation in the capacities, and independence to the direction and value of initial geometric imperfections.
- Reinforcing a preloaded beam by welding a cover plate at the bottom flange increased the ultimate capacity and stiffness of the beams. Also, for the recommended welding sequence (welding sequence 2 of this paper), lateral residual deformations due to welding of the reinforcing plate were similar for the I-beams with different preload levels. On the other hand, a difference in the vertical deformation was observed for welding the reinforcing plate at different preload levels. Nevertheless, the overall behaviour and ultimate capacities of the beams reinforced by welding a cover plate at the bottom flanges were similar. Also, for the beams with cross-section yielding and lateral-torsional buckling failure mode, preloading did not have any significant effect on the ultimate capacity of the I-beams reinforced at a preload level up to 50% of the strength of the

unreinforced beam. In addition, vertical deformation (plateau) induced from welding of a cover plate to the bottom flange of a simply supported beam increased with an increase in the preload level for the reinforced beams.

- Shorter welding segments reduced the welding residual deformation in the lateral direction for the recommended welding sequence (welding sequence 2 of this paper). However, vertical residual deformation induced by the welding was not sensitive to the welding segment length for the recommended welding sequence. Also, the ultimate capacity of the reinforced beam increased by reducing the weld segments. However, it was observed that the difference in ultimate moment capacity between weld segment L/9 and L/15 (where L is the length of the I-beam) was very small, and for practical applications, a welding segment length of L/9 can be used.

5. REINFORCING OF STEEL I-BEAMS WITH WELDED COVER PLATES IN THE NEGATIVE BENDING MOMENT REGION

5.1. ABSTRACT

Steel I-beam bridges often require rehabilitation or strengthening due to changes in loading requirements or to increase the design life of the bridges. Steel I-beams are reinforced after they have been placed in service and are loaded with dead loads and partial live loads. As the bottom flange of the I-beam is accessible most of the time, an economical option is to weld a steel cover plate to the bottom flange of the existing beam. In continuous span beams, a challenging issue is to reinforce the preloaded steel beams when they are subjected to negative moments. This paper presents a numerical study on preloaded steel I-beams reinforced with steel cover plates welded at the compression flanges of the beams. The details of the development of the FE model are presented and with the developed FE model, a series of steel I-beams are analyzed to study the behaviour of I-beams strengthened by welding a cover plate at the compression flange. Three-point loading condition was considered to simulate continuous span bridges. FE analyses show that adding a cover plate to each span of the beam can increase the ultimate capacity and stiffness of the beam. Also, the reinforcement can prevent the beam from lateral torsional buckling failure mode and the beam can reach its capacity. Furthermore, the preloading level has an insignificant effect on the behaviour and ultimate capacity of the reinforced beam. The maximum difference of the capacity for the considered cross-sections is less than 3% up to a preload level of 60% of the base beam capacity.

5.2. INTRODUCTION

A large number of steel girder bridges in North America are in urgent need of strengthening. Strengthening of steel bridges is needed to address many issues such as inappropriate design, defective constructions, structure aging, additional bearing requirements, material deterioration or accidental damage. Replacing the steel beams can be more expensive, time-consuming, and often requires a long-time traffic closure for vital bridges. To avoid deconstruction and replacement, steel beams can be reinforced and strengthened. On the other hand, beams that require strengthening often are in service, and complete relieving of their loads is not either possible or not economical. Thus, steel beams may need to be reinforced while under load.

Reinforcing a steel beam is done to increase the strength and stiffness of the reinforced beam or to change the failure mode and structural behaviour of the beam. One of the practical and economical options for reinforcing is welding a cover plate to the bottom flange because of the accessibility of the bottom flange of the steel I-beam. Current practice is to ignore the effect of preload and select a cover plate to resist the additional moment that is applied in the beam. It is possible that the locked-in stresses due to service loads present during the reinforcement, adversely affect the behaviour of the reinforced beam.

Very limited studies have been conducted on the behaviour of steel I-beams reinforced while they are under load. Liu and Gannon (2009) conducted experimental studies to investigate the behaviour of the steel I-beams reinforced while under preload. The steel I-sections were reinforced using welded cover plates. Two reinforcing patterns, a plate welded to the bottom flange only (pattern A) and two plates parallel to the web and welded with the flange tips (pattern B), were considered. The selected specimens were tested for different preload levels. It was observed that an increase in the preload level resulted in a decrease in the lateral-torsional buckling capacity of beams reinforced with pattern A reinforcement than the specimen reinforced with no preload. It was also reported that preload level did not have any significant effect on the ultimate strength of beams with flexural yielding failure mode. Yuan-qing et al. (2015) conducted an experimental investigation on steel I-beams reinforced while under load. The I-beams were reinforced by welding cover plates to both top and bottom flanges. Three reinforced I-beams with a preload level of 0%, 37%, and 74% of the unreinforced beam capacity were tested. It was observed that the beam with the 37% preload level failed in lateral-torsional buckling. In addition, the ultimate strength was reduced in comparison to the capacity of the beam when reinforced without any preload. However, for the beam reinforced at 74% preload level, the ultimate capacity increased and the failure mode for this beam was flange local buckling. Thus, no concrete and conclusive relationship was obtained between the preload level and the capacity of the reinforced beam from the study of Yuan-qing et al. (2015). Mohammadzadeh and Bhowmick (2022) conducted a numerical study to investigate the effects of preload level, initial and welding residual stresses, and steel grade on the behaviour of simply supported steel I-beams reinforced with a cover plate to the bottom flange. It was observed that preloading did not have a significant effect on the behaviour and ultimate capacity of beams with flexural yielding failure mode (Mohammadzadeh and Bhowmick 2022). However, preloading had some effect on the behaviour of beams with linear and nonlinear LTB failure modes. Also, it was stated that for the nonlinear LTB, the buckling and ultimate capacities decreased when the preload magnitude was increased. The reduction in ultimate capacity was smaller than 5% for a preload of up to 60% of the

strength of the unreinforced beam. Also, it was observed that initial and welding residual stresses did not affect the capacity and behaviour of I-beams reinforced while under load.

In continuous steel beams, a challenging issue is to reinforce steel beams subjected to negative moments while they are under preloading. In the positive moment region in composite steel bridges, because the concrete slab provides a large compression area and lateral restraining to the flange subjected to compression force, lateral-torsional buckling failure of the compression flange and local buckling of the flange and web are not common and the beam can reach to its plastic moment capacity. In the negative moment region in composite steel bridges, usually, it is assumed that the concrete slab does not carry any tension stress. Besides, lateral restraint of the compression flange is provided just by cross-frames. Therefore, the beam is susceptible to lateral-torsional buckling failure mode while subjected to a negative bending moment. If the lateral-torsional buckling failure is prevented, the pier section can reach its plastic capacity, which would allow the formation of the second hinge at the midspan, and this could increase the load-carrying capacity of the beam significantly. The main objective of this study is to investigate the behaviour of steel I-beams that are reinforced by welding cover plates to the compression flanges while the beams are under load. A numerical study is carried out to see whether adding a cover plate to the spans adjacent to piers can prevent the lateral-torsional buckling failure mode or not. To accomplish this objective, three-point loading numerical test specimens were considered to simulate the continuous-span beams and a numerical parametric study was conducted. Reinforcement was carried out for different cross-sections with different unbraced lengths and under different preload levels. In addition, the effects of two important parameters, (1) use of higher steel grade for reinforcing plate (hybrid sections), and (2) use of different reinforcing plate lengths (cut-off point), on the behaviour of preloaded steel beams reinforced by welding cover plates to the compression flange are studied.

5.3. FE ANALYSIS OF STEEL I-BEAMS REINFORCED WHILE UNDER LOAD

Using the commercial FE software Abaqus (2019), a FE model of steel I-section reinforced while under load was developed. Reinforcing was carried out by welding cover plates at the compression flange of the steel beam. Three-point loading pattern was used as a representative of continuous steel beams reinforced while subjected to a negative bending moment. This section provides the details of the finite element model development for the reinforced steel I-beam.

5.3.1 Finite element model development

The main scope of this study was to investigate the behaviour of preloaded continuous steel I-beams reinforced by welding cover plates to their bottom flanges while subjected to a negative bending moment. A generic configuration of the numerical test specimen in this research is presented in Figure 5.1. In this figure, L is the length of each span, Lb1 is the internal unbraced length, and Lb2 is the external unbraced length. All the numerical tests included three-point loading to simulate the behaviour of continuous span I-beams within the negative bending moment region. The same procedure was implemented to simulate continuous-span bridges in earlier research (Barth et al. 2000, Sause and Fahnestock 2001). It is assumed that 20% of the span is under the negative bending moment. To simulate the pier section, the test specimens have multiple unbraced segments on each side of the maximum bending moment location. Furthermore, to include the warping and lateral bending restrain of the beam, as well as to be able to study the cover plate length effect, the test specimen was extended by 0.1L beyond the inflection point (simulated by supports) from each end. The developed FE model for the three-point loading includes a base beam that is a build-up I-section, a reinforcing cover plate, an identical reinforcing plate with zero stiffness, and rigid beam connectors. Shell element S4R was used in Abaqus to model the components of the base beam, reinforcing cover plate, and identical reinforcing plate with zero stiffness. To connect the identical reinforcing plate to the base beam at the welding location, two-node rigid beam connectors were used. To activate the reinforcing plate in the right position after preload application, the nodes of the identical reinforcing plate were tied to the nodes of the reinforcing plate. The identical reinforcing plate has zero stiffness, and it was not removed during the analysis. The thickness and material properties of the identical plate were assigned in a way that did not affect the reinforced beam behaviour and did not cause any numerical problems. To define contact between the reinforcing cover plate and the compression flange in the developed FE model, the distance between the reinforcing cover plate and the compression flange of the I-beam was taken to be zero and the effect of the thickness was incorporated by using shell offset in the Abaqus software. Between the compression flange and the identical reinforcing plate, a surface-to-surface contact with a penalty in the tangential direction and hard contact in the normal direction was applied.

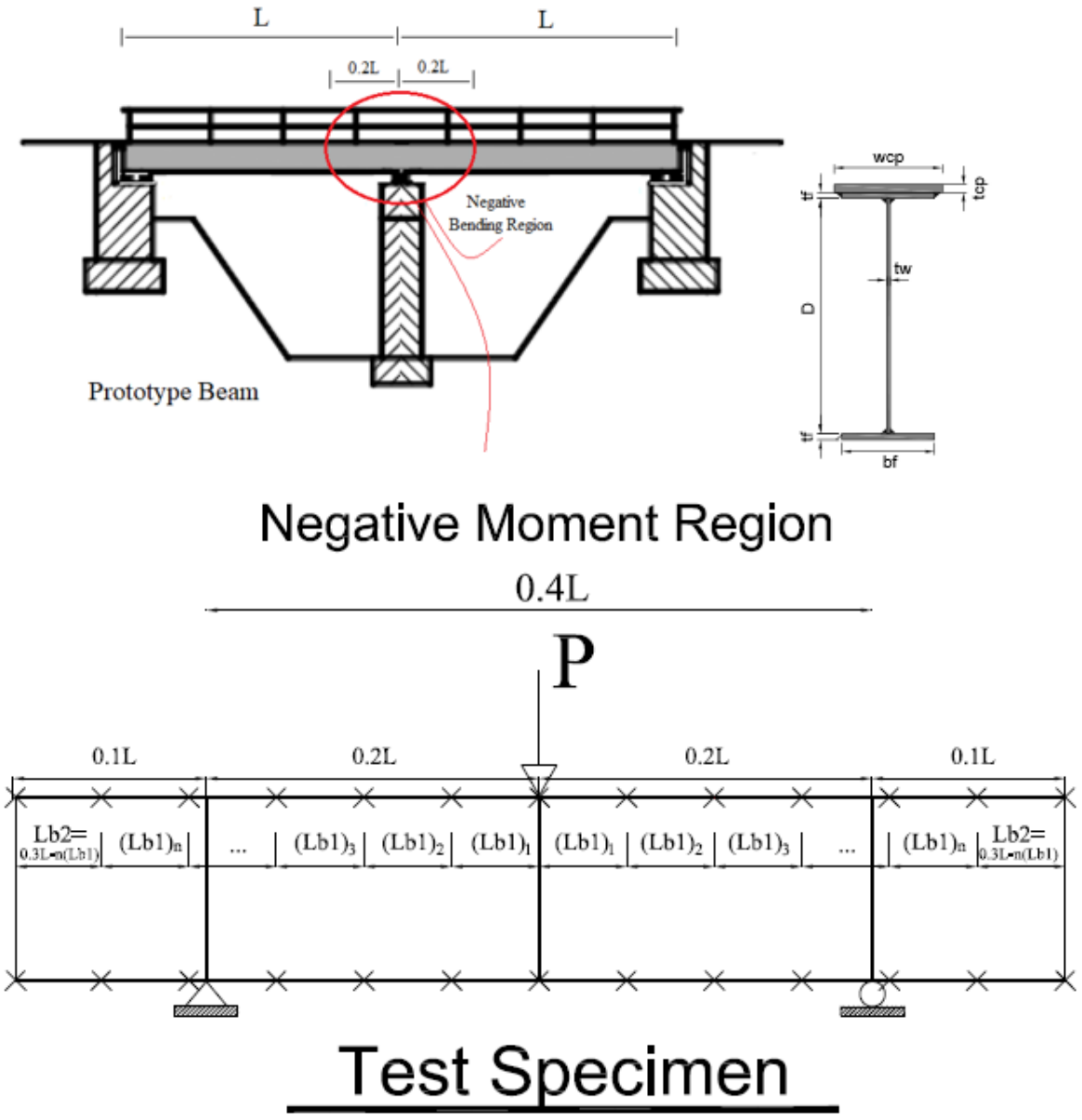

Figure 5.1: A generic configuration of the numerical test specimen

In this paper, a multi-linear stress-strain curve with isotropic hardening steel material was used for the base beam components and reinforcing cover plates. For the steel material, poison ratio, ν, and modulus of elasticity, E, were selected as 0.3 and 200,000 MPa, respectively. For the stress-strain curve, the tangent stiffness in the region of yield plateau up to strain-hardening strain (ε_{sh}) was considered as $\frac{1}{1000}$E. The strain-hardening strain (ε_{sh}) was considered equal to $10\varepsilon_y$ $\left(\varepsilon_{sh} = 10\varepsilon_y\right)$, where ε_y is the material yield strain. A constant strain-hardening modulus of $\frac{1}{50}$ E was used from strain-hardening strain to the strain hardening strength (Kim 2010). Also, von Mises yield criterion was used.

The base beam's initial residual stresses were introduced in the initial step of the analysis as uniform stresses on each element of the beam section in the form of an initial stress field. A longitudinal temperature gradient was used to apply both welding residual stress and reinforcing cover plate initial residual stress. As shown in Figure 5.2, Best-Fit Parel (Kim 2010) residual stress pattern proposed for welded steel I-beams was incorporated for the base beam, and for the cover plate, an initial residual stress pattern considered by Wu and Grondin (2002) was adopted in the finite element models. For the residual stress induced from welding of reinforcing plate to the base beam, a magnitude of 100% material yield strain was considered in the finite element models. More details about the application and verification of the initial and weld-induced residual stresses can be found elsewhere (Mohammadzadeh and Bhowmick 2022).

In the developed finite element model, 12 elements throughout the flange width and 40 elements across the web depth were used. The size of the mesh in the longitudinal direction was selected so that the aspect ratio of shell elements remained smaller than 2.

As mentioned earlier, three-point loading was considered for the FE model to simulate the continuous span beams. In this loading case, a concentrated load was applied at the center of the beam as the representative of the pier reaction. Simply supported bearings were imposed at the inflection points: vertical and transverse displacements were restrained across the tension flange in both bearings while longitudinal displacement was restrained only at one of the bearings. Furthermore, lateral braces were located at concentrated load location, each end of the beam, and unbraced segment boundaries along the beam at the tension and compression flanges. Besides, transverse stiffeners were incorporated at the concentrated load and the bearing locations.

For the geometrical imperfection induced from the erection and fabrication of the base steel beam along with weld shrinkage deformation, induced from welding of reinforcing plate, three different geometrical imperfections (compression flange sweep, flange tilt and web out of flatness) are superimposed and applied in the first step of the loading (Mohammadzadeh and Bhowmick 2022). Based on the American Welding Society (2020) limitation/tolerance for the repairing of existing structures, a value of $L_b/1000$ regardless of preload level and the welding process was applied at the mid-point of the unbraced lengths as the compression flange sweep. For the flange tilt, a value maximum of $\frac{1}{200}$ of flange width or 1.6mm was applied as the imperfection (Subramanian and White 2017). In addition, a value of D/300 (where D is web depth) was applied as the geometrical imperfection value of web out of flatness

for the welded beams (Subramanian and White 2017). To apply the flange tilt and the web out of flatness, a sinusoidal function with the half-sine length equal to the lesser of the unbraced length and the web depth was used. Initially, the base beam was analyzed to obtain the ultimate capacity of the unreinforced beam to have the preloading values. Analyzing the base beam was straightforward, in which initial residual stresses along with the geometrical imperfections were applied at the first loading step and the residual stress equilibrium was ensured by going through an equilibrium step. Then, the beam was analyzed for three-point loading using the modified Risk method to obtain the equilibrium path of the beam. The following steps were considered to analyze the reinforced beams:

1. The components of the reinforced steel I-beam were constructed. Both geometrical imperfection and initial residual stresses of the base beam were applied. Furthermore, all reinforcing plate elements were deactivated.
2. The considered preload level was applied. In this study four preload values, 0%, 20%, 40%, and 60% of base beam strength, were considered.
3. Reinforcing plate elements were reactivated to simulate the reinforcement of the beam by welding a cover plate at the compression flange of the beam.
4. Surface-to-surface contact between the identical cover plates and compression flange was introduced. Furthermore, the reinforcing plate's initial residual stresses were incorporated by temperature gradient and self-equilibrium was obtained.
5. Residual stresses of welding the cover plates to the compression flange were applied by changing the temperature at the weld location. The temperature at the compression flange tip and the corresponding location on cover plates was varied to reach 100% of material yield strain and a self-equilibrating residual stress pattern was developed in the cross-section of the reinforced beam.
6. In the last step, loading increased in the reinforced beam to obtain the equilibrium path and the ultimate capacity of the beam.

For all steps except step number 6, nonlinear static stress analysis was conducted. For loading step 6, the modified Risk method was used.

More details about the finite element modeling procedure along with the validation of the reinforced steel I-beams can be found elsewhere (Mohammadzadeh and Bhowmick 2022).

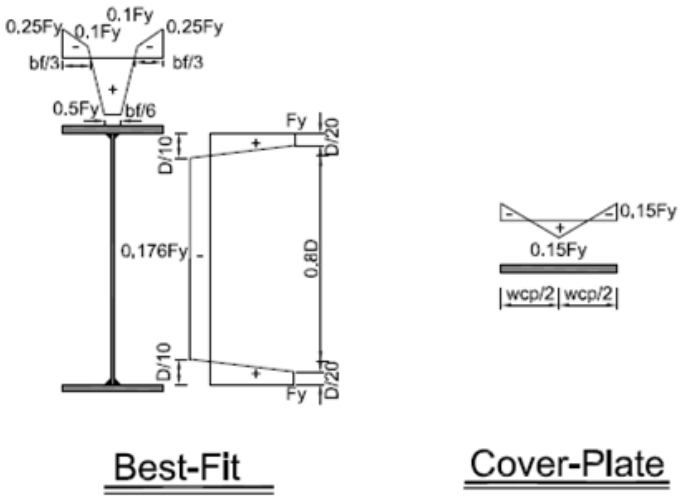

Figure 5.2: Initial residual stress patterns for I-beam and cover plate

5.4. PARAMETRIC STUDIES

In total, 220 FE models were developed to conduct a parametric study to investigate the effects of important parameters, such as preload level, cover plate thickness, unbraced length of the beam, material grade difference between the original I-beam and the reinforcing plate, length of the cover plate, on the strength and behaviour of I-beam reinforced with a cover plate at the bottom flange when subjected to negative bending moment. Three different base beam sections, as shown in Table 5.1, were considered in this study. For cross-section B1, two different reinforcing plate sizes, 196 mm×12 mm ($w_{cp} \times t_{cp}$) and 196 mm×6 mm, were considered. Cross-section B1 with a reinforcing plate of 196 mm×12 mm is named section B1-1, and cross-section B1 with a reinforcing plate of 196 mm×6 mm is named B1-2 in this paper. Similarly, for cross-section B2, two different reinforcing plate sizes of 385 mm×24 mm and 385 mm×12 mm were considered and named B2-1 and B2-2, respectively. For cross-section B3, a reinforcing plate size of 385 mm×24 mm was considered. The parametric studies were conducted for the beams with three different reinforcing plate cut-off lengths: (a) cover plate with no cut-off, (b) cut-off at zero bending moment location (where the cover plate was extended up to support location), and (c) cut-off at the end of the critical unbraced length. The geometrical properties of the cross-sections along with the flange and web classifications based on AASHTO (2022) and CAN/CSA-S6-19 (2019), and considered unbraced lengths are presented in Table 5.1. Also, the geometrical proportioning of the selected base sections is provided in Table 5.2. It should be noted that the ratio of the continuous beam span lengths to the depth of the beams was kept constant at the value of (L/D=30). Furthermore, Lb1

values, indicated in Table 5.1, are the interior unbraced lengths that were considered equal along the length of the beam. In this study, Lb1 varies to investigate the effect of welding the cover plate to the compression flange in the beams with cross-section yielding and lateral-torsional buckling failure modes. Also, as shown in Figure 5.1, Lb2 is the remaining length which is considered as the exterior unbraced length. Unless otherwise stated, in the parametric studies, the initial residual stress considered was the 'Best-Fit' pattern (shown in Figure 5.2), welding residual stress considered was 100% yielding strength of the steel cover plate, geometrical imperfection considered was the imperfection pattern as discussed earlier in section 2.1, loading pattern considered was the 3-point loading, welding type considered was continuous welding, reinforcing plate with a length corresponding to cut-off at the point with zero bending moment i.e. extending of cover plate up to the support locations, and cross-section considered was a homogeneous cross-section with a yield strength (F_y) of 345 MPa and ultimate strength (F_u) of 450 MPa.

Table 5.1: Geometrical properties of the cross-sections, classifications, and unbraced lengths

Base beam cross-sections	Compression FL $(b_f \times t_f)$ mm x mm	Tension FL $(b_f \times t_f)$ mm x mm	Web $D \times t_w$ mm x mm	AASHTO		CSA S6:19		Unbraced span length, L_{b1} (mm)			
				Compression Flange	Web	Compression Flange	Web				
B1 (Doubly symmetric)	168×10	168×10	1000×12	Compact	Compact	2	2	900	1800	3000	4500
B2 (Doubly symmetric)	330×20	330×20	1500×10	Compact	Slender	2	4	2000	5000	6700	8900
B3 (Doubly symmetric)	330×20	330×20	1500×18	Compact	Compact	2	2	2000	5000	6700	8900

Table 5.2: Geometrical proportioning of the selected base sections

Base beam cross-sections	$b_f/2t_f$	D/t_w	D/b_{fc}
	Compression FL		
B1 (Doubly symmetric)	8.4	83.3	5.95
B2 (Doubly symmetric)	8.25	150	4.55
B3 (Doubly symmetric)	8.25	75	4.55

5.4.1 Effect of preload magnitude

To study the effect of preload magnitude on the behaviour of beams reinforced while under-load by welding cover plates to the compression flange, four levels of preloading, 0% (CP-NPL), 20% (CP-20% Preload), 40% (CP-40% Preload), and 60% (CP-60% Preload) of the capacity of the unreinforced beam at the time of strengthening, were considered. Maximum moment-vertical deflection diagrams at the mid-span of the beams under considered preload levels along with maximum moment-lateral deflection of the compression flange at the mid-span of the critical unbraced length are depicted in Figure 5.3. These diagrams are for cross-section B2-1 with Lb1=2000 mm, 5000 mm, 6700 mm, and 8900 mm, respectively. As shown in the diagrams, reinforcing a beam by welding a cover plate at the compression flange increases the ultimate capacity and stiffness of the beam regardless of the preload level. Moreover, variation of preload does not have a significant effect on the ultimate capacity of the beams for the considered unbraced lengths.

Maximum lateral and vertical deflections at the ultimate capacity of the reinforced beams for the studied preload levels are presented in Table 5.3. Based on Table 5.3 and Figure 5.3, it can be observed that the lateral deflections of the reinforced beams are small in comparison to the unreinforced beams. However, for longer unbraced lengths, lateral deflections of the reinforced beams, at their ultimate capacity, increase with an increase in the preload level. For instance, the lateral deflection of the reinforced beam with an unbraced length of 8900 mm, without any preload is 6.29 mm, while the lateral deflection reaches 15.6 mm for the beam reinforced under 60% of preload level. Despite the difference

in lateral deformation in the beams reinforced while under load, the failure mode for the beams is similar. Figure 5.4 compares the failure mode and von Misses stress distribution at the ultimate loading stage for the unreinforced I-beam (Figure 5.4(a)), I-beam reinforced without any preload (Figure 5.4 (b)), and I-beam reinforced under 60% of preload level (Figure 5.4 (c)) for the unbraced length of 8900 mm. It is observed from Figure 5.4 that the failure mode of the unreinforced beam is lateral-torsional buckling. On the other hand, failure modes for the beams reinforced at preload levels of 0% and 60% of the capacity of the unreinforced beam at the time of strengthening are cross-section yielding. Therefore, reinforcing a beam by welding a cover plate to the compression flange can prevent the beam from lateral-torsional buckling failure mode.

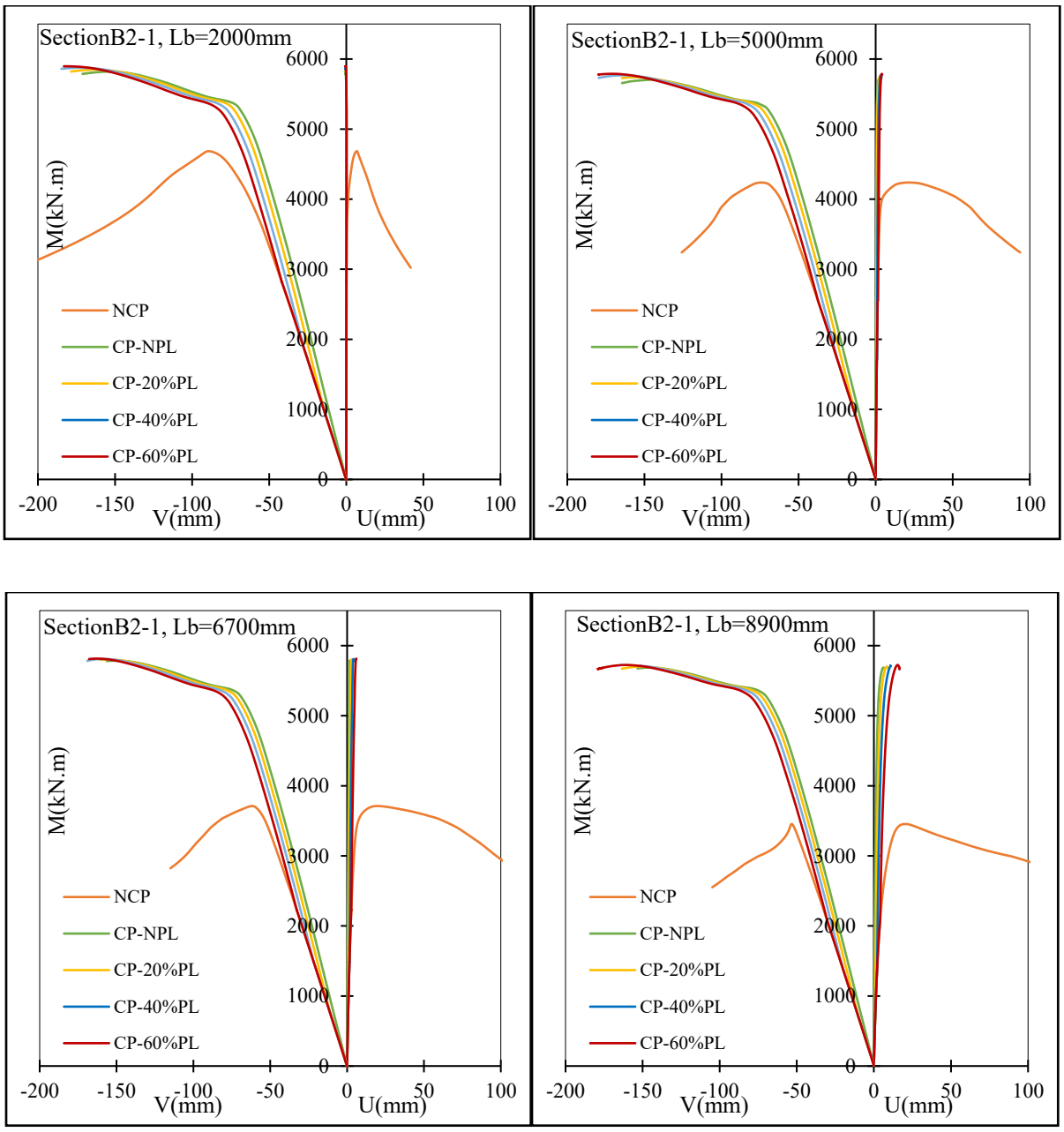

Figure 5.3: Moment- deflection diagrams of the beams reinforced under preload for Section B2-1

Table 5.3: Lateral and vertical deflections corresponding to the ultimate capacity of the reinforced beams for different preload levels in Section B2-1

Base beam cross-sections	Unbraced Length (mm)	Preload Level (%)	Lateral deflection at ultimate load (mm)		Vertical deflection at ultimate load (mm)	
			Unreinforced	Reinforced	Unreinforced	Reinforced
B2-1	2000	0	6.76	0.46	89.05	155.55
		20	6.76	0.42	89.05	161.81
		40	6.76	0.48	89.05	171.07
		60	6.76	0.43	89.05	182.09
	5000	0	21.62	1.81	74.01	145.39
		20	21.62	2.42	74.01	154.61
		40	21.62	3.27	74.01	163.56
		60	21.62	4.01	74.01	170.81
	6700	0	19.6	1.63	61.67	150.28
		20	19.6	2.82	61.67	160.63
		40	19.6	4.05	61.67	156.24
		60	19.6	5.91	61.67	163.11
	8900	0	20.28	6.29	53.31	147.04
		20	20.28	8.36	53.31	150.29
		40	20.28	10.96	53.31	151.49
		60	20.28	15.60	53.31	163.12

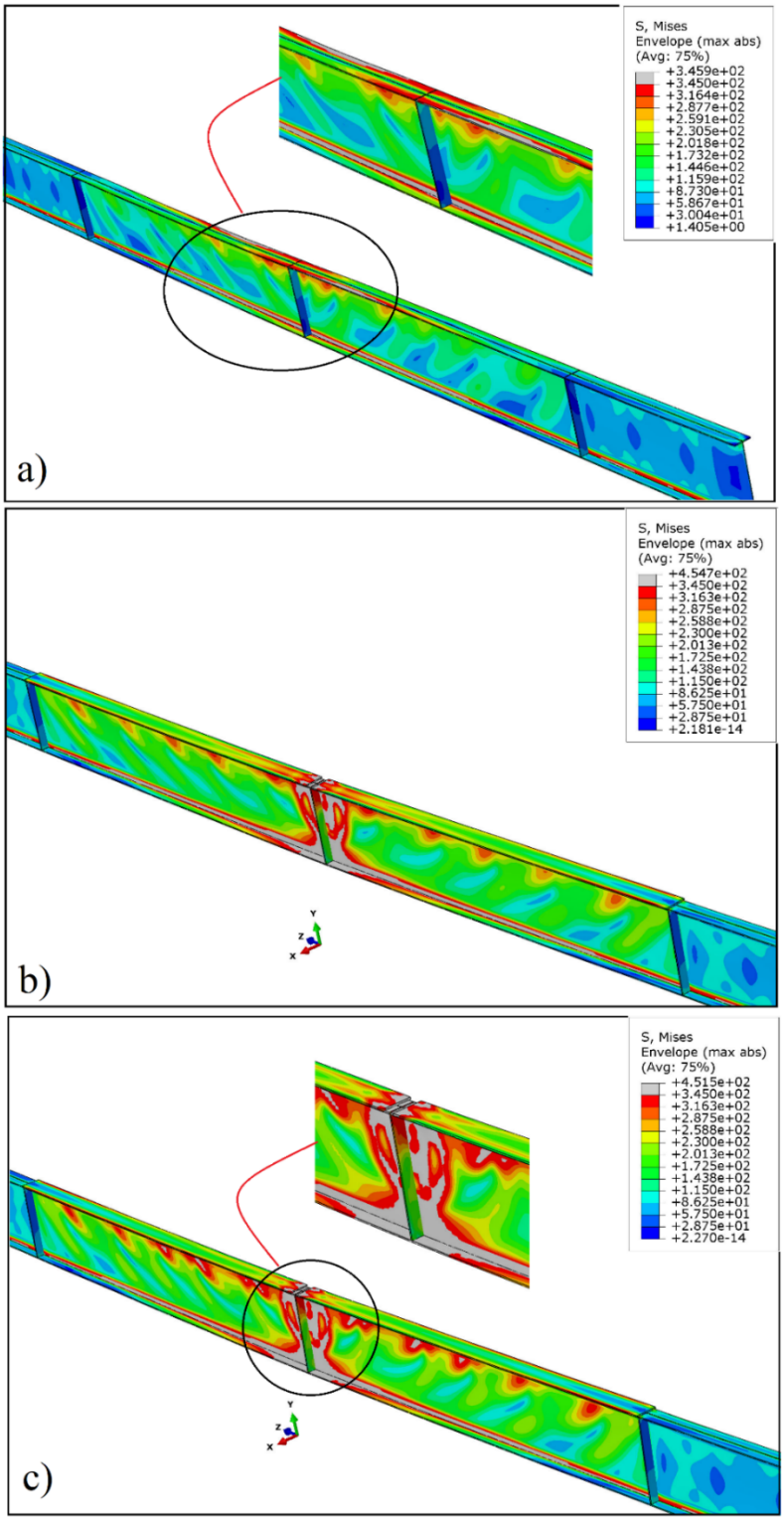

Figure 5.4: Failure mode and von-Misses stress distribution at ultimate loading stage; (a) unreinforced I-beam, (b)reinforced without any preload, (c) reinforced at preload level of 60% of the capacity of the unreinforced beam

5.4.2 Effect of cover plate thickness

To study the effect of cover plate thickness on the behaviour of preloaded I-beams when reinforced with welded cover plate to the compression flanges, beams with cross-sections B1-1 and B1-2 as well as B2-1 and B2-2 were considered. The size of the reinforcing plate was 196 mm×12 mm and 196 mm×6 mm for the B1-1 and B1-2 sections, respectively. Also, the cover plate size for B2-1 and B2-2 sections was 385 mm×24 mm and 385 mm×12 mm. It is acknowledged that a thickness of 6 mm is not a structural thickness for a cover plate and the objective here is just to investigate the effect of a thin cover plate on the behaviour of reinforced steel I-beams. In these beams, four different unbraced lengths and preload levels were considered. Maximum moment-vertical deflection at the mid-span of the beam under considered preload levels along with maximum moment-lateral deflection of the mid-length compression flange of critical unbraced length are depicted in Figure 5.5 for B2-2 with L_b=2000 mm and 6700 mm, respectively. It can be observed from Figure 5.5 that reinforcing a beam by welding a cover plate at the compression flange increases the capacity and stiffness of the beam regardless of the cover plate thickness. Also, preloading has an insignificant effect on the increased capacity.

Comparing the capacity increase for the cross-sections B1-1 and B1-2 along with the cross-sections B2-1 and B2-2 with no-preload in Table 5.4 shows that for the same base beam section the capacity increase is higher when the reinforcing plate thickness is higher, mainly in the reinforced beams with longer unbraced length and lateral-torsional buckling failure mode. Figure 5.6 compares the ultimate capacities of the unreinforced and reinforced beams with 0%, 20%, 40% and 60% preload levels and unbraced lengths for the considered cross-sections along with the yield moment (M_y) and plastic moment (M_p) of the base beam. In the cross-sections B2-1 and B2-2, the failure of the reinforced beam is the cross-section yielding of the base beam. Therefore, increasing the thickness of the cover plate has an insignificant effect on the capacity increase of the beam. However, for the reinforced beams with cross-section B1-2, failure of the reinforced beam for longer unbraced length is lateral-torsional buckling of the beam and welding a reinforcing plate could not change the failure mode. Therefore, increasing the reinforcing plate thickness can significantly increase the capacity of the beam. For instance, the capacity increase for the beam with cross-section B1-2 with an unbraced length of 4500 mm is 65.74%, while the capacity increase for the B1-1 with the same unbraced length is 122.02%. Also, increasing the thickness of this beam changes the failure from LTB to the cross-section yielding. For the beams with different reinforcing plate thicknesses, lateral and vertical deflections of the base and reinforced beams (with no-preloading) at the ultimate loading stage are presented in Table 5.5. Based on Table 5.5, for the reinforced

beams with the cross-section yielding failure mode (failure mode after reinforcement), lateral deformation decreases with an increase in the cover plate thickness, especially in the beams with longer unbraced lengths. For example, beam B2-2 with an unbraced length of 8900 mm has a lateral deflection of 36.9 mm, while for a thicker cover plate (cross-section B2-1) lateral deflection is limited to 6.29 mm. Therefore, increasing the cover plate thickness can reduce the excessive lateral deformation for the beams with the same failure mode and capacity.

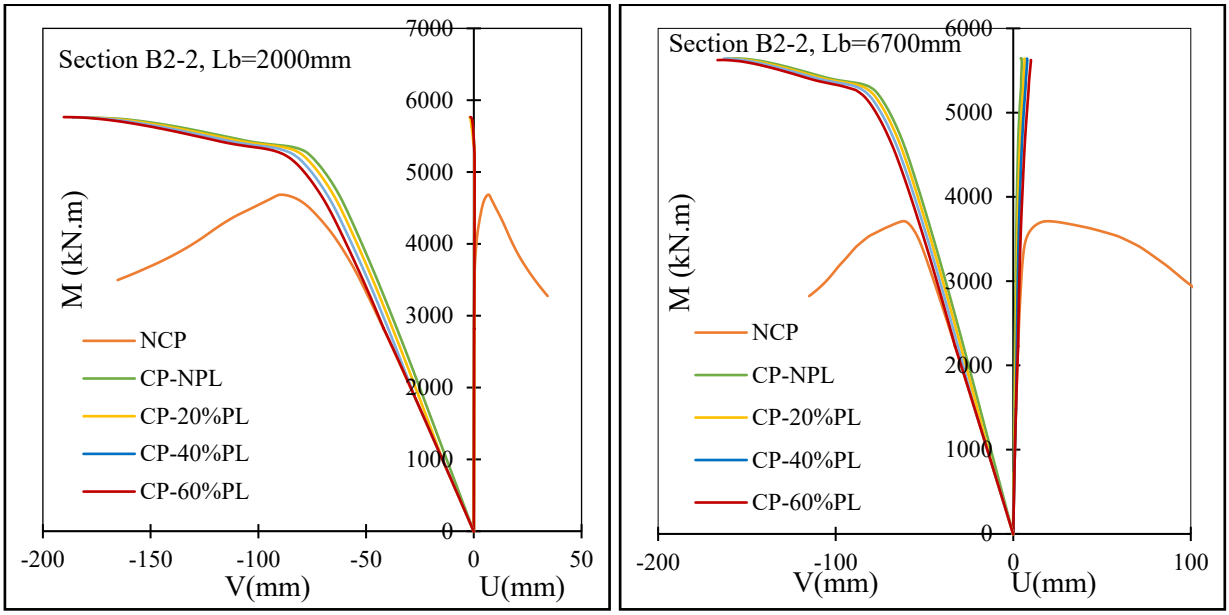

Figure 5.5: Moment- deflection diagrams of the beams reinforced under preloading for Section B2-1

Table 5.4: Capacity increase of beams reinforced with welded cover plates of different thicknesses (without any preloading)

Base beam cross-sections	Unbraced Length (mm)	Capacity (kN·m)			Capacity increase (%) ($B_{i1\&i=1,2}$)	Capacity increase (%) (($B_{i2\&i=1,2}$)
		Unreinforced	Reinforced ($B_{i1\&i=1,2}$)	Reinforced (($B_{i2\&i=1,2}$)		
B1	900	1390.80	1611.98	1585.99	15.90	14.03
	1800	1247.35	1656.61	1636.5	32.81	31.2
	3000	941.27	1656.32	1588.21	75.97	68.73
	4500	746.02	1656.29	1236.42	122.02	65.74
B2	2000	4684.48	5819.53	5754.55	24.23	22.84
	5000	4237.3	5706.89	5593.84	34.682	32.01
	6700	3711.15	5785.89	5643.58	55.906	52.07
	8900	3454.36	5686.58	5518.24	64.62	59.75

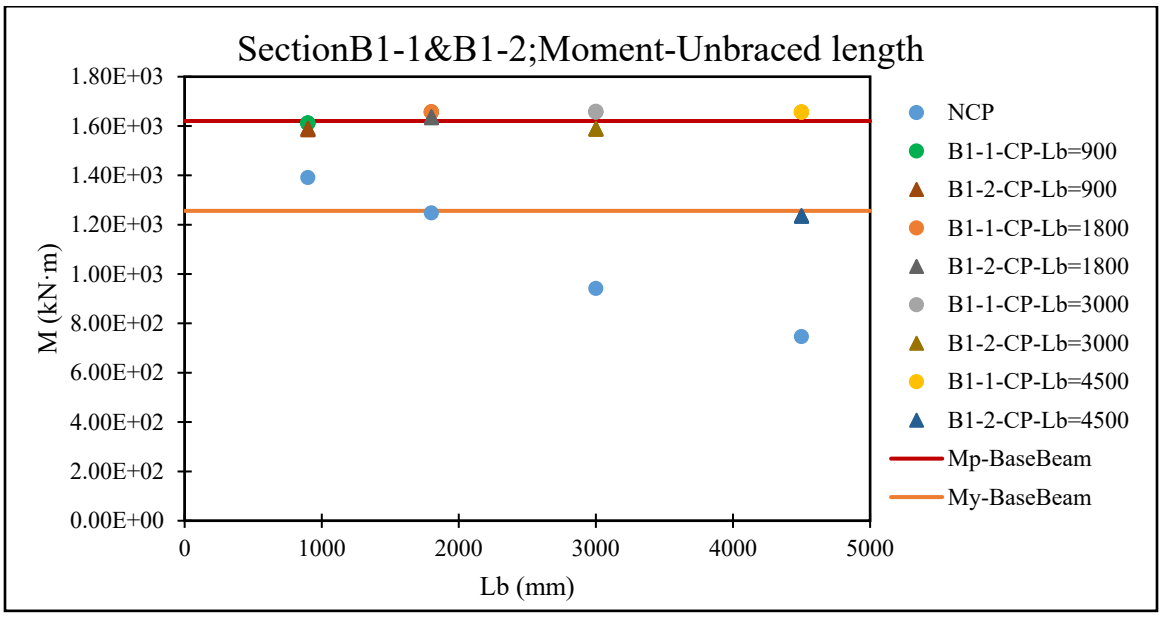

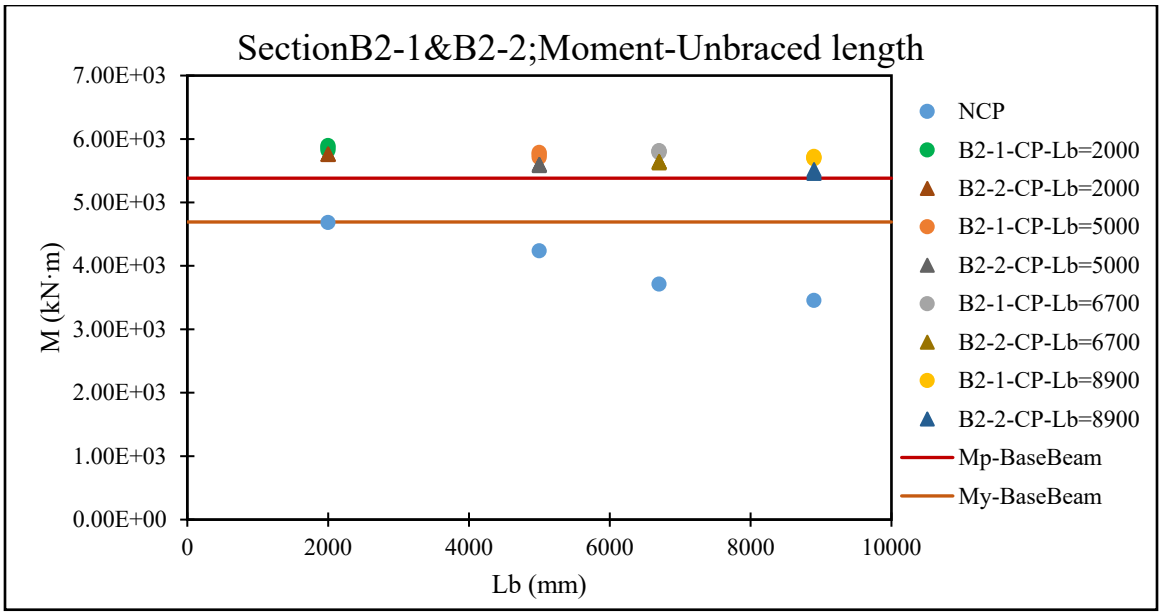

Figure 5.6: Comparison of the ultimate capacities of the unreinforced and reinforced beams with different cover plate thickness and preloading levels with M_y and M_p of the base beam.

Table 5.5: Lateral and vertical deflections at the ultimate capacity of the beams for different cover plate thicknesses with no-preloading

Base beam cross-sections	Unbraced Length (mm)	Lateral deflection at ultimate load (mm)			Vertical deflection at ultimate load (mm)		
		Unreinforced	Reinforced ($B_{i1\&i=1,2}$)	Reinforced (($B_{i2\&i=1,2}$)	Unreinforced	Reinforced ($B_{i1\&i=1,2}$)	Reinforced (($B_{i2\&i=1,2}$)
B1	900	4.97	0.38	0.55	63.63	57.79	61.34
	1800	10.09	0.21	0.33	52.34	60.49	65.92
	3000	8.65	1.94	13.63	35.62	58.49	62.83
	4500	15.13	24.11	20.15	28.06	66.05	44.24
B2	2000	6.76	0.46	1.67	89.05	155.55	177.28
	5000	21.62	1.81	5.62	74.01	145.39	161.04
	6700	19.6	1.63	4.42	61.67	150.28	158.14
	8900	20.28	6.29	36.9	53.31	147.04	152.87

5.4.3 Effect of type of cross-section of I-beam

To examine the cross-section effect on the behaviour of preloaded I-beams reinforced by welding cover plates at the compression flanges, cross-sections B1-1, B2-1, and B3 with a yield strength of 345 MPa were used. The ratio of the reinforcing plate area to the compression flange area was kept constant at a value of 1.4. Cross-section B1-1 has a one-meter web depth with a compact web and compact compression flange. In this section, the ratio of the web depth to the compression flange (D/b_{fc}) is very

close to the AASHTO's limitation (2020) (the upper bound value is 6 in AASHTO). Cross-section B2-1 has a slender web and a compact compression flange with a web depth of 1.5m. For this section, the ratio of the web depth to the web thickness (D/t_w) is equal to the upper bound limitation of the AASHTO which is equal to 150. All the cross-section geometrical properties are the same for cross-sections B3 and B2-1 except for the web thickness. In this section, the web is compact with a depth-to-web thickness ratio equal to 75. To present the behaviour of the considered sections, maximum moment-vertical deflection diagrams at the mid-span of the beams under considered preload levels along with maximum moment-lateral deflection of the compression flange at the mid-span of the critical unbraced length are depicted in Figure 5.7 for B1-1 with unbraced length 900 mm and 3000 mm and B3 with unbraced length 5000 mm and 8900 mm for different preloading levels. Based on Figure 5.7 and Figure 5.3, the selected I-beam sections when reinforced by welding cover plates to the compression flange have similar behaviour in terms of stiffness and capacity increase. Also, for the selected beam sections, the preloading level has an insignificant effect on the ultimate capacity of the beams. However, there is a slight difference in the diagrams of B2-1 (with the slender web), as shown in Figure 5.3, with B1-1 and B3 (with compact webs) near the ultimate stage of loading. B2-1 shows more nonlinearity before reaching the ultimate capacity. To clarify this difference, the stress distribution of the I-beams under 60% of the preloading for B1-1 and B3 at the ultimate loading stage for the maximum moment location is depicted in Figure 5.8. A comparison between the stress distributions from Figure 5.8 and Figure 5.4 shows that in B2-1, yielding at the compression flange extends to the reinforcing cover plate while in B1-1 and B3, the yielding is limited to the base beam compression flange. Also, a wider web area of the B2-1 yields at the ultimate loading stage comparing with the webs of B1-1 and B3.

Lateral and vertical deflections at the ultimate load of the base and reinforced beams without any preload level for cross-section B3 are presented in Table 5.6. Based on Tables 5.6 and 5.5, reinforcing a beam by welding a cover plate at the compression flange can control and reduce the excessive out-of-plane deformation of the reinforced beam. Furthermore, the vertical deformation of the reinforced beam is greater than the base beam, which means that reinforcing a beam can improve the lateral-torsional behaviour of the beam, and based on the size of the cover plate, it can change the failure mode of the beam from lateral torsional buckling to the cross-section yielding. Table 5.7 presents the capacity increase in beams with cross-section B3 for different unbraced lengths as the beams were reinforced with welding cover plates at no preloading level. Based on Table 5.7 and Table 5.4 for cross-sections B1-1 and B1-2, the capacity increase rate is more for the beams with longer unbraced lengths. As an example, the capacity increase rate for cross-section B3 with an unbraced length of 2000 mm is 15.3% while for

the unbraced length of 8900 mm, it reaches 72.57%. Figure 5.9 compares the ultimate capacities of the unreinforced and reinforced beams with different preloading levels and unbraced lengths for cross-section B3 with the yield moment (M_y) and plastic moment (M_p) of the base beam. Based on Figure 5.9 reinforced beams can reach the plastic capacity of the unreinforced beam.

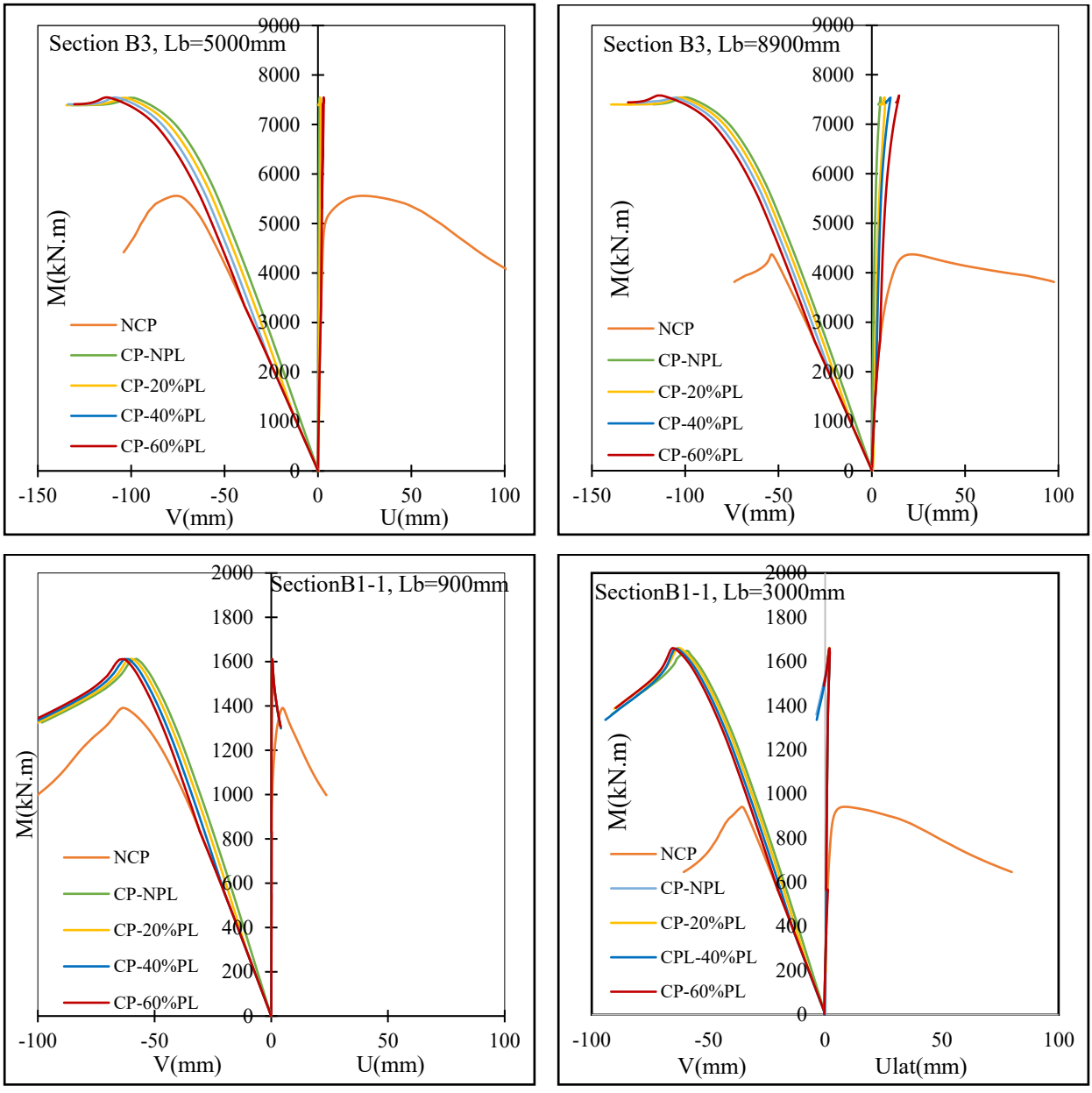

Figure 5.7: Moment-deflection diagrams of the beams reinforced under preload for sections B1-1 and B3.

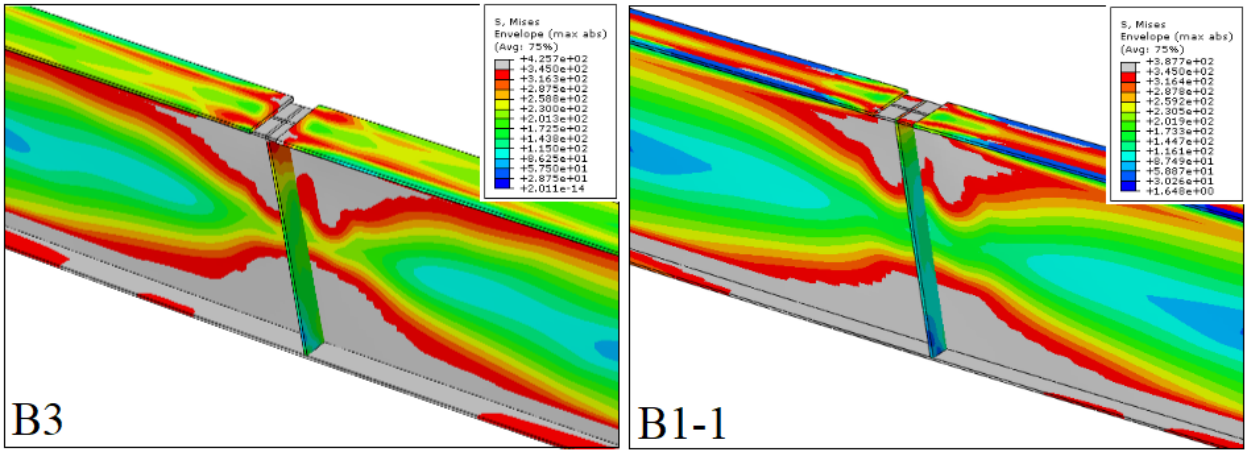

Figure 5.8: Stress distribution of the I-beams under 60% of the preloading for B1-1 and B3 at the ultimate loading stage for the maximum moment location.

Table 5.6: Lateral and vertical deflections at ultimate load of the base and reinforced beams without any preloading for cross-section B3

Base beam cross-sections	Unbraced Length (mm)	Lateral deflection at ultimate load (mm)		Vertical deflection at ultimate load (mm)	
		Unreinforced	Reinforced	Unreinforced	Reinforced
B3	2000	8.23	0.106	97.69	93.36
	5000	22.2	0.86	74.95	100.84
	6700	25.15	3.06	63.15	92.66
	8900	21.25	4.61	53.65	100.85

Table 5.7: Lateral and vertical deflections at the ultimate load of the reinforced beams for cross-section B3 with no-preloading

Base beam cross-sections	Unbraced Length (mm)	Capacity (kN·m)		Capacity increase (%)
		Unreinforced	Reinforced ($B_{i1\&i=1,2}$)	
B3	2000	6429.41	7413.85	15.31
	5000	5558.84	7539.17	35.63
	6700	4766.38	7540.39	58.2
	8900	4370.6	7542.41	72.57

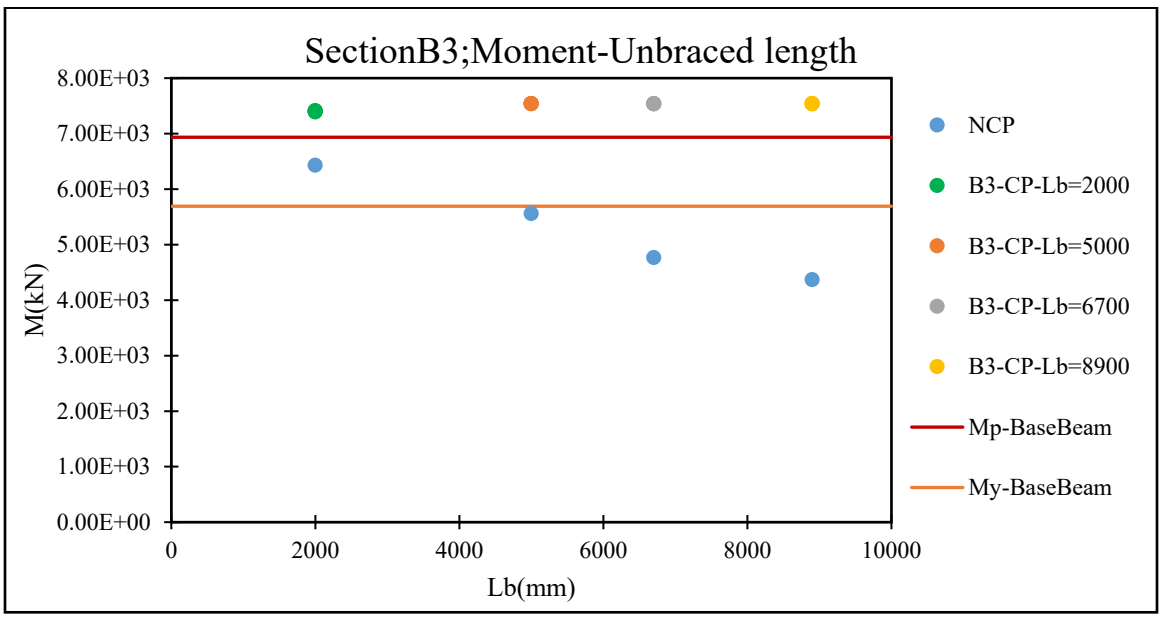

Figure 5.9: Comparison of the ultimate capacities of the B3 beams with different preloading levels with M_y and M_p of the base beam.

5.4.4 Effect of Hybrid Sections

To study the effect of steel grade difference between the base beam and reinforcing cover plate on the behaviour of steel I-beams reinforced while under load by welding cover plates to compression flange, two different grades of steel were considered. The base steel I-beam was constructed from ASTM A36 steel material in which F_y (yield strength) was 250 MPa and F_u (ultimate strength) was 400 MPa. The reinforcing plate was made of previously considered ASTM A572 grade 50 with F_y of 345 MPa and F_u of 450 MPa. Also, two different cross-sections B1-1 and B2-1 were considered to study the effect of higher-grade steel reinforcing plates. From the numerical study, it was observed that the overall behaviour of steel beams reinforced while under load with cover plates of higher steel grade was similar to the steel beams reinforced with the same steel grade cover plate. Figure 5.10 illustrates moment-vertical deflection diagrams at the mid-span and moment-lateral deflection of the compression flange at the mid-span of critical unbraced length under different preloading levels for the hybrid cross-section B1-1 with an unbraced length of 4500 mm and hybrid cross-section B2-1 with an unbraced length of 8900 mm. Based on Figure 5.10, it is observed that preloading has an insignificant effect on the behaviour and ultimate capacity of the reinforced beams with higher-grade steel reinforcing plates. Table 5.8 presents a capacity increase for the hybrid beams with no preloading while reinforced at the compression flange with higher-grade steel cover plates. Based on Table 5.8 for hybrid beam B1-1, the smallest capacity increase is 10.70% for the unbraced length of 900 mm and the largest capacity increase is 94.47% for the unbraced length of 4500 mm. For hybrid beam B2-1, the maximum capacity increase is 60.7% for an unbraced length of 8900 mm and the minimum capacity increase is 33.36% for an unbraced length of 5000. However, the minimum capacity increase is very close to the capacity increase for the unbraced length of 2000 mm, which is 34.16%. Based on Tables 5.8 and 5.4, in general capacity of the steel I-beams increases more for beams with longer unbraced lengths when reinforced by welding cover plates to the compression flanges of hybrid and homogeneous cross-sections.

Figure 5.11 shows the comparison of the ultimate capacities of the unreinforced and reinforced beams for considered preloading levels and unbraced lengths for hybrid cross-sections B1-1 and B2-1. Also included in Figure 5.11 are the yield moment (M_y) and plastic moment (M_p) capacities of the base beams. Based on Figure 5.10, Figure 5.11, and Table 5.9, reinforcing the beams can increase their capacity to their plastic capacity and can change the failure of the hybrid beams from lateral torsional buckling failure mode to the cross-section yielding of the base beam. Also, Figure 5.11 shows that for cross-section B2-1, which is a more practical section in bridge engineering in terms of geometrical

proportioning, the difference between the ultimate capacity and plastic moment of the base section is more for hybrid section B2-1 compared with the homogeneous section.

Lateral and vertical deflections of the base and reinforced (with no-preloading) hybrid beams at their ultimate capacities are presented in Table 5.9. Table 5.9 shows that reinforcing a beam by welding a cover plate to the compression flange can reduce the lateral deflection and increase the vertical deflection of the beam before the beam reaches its moment capacity.

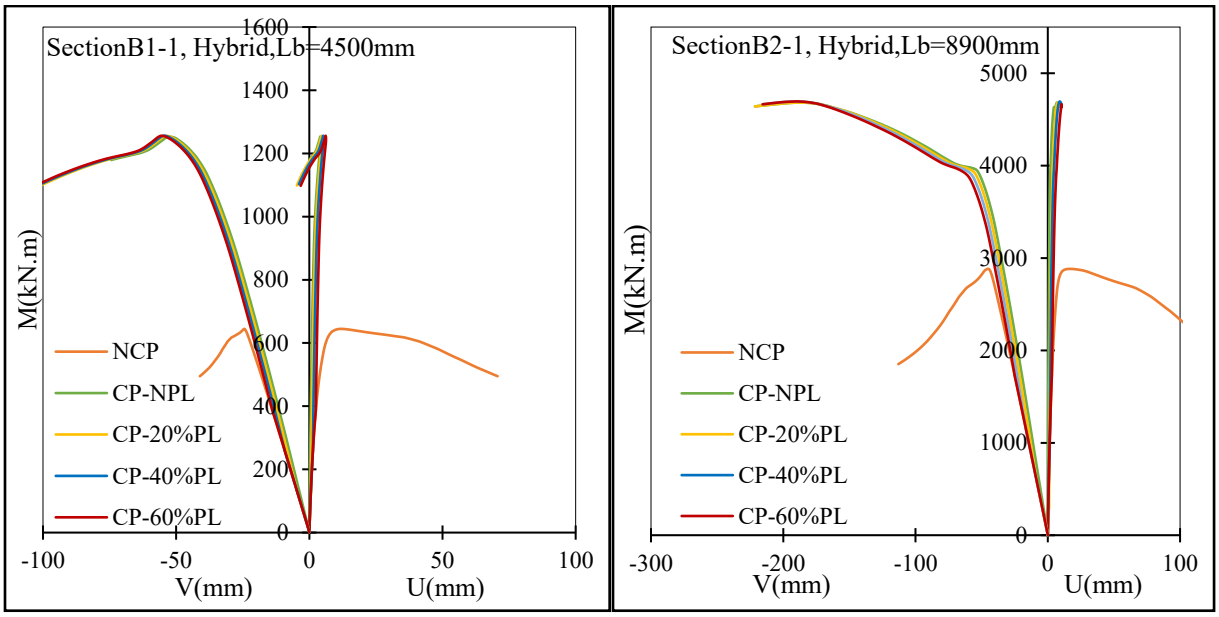

Figure 5.10: Moment-deflection diagrams of the beams reinforced under preloading for Hybrid sections B1-1 & B2-1.

Table 5.8: Capacities of the beams reinforced with cover plates with higher steel grade material without any preloading

Base beam cross-sections with F_y of $250MPa$	Unbraced Length (mm)	Capacity (kN.m)		Capacity increase (%)
		Unreinforced	Reinforced	
B1-1	900	1097.668	1215.14	10.70
	1800	1051.388	1242.95	18.22
	3000	805.07	1249.88	55.25
	4500	644.48	1253.34	94.47
B2-1	2000	3581.19	4804.5	34.16
	5000	3512.64	4684.3	33.36
	6700	3108.37	4822.26	55.14
	8900	2882.4	4682.45	60.7

Table 5.9: Lateral and vertical deflections (at ultimate load) of the reinforced hybrid cross-sections with no preloading

Base beam cross-sections with F_y of $250MPa$	Unbraced Length (mm)	Lateral deflection at ultimate load (mm)		Vertical deflection at ultimate load (mm)	
		Unreinforced	Reinforced	Unreinforced	Reinforced
B1-1	900	3.31	0.27	50.80	46.43
	1800	-7.87	0.01	47.56	49.34
	3000	16.17	0.82	33.21	52.05
	4500	11.32	4.12	24.34	52.58
B2-1	2000	4.32	0.65	66.05	211.37
	5000	19.09	1.84	64.90	188.34
	6700	23.05	0.27	56.24	218.00
	8900	17.55	7.03	45.37	187.29

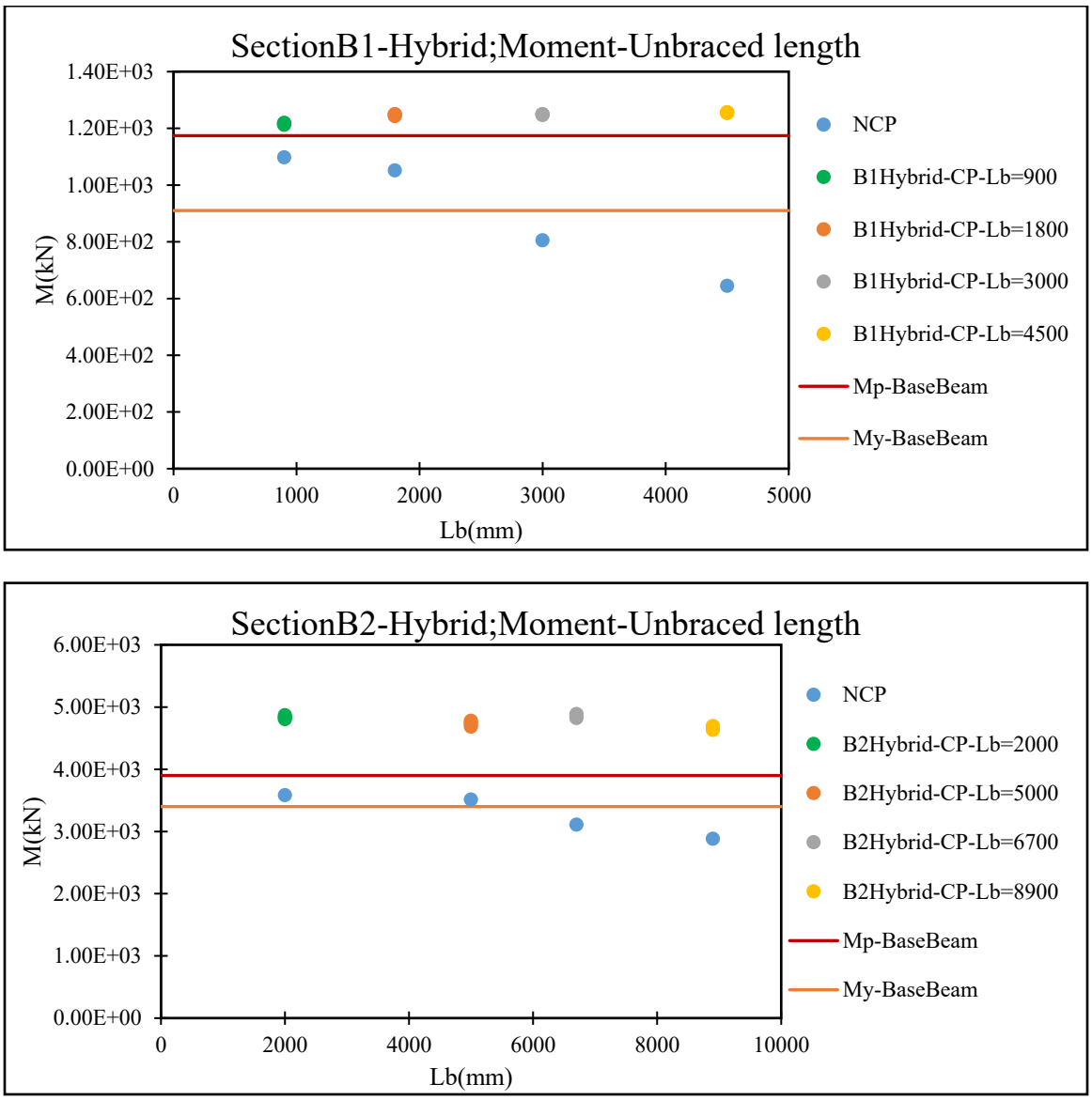

Figure 5.11: Comparison of the ultimate capacities of the unreinforced and hybrid reinforced beams for different preloading levels with M_y and M_p of the base beam.

5.4.5 Effect of Reinforcing Plate length

To study the effect of reinforcing plate length and cut-off point on the behaviour of steel I-beams reinforced by welding cover plates at the compression flange, three different lengths/cut-off points of cover plates, (a) cover plate with no cut-off, (b) cut-off at zero bending moment location (M=0), and (c) cut-off at the end of the critical unbraced length, were considered. For this study, cross-sections B1-1 and B2-1 under different preloading levels and unbraced lengths were used. A schematic view of the

considered cover plate lengths corresponding to their practical cut-off points is shown in Figure 5.12. It should be mentioned that for the cover plate with the length of L_b, the cover plate was extended beyond the theoretical cut-off point and connected to the flange by a weld connection to develop a force in the cover plate at the theoretical cut-off point not less than the value provided in equation [5-1] which was taken from CSA (CSA S16-19).

$$P = \frac{AM_{fc}Y}{I_g} \qquad [5\text{-}1]$$

In this equation, P is the force that is required to be developed in the reinforcing plate, A is the reinforcing plate area, Y is the distance of the reinforcing plate center from the elastic neutral axes of the reinforced cross-section of the beam, I_g is the moment of inertia of the reinforced cross-section and finally M_{fc} is the moment at the theoretical cut-off point which is obtained by assuming that the plastic moment will be developed in the unreinforced beam at the peak bending moment location of the beam. A schematic view of the considered moment diagram for calculating the theoretical cut-off point is presented in Figure 5.13.

Also, for cross-section B2-1, unbraced length with the value of 8900 was not considered for the cut-off at L_b since the length is very close to the case of the 'M=0' cut-off point. To investigate the behaviour of the reinforced steel I-beams with different reinforcing plate cut-off points, moment-vertical deflection diagrams at the mid-span and moment-lateral deflection of the compression flange at the mid-span of the critical unbraced length for the considered preloading levels are depicted in Figure 5.14. These diagrams are for cross-section B1-2 with an unbraced length of 4500 mm and cross-section B2-1 with an unbraced length of 6700 mm for the beams with a cut-off point at L_b location and for the beams with whole-length cover plate (no cut-off point). It can be observed that the overall behaviour of steel I-beams reinforced by welding cover plates at the compression flange for considered cut-off points is similar, and preloading does not have a significant effect on capacity reduction. Also, it is observed that reinforcing at the compression flange can increase the ultimate capacity and stiffness of the reinforced beams. Table 5.10 presents the capacity increase for the beams reinforced by welding cover plates with a cut-off point at the critical unbraced length (L_b) and with no cut-off point. Comparing the results of Table 5.10 and Table 5.4 shows that the capacity increase is higher when the cover plate length is increased. However, the difference in capacity increase is insignificant for the beams with considered cover plate lengths except for the cross-section B1-1 with an unbraced length of 4500 mm. For this unbraced length, the capacity increase for the cut-off at L_b is 109.69% while for the beam with a cover

plate cut-off at zero bending moment location (M=0) and no cut-off point the capacity increase is equal to 122.02% (as presented in Table 5.4) and 122.20%, respectively.

Figure 5.15 compares the ultimate capacities of the base and reinforced beams for different cover plate lengths with considered preloading levels and unbraced length for homogeneous cross-sections B1-1 and B2-1. Both the yield moment (M_y) and plastic moment (M_p) capacities of the base beams are also included in Figure 5.15 for comparison. Based on this figure, for the studied cut-off point of the cover plates, reinforced beams are able to reach the plastic moment capacity of the base beam regardless of the unbraced length except for B1-1 with an unbraced length of 4500 mm with reinforcing plate cut-off at L_b (critical unbraced length). Therefore, it can be concluded that the general behaviour of the reinforced beams with no cut-off point and cut-off at zero bending moment location (M=0) is very similar and there is no need to extend the cover plate beyond the zero-moment location (M=0) to increase the capacity of the beam.

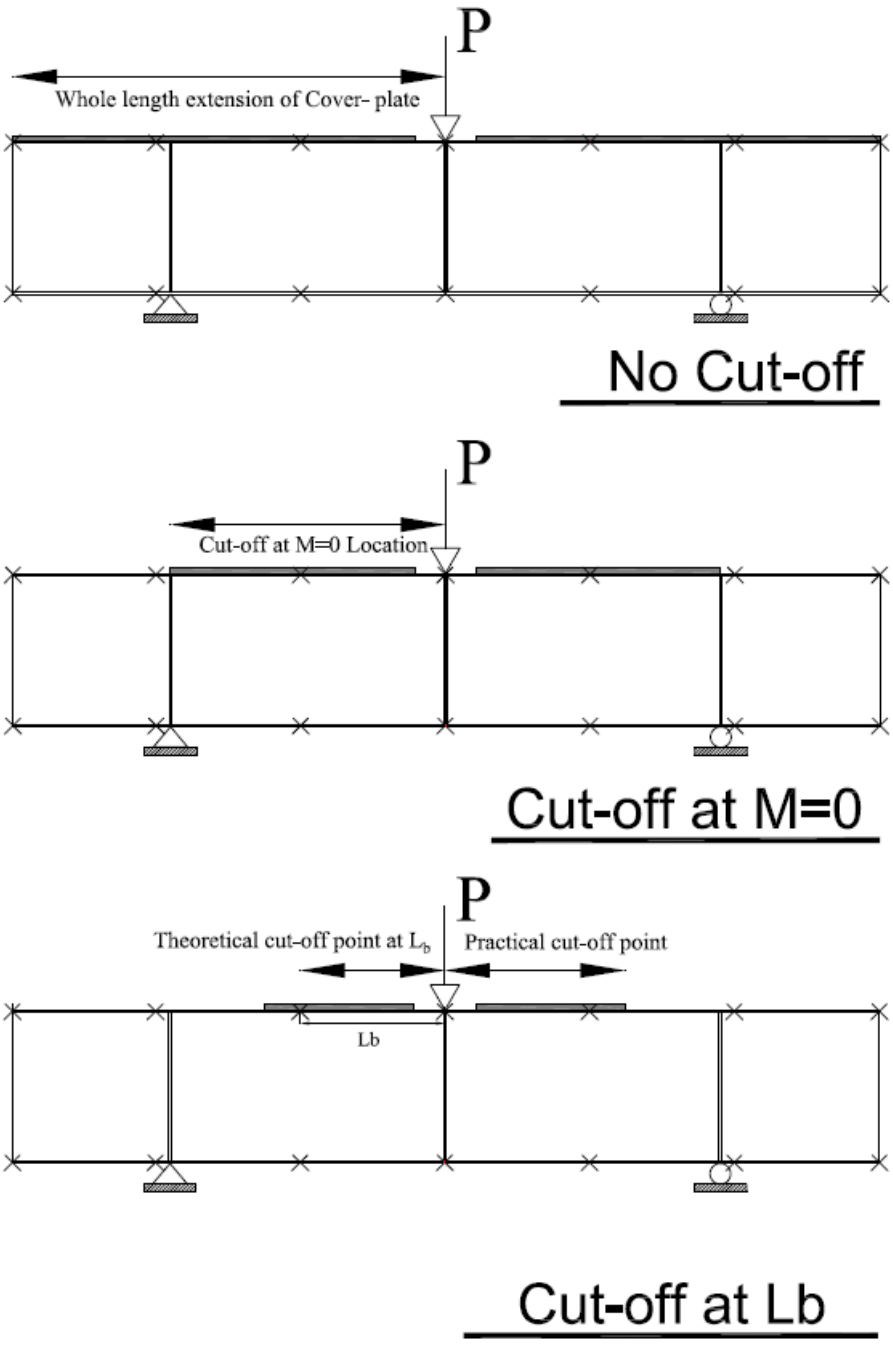

Figure 5.12: Schematic view of the considered cover plate lengths

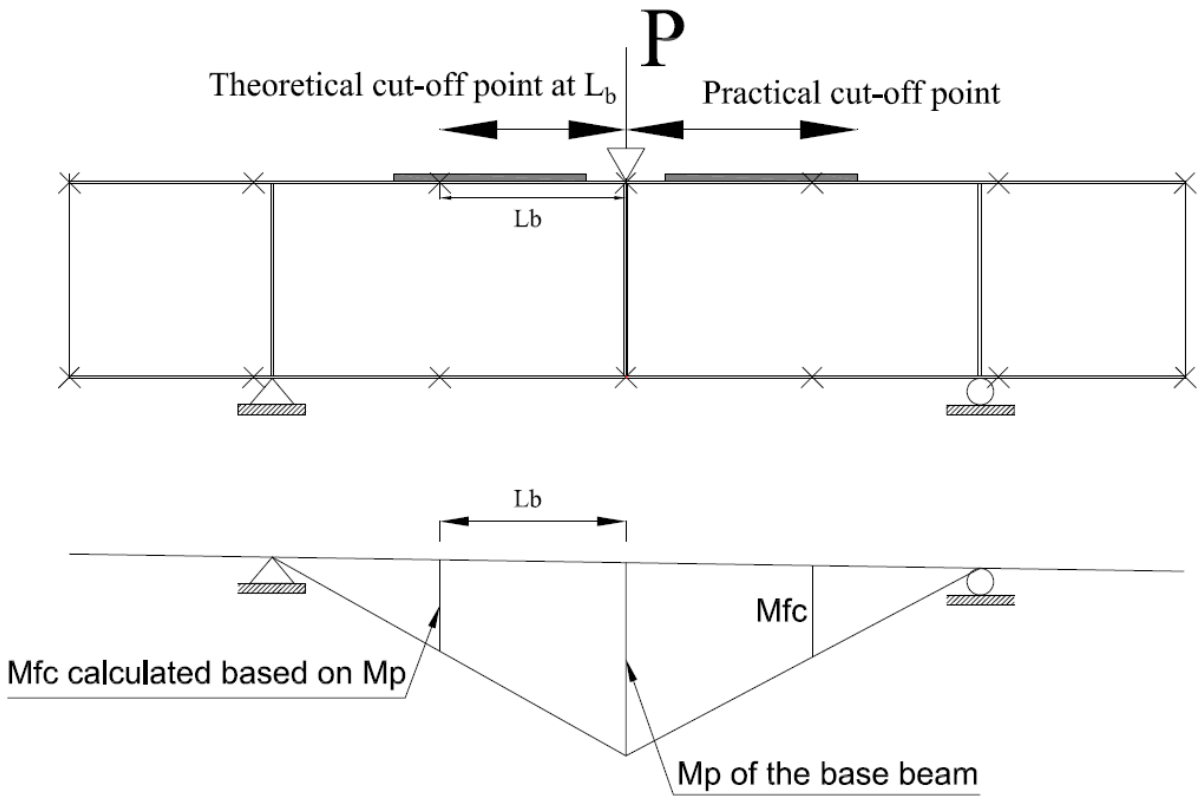

Figure 5.13: Schematic view of the considered moment diagram for calculating M_{fc}

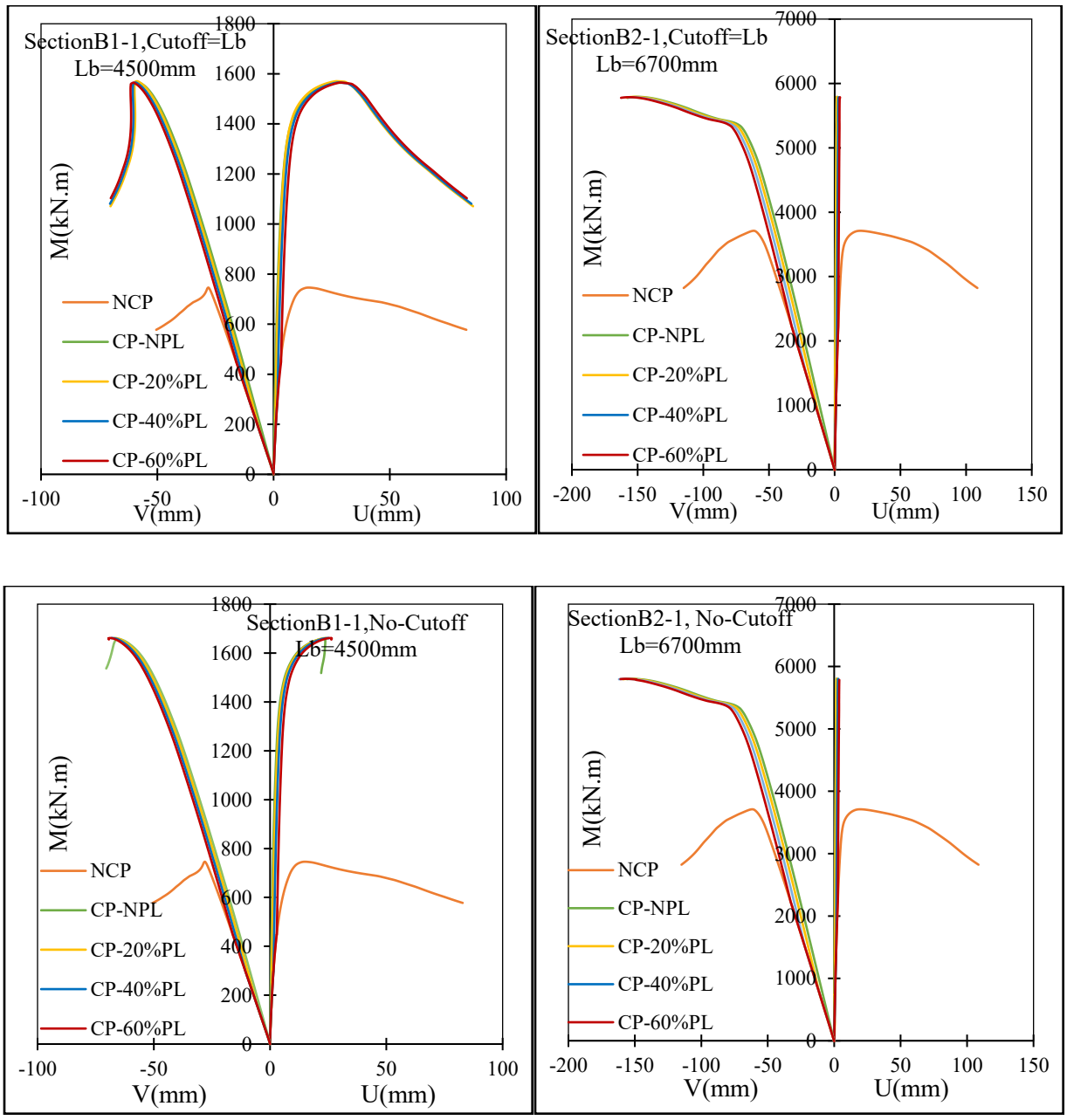

Figure 5.14: Moment-Deflection diagrams of the beams reinforced under different preload levels and with different cover plate lengths

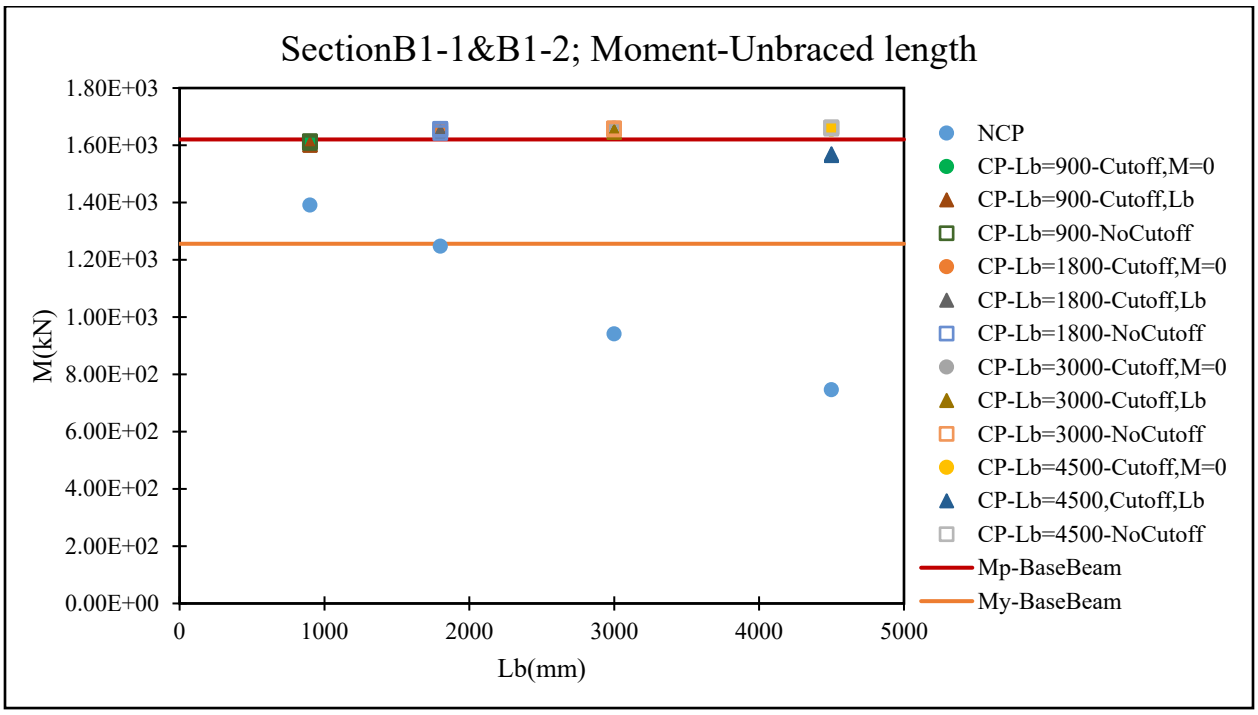

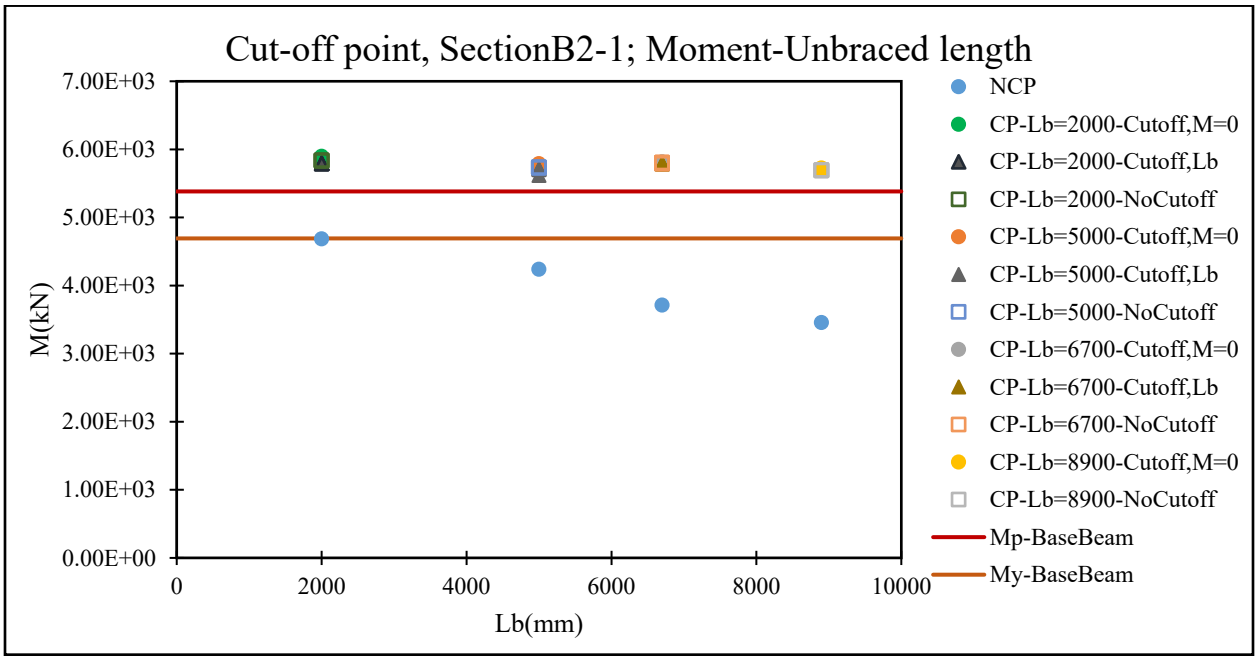

Figure 5.15: Comparison of the ultimate capacities of the unreinforced and reinforced beams with different cover plate lengths and preload levels

Table 5.10: Capacity increase of beams due to welding of cover plate with different lengths and with no preload

Base beam cross-sections	Unbraced Length (mm)	Capacity (kN·m)			Capacity increase (%)	Capacity increase (%)
		Unreinforced	Reinforced (Cut-off Point=Lb)	Reinforced (No Cut-off)	Cut-off Point = Lb	(No Cut-off)
B1	900	1390.80	1600.45	1607.9	15.07	15.61
	1800	1247.35	1645.94	1656.88	31.95	32.83
	3000	941.27	1645.57	1656.79	74.82	76.01
	4500	746.02	1564.3	1657.66	109.69	122.20
B2	2000	4684.48	5793.76	5833.62	23.68	24.53
	5000	4237.3	5701.52	5731.09	34.56	35.25
	6700	3711.15	5792.11	5802.05	56.07	56.34
	8900	3454.36	-	5687.01	-	64.63

5.5. CONCLUSIONS

A detailed finite element study was carried out to investigate the behaviour of steel I-beams reinforced with steel cover plates welded to the compression flanges of I-beams while the beams are under load. Effects of preload, cover plate thickness, reinforcing plate length, different cross-sections, and higher grade of steel for reinforcing plate on the behaviour of reinforced I-beams were investigated. The following conclusions can be summarized d from this study.

- Reinforcing a beam by welding a cover plate to the compression flange increased the ultimate capacities and stiffness of the beams regardless of preload level, and variation of preload did not have a significant effect on the ultimate capacity and failure mode of the steel I-beams reinforced at the negative bending moment region for continuous steel I-beams.
- Reinforcing steel-I beams, including homogeneous and hybrid cross-sections, could control and reduce the excessive out-of-plane deformation of the reinforced beams. Also, reinforcing the base beam at the compression flange changed the failure mode of the beam from lateral torsional buckling to cross-section yielding. In addition, I-beam reinforced by welding cover plate to the compression flange can increase the capacity of the beam to the plastic capacity of the unreinforced beam.
- Lateral deflections of the reinforced beams increased when the preload level was increased, mainly for the beams with longer unbraced lengths. Despite the difference in lateral deformation in the beams reinforced while under load, the failure mode and ultimate capacity of the beams were similar. Therefore, preloading and deformations induced by it did not have a significant effect on the behaviour of reinforced steel I-beams.
- It was observed that the thickness of the cover plate could change the failure mode of the reinforced beam. In this study, the failure mode of the reinforced beams was either lateral-torsional buckling of the reinforced beam or cross-section yielding. Increasing the cover plate thickness changed the failure mode of the reinforced beam from LTB to the cross-section yielding of the base beam (beam with cross-section B1). Also, the capacity increase due to increased reinforcing plate thickness was higher for reinforced beams with longer unbraced length and lateral-torsional buckling failure mode. Also, increasing the cover plate thickness was found to reduce the excessive lateral deformations for the beams with the same failure mode and capacity.

- In general, the capacity of the steel I-beams increased more for the beams with longer unbraced lengths when the beams were strengthened by welding cover plates to the compression flanges of both hybrid and homogeneous cross-sections.
- The moment capacity increased slightly with a change in the cover plate length. The difference in the capacity increase was negligible for the reinforced beams with a cover plate cut-off at zero bending moment location and a cover plate with no cut-off point. Therefore, there is no need to extend the cover plate beyond the M=0 location to increase the capacity of steel I-beam for negative bending moment. Moreover, preloading has an insignificant effect on the behaviour of steel I-beams reinforced with welded cover plates of different cut-off lengths.

6. Summary, Conclusions, and Recommendations for Future Work

6.1. SUMMARY

The purpose of the current study was to investigate the flexural behaviour and ultimate capacity of preloaded steel I-beams reinforced by welding a cover plate at the bottom flange. FE models were developed to simulate the steel I-beams welded with steel cover plates while under load. To the best of the author's knowledge, very limited research has been conducted on the strengthening of steel beams while they are in service. Proposed numerical models were validated against available experimental results. With the verified FE models, a series of steel I-beams reinforced with steel cover plates at the bottom flanges were analyzed. The considered failures for these beams were cross-section yielding and lateral-torsional buckling limit state flexural resistance. The behaviour and ultimate capacity of simply supported I-beams subjected to positive moment; and continuous-span I-beams subjected to negative moment by welding a cover plate while under load were studied.

Past studies have shown that an increase in the preload level resulted in a decrease in the lateral-torsional buckling capacity of beams reinforced by welding a cover plate at the bottom flange of a simply supported beam than the specimen reinforced with no preload. Also, no clear and definable relationship was obtained between the preload and strength of the reinforced beam for the I-beams reinforced by welding cover plates to both top and bottom flanges.

The numerical study included the following:

- Developing a numerical model to simulate the behaviour and ultimate capacity of the reinforced steel I-beams by considering the welding effects such as welding residual stress and deformation as the inputs.
- Developing a numerical model to simulate the behaviour and ultimate capacity of the reinforced steel I-beams by considering welding procedure simulation
- Studying the behaviour of simply supported steel I-beams reinforced with a welded cover plate at the bottom flange using detailed FE analysis by considering the effects of preloading, initial and welding residual stress, initial geometric imperfection, cover plate thickness, loading pattern, welding type (continuous or intermittent welding), different cross-section class for I-beams, and different steel grades of the beam components and reinforcing plate for the beams with cross-section and lateral torsional buckling failure modes.
- Investigating the effectiveness of the flexural strength equations of AISC 360-16 (Specifications for Structural Steel Buildings, ANSI/AISC 360-16. American Institute of Steel Construction) and

CAN/CSA-S16-19 (National Standard of Canada: Design of steel structures) for the design of simply supported I-shape beams reinforced with welded cover plate at the bottom flanges of the beams.

- Investigate the effect of welding heat input, welding sequences, and weld length on the residual deformation (plateau) due to welding, behaviour, and ultimate capacity of the simply supported I-beams when reinforced by welding a cover plate at the bottom flange.
- Studying the effect of initial geometric imperfection value and direction, as well as preloading level on the welding residual deformation (plateau), behaviour and capacity reduction of reinforced simply supported I-beams by considering welding procedures.
- Investigating the behaviour of steel-I beams that were reinforced by welding cover plates to the compression flanges while the beams were under load by considering the effects of cross-sections, unbraced lengths, preload levels, steel grade for reinforcing plate (hybrid sections) and reinforcing plate length (cut-off point). The numerical study was carried out to see whether adding a cover plate to the spans adjacent to piers could prevent the lateral-torsional buckling failure mode or not.

6.2. CONCLUSION

The main findings of the research study are categorized into three different subsections for reinforced steel I-beams while under load as follows:

- Simply supported beams reinforced by welding a cover plate at the bottom flange considering welding effects such as welding residual stresses and deformations as inputs in FEM.
- Simply supported beams reinforced by welding a cover plate at the bottom flange considering weld heat effects.
- Reinforcing continuous spans beams with welded cover plates in the negative bending moment region

6.2.1 Conclusions obtained for simply supported beams (welding effects as inputs in FEM)

A numerical study was conducted to investigate the effects of preloading, initial and welding residual stress, initial geometric imperfection, cover plate thickness, loading pattern, welding type; continuous or intermittent, different cross-section classes and steel grades of the beam components and reinforcing plate on the behaviour of steel I-beams reinforced by welding a cover plate to the bottom flange. The following results are drawn from this investigation.

- Preload did not have a significant effect on the behaviour and ultimate capacities of reinforced I-beams with flexural yielding failure modes. However, preload had some effect on the behaviour of beams with linear and nonlinear LTB failure modes. For the nonlinear LTB, the ultimate capacities decreased when the preload magnitude was increased; however, the reduction was smaller than 5% for a preload level of up to 60% of the strength of the unreinforced beam. For the beams with linear LTB, the presence of preload changed the buckling behaviour of the reinforced beams and reduced the buckling capacity.

- Initial residual stress has a negligible effect on the capacity reduction of I-beams with flexural yielding and linear LTB failures. However, the capacity reduction was different for different initial residual stress patterns and the difference increased with an increase in the preload level in the I-beams with nonlinear LTB failure. It was observed that the minimum capacity reduction was for the 'Chacon' initial residual stress pattern and the maximum capacity reduction (up to 5% for beams with 60% preloading) was for the 'ECCS' initial residual stress pattern.

- Variation of the maximum welding residual stress from 70% up to 100% yielding strength of the material did not change the capacity and behaviour of I-beams reinforced while under load.

- For the beams with different geometrical imperfection magnitudes, the flexural capacity was reduced when the preload level was increased. This was clear for the slender and intermediate beams with higher imperfection magnitude. However, the capacity reduction was small for beams with an imperfection magnitude of L/1000 (AWS limitation) and a preload level up to 60% of the capacity of the base beam. Also, the capacity reduction was negligible for the stocky beams, regardless of the preload level.
- In general, the behaviour of the reinforced I-beams with different reinforcing plate thicknesses was similar. The thickness of the cover plate did not affect the capacity increase in the stocky beams (with no preload). However, for the intermediate and slender beams, increasing the cover plate thickness affected the capacity increase. In intermediate and slender beams, the capacity reduction under preloading was more significant in the beams with thicker reinforcing plates, mainly in the intermediate ones.
- The overall behaviour of the beams with different loading patterns and preload levels was similar. When no preload was present, the capacity increase of the reinforced beam was different for beams with different loading patterns. When reinforced under preload, the loading pattern did not have a significant effect on the capacity reduction for the stocky beams. For the intermediate and

slender beams, the capacity reduction was more for the uniformly distributed loading pattern without any intermediate stiffener in the web, mainly in the slender beams under preload levels of 40% and 60%. However, for all loading patterns, the capacity reduction of reinforced beams was under 5%, up to a preload level of 60% of the capacity of the base beams.

- From this study, it was observed that the overall behaviour of I-beams reinforced with cover plates using continuous and intermittent welding was similar. For the stocky beams, the capacity increase was similar for I-beams reinforced with intermittent and continuous welding. However, for the intermediate and slender beams with no preload, cover plates welded with continuous welding, in comparison to the intermittent welding, provided higher capacities. For the beams reinforced under preload, capacity reduction for intermittent and continuous welding was almost similar.
- For the different considered cross-sections, the rate of buckling and ultimate capacity reduction for the beams reinforced under load was different. This difference was more noticeable in the intermediate and slender beams.

- For the homogeneous base (I-) beams, using higher strength material for welded cover plate did not have a significant effect on the capacity increase. For the hybrid base (I-) beams, using high strength reinforcing plate did not have any noticeable effect on the capacity increase of I-beams with no preload. Also, steel grade did not have any significant effect on the capacity reduction of the beams reinforced while under load.

- The capacities predicted by AISC were close to the FE capacities with slight overestimation for homogeneous cross-sections with compact and non-compact webs in stocky beams, while CSA S16-19 significantly overestimated the capacities for these beams. For the homogeneous intermediate beams, AISC without considering the effect of loading position and CSA with and without considering the effect of loading height into account significantly overpredicted the flexural capacities. Predicated capacities for AISC with modification factor of loading position were close to FE results with slight overestimation. For the elastic beams, AISC and CSA, considering the effect of loading height, could predict the capacity with reasonable accuracy. In addition, using the minimum yield strength of the cross-section components to find the capacities of reinforced I-beams with higher steel grades just for the reinforcing plate was shown to be a reasonable assumption. This assumption gave a conservative capacity prediction for stocky and

somewhat intermediate reinforced beams with cross-sections having different steel grades for web, flanges, and reinforcing plate.

6.2.2 Conclusions obtained for simply supported beams (Considering welding procedure simulation)

A finite element study was carried out to investigate the effects of local but intense welding heat, welding sequence, and welding length on the behaviour of reinforced steel I-beams by welding procedure simulation. Also, the effects of initial geometrical imperfection and preloading were studied numerically on the welding residual deformation and behaviour of the reinforced beams while under load by welding a cover plate to the bottom flange of the I-beam. The following conclusions were obtained from this paper:

- There was deformation induced due to the welding of reinforcing plate to the bottom flange of the base beams similar to the plateau observed in the experimental results in the lateral and vertical directions. The value and direction of residual out-of-plane deformation were dependent on the welding sequence. However, in-plane welding residual deformation was equal for all considered welding sequences. Also, it was shown that the conventional welding sequence recommended in the literature had the least welding residual deformation in the lateral direction. Therefore, using this welding sequence will lead to a reliable behaviour of the reinforced steel beam mainly for the beams which might have lateral-torsional buckling failure.
- For a specific welding sequence, the direction and value of welding lateral deformation changed for different initial geometric imperfection values and directions of the reinforced steel beams. However, welding-induced vertical deformation was not sensitive to the initial geometric imperfection. Also, the conventionally recommended welding sequence (welding sequence 2 in this study) was a preferable welding sequence for the reinforced steel I-beams because of the small variation of lateral residual deformations, low variation in the capacities, and independence to the direction and value of initial geometric imperfections.
- Reinforcing a preloaded beam by welding a cover plate at the bottom flange increased the ultimate capacity and stiffness of the beams. Also, for the recommended welding sequence (welding sequence 2 of this paper), lateral residual deformations due to welding of the reinforcing plate were similar for the I-beams with different preload levels. On the other hand, a difference in the vertical deformation was observed for welding the reinforcing plate at different preload levels.

Nevertheless, the overall behaviour and ultimate capacities of the beams reinforced by welding a cover plate at the bottom flanges were similar. Also, for the beams with cross-section yielding and lateral-torsional buckling failure mode, preloading did not have any significant effect on the ultimate capacity of the I-beams reinforced at a preload level up to 50% of the strength of the unreinforced beam. In addition, vertical deformation (plateau) induced from welding of a cover plate to the bottom flange of a simply supported beam increased with an increase in the preload level for the reinforced beams.

- Shorter welding segments reduced the welding residual deformation in the lateral direction for the recommended welding sequence (welding sequence 2 of this paper). However, vertical residual deformation induced by the welding was not sensitive to the welding segment length for the recommended welding sequence. Also, the ultimate capacity of the reinforced beam increased by reducing the weld segments. However, it was observed that the difference in ultimate moment capacity between weld segment L/9 and L/15 (where L is the length of the I-beam) was very small, and for practical applications, a welding segment length of L/9 can be used.

6.2.3 Conclusions obtained for steel I-beams with welded cover plates in the negative bending moment region

A detailed finite element study was carried out to investigate the behaviour of steel I-beams reinforced with steel cover plates welded to the compression flanges of I-beams while the beams are under load. Effects of preload, cover plate thickness, reinforcing plate length, different cross-sections, and higher grade of steel for reinforcing plate on the behaviour of reinforced I-beams were investigated. The following conclusions can be summarized from this study.

- Reinforcing a beam by welding a cover plate to the compression flange increased the ultimate capacities and stiffness of the beams regardless of preload level and the variation of preload did not have a significant effect on the ultimate capacity and failure mode of the steel I-beams reinforced at the negative bending moment region for continuous steel I-beams.
- Reinforcing steel-I beams, including homogeneous and hybrid cross-sections, could control and reduce the excessive out-of-plane deformation of the reinforced beams. Also, reinforcing the base beam at the compression flange changed the failure mode of the beam from lateral torsional buckling to cross-section yielding. In addition, I-beam reinforced by welding the cover plate to the compression flange can increase the capacity of the beam to the plastic capacity of the unreinforced beam.

- Lateral deflections of the reinforced beams increased when the preload level was increased, mainly for the beams with longer unbraced lengths. Despite the difference in lateral deformation in the beams reinforced while under load, the failure mode and ultimate capacity of the beams were similar. Therefore, preloading and deformations induced by it did not have a significant effect on the behaviour of reinforced steel I-beams.
- It was observed that the thickness of the cover plate could change the failure mode of the reinforced beam. In this study, the failure mode of the reinforced beams was either lateral-torsional buckling of the reinforced beam or cross-section yielding. Increasing the cover plate thickness changed the failure mode of the reinforced beam from LTB to the cross-section yielding of the base beam (beam with cross-section B1). Also, the capacity increase due to increased reinforcing plate thickness was higher for reinforced beams with longer unbraced length and lateral-torsional buckling failure mode. Also, increasing the cover plate thickness was found to reduce the excessive lateral deformations for the beams with the same failure mode and capacity.
- In general, the capacity of the steel I-beams increased more for the beams with longer unbraced lengths when the beams were strengthened by welding cover plates to the compression flanges of both hybrid and homogeneous cross-sections.
- The moment capacity increased slightly with a change in the cover plate length. The difference in the capacity increase was negligible for the reinforced beams with cover plate cut-off at zero bending moment location and cover plate with no cut-off point. Therefore, there is no need to extend the cover plate beyond the M=0 location to increase the capacity of steel I-beam for negative bending moment. Moreover, preloading has an insignificant effect on the behaviour of steel I-beams reinforced with welded cover plates of different cut-off lengths.

6.3. RECOMMENDATIONS FOR FUTURE RESEARCH

The conclusions of this study were limited to the parameters and numerical specimens considered for the analysis. However, to further expand the knowledge, some areas merit further investigations, some of which are listed below:

- It is recommended that further studies be conducted on the welding heat effects for the beams reinforced by a cover plate at the negative bending moment region.
- Based on the result of this study, there is a permanent welding residual deformation in the vertical direction for the beams reinforced while under load. There is merit in studying the beams for serviceability limit states for different cross-sections, loading and boundary conditions, and preloading levels.

- Considered beams for this study are isolated beams from the system. There is merit in considering the beams reinforced while under load within the structure system to see the effects of the adjacent members on the behaviour of the beams.
- Based on the results of this study, welding cover plates in the negative bending moment region can prevent the beam from LTB failure mode depending on the cover plate size. It is recommended to further study the size of cover plates and formulate an equation in terms of the reinforcing plate size for preventing the LTB failure modes.

7. REFERENCES

Abaqus 2019. Simulia, Inc., Providence, RI.

AISC. 2016. Specifications for structural steel buildings. ANSI/AISC 360-16. Chicago.

ANSYS 2006 standard user's manual. ANSYS.

AWS. 2020. Structural welding code–steel, AWS D1 .1 /D1 .1 M:2020, 24th ed., American Welding Society (AWS) D1 Committee on Structural Welding.

Barth, K.B., White, D.W, Bobb, B.M. 2000. Negative bending resistance of HPS70W girders. Journal of Constructional Steel Research, 53:1-31.

Bhowmick, A. K. Grondin, G. Y. 2016. Limit state design of steel columns reinforced with welded steel plates. Engineering Structures, 114: 48–60.

CAN/CSA S16-14. 2014. Handbook of steel construction. Mississauga (Ontario, Canada): Canadian Institute of Steel Construction.

Chacon, R. Serrat, M. Real, E. 2012. The influence of structural imperfections on the resistance of plate girders to patch loading, Thin-Walled Structures, 53:15–25.

Diana E. Chernenko, D.J. Kennedy, L. 1991. An analysis of the performance of welded wide flange columns, Canadian Journal of Civil Engineering, 180 (4): 537–555.

ECCS, 2000, New Lateral Torsional Buckling Curves kLT - Numerical Simulations and Design Formulae, European Convention for Constructional Steelwork Technical Committee No. 8.

Fu, G., Lourenco, M. Duan, M. Surjak, M. Estefen, F.E. 2014. Effect of boundary conditions on residual stress and distortion in T-joint welds. Journal of constructional steel research, 102:121–135.

Galambos, TV. 1998. Guide to stability design criteria for metal structures. Structural stability research council. 5th ed. New York: John Wiley & Sons, Inc.

Gao a, R. Cao, Q. Hu, F. Gao, Z. Li, F. 2017. Experimental study on flexural performance of reinforced concrete beams subjected to different plate strengthening. Composite Structures, 176: 565–581.

Goldak, J. Chakravarti, A. Bibby, M. 1984. A new finite element model for welding heat

sources. Metall Trans B,15B:299–305.

Kim, Y. D. 2010. Behavior and design of metal building frames using general prismatic and web-tapered steel I-section members. Doctoral dissertation, School of Civil and Environmental Engineering, Georgia Institute of Technology.

Gannon, L. 2007. Strength and behaviour of beams strengthened while under load. M.Sc. thesis,

Department of Civil and Resource Engineering, Dalhousie university.

Liu, Y. Gannon, L. 2009. Finite element study of steel beams reinforced while under load. Engineering Structures, 31(11): 2630–42.

Marzouk, H. Mohan, S. 1990. Strengthening of wide-flange columns under load. Canadian Journal of Civil Engineering, 17(5):835_43.

Mohammadzadeh, M., Bhowmick, A.K. 2022. Behavior of steel I-beams reinforced while under load. Engineering Structures, 257 (6):114080.

Mohammadzadeh, M., Bhowmick, A.K. Behavior of steel I-beams reinforced while under load. Proceedings of the Canadian Society of Civil Engineering Annual Conference 2021, 244: 67–79

Mohammadzadeh, M., Bhowmick, A.K. Reinforcing of steel I-beams in the negative moment region with welded cover plates" 11th International Conference on Short and Medium Span Bridges, Toronto, ON 2022.

Nagaraja Rao NR, Tall L. 1962. Columns reinforced under load. Fritz Laboratory Report No.286.1. Bethlehem, PA: Lehigh University.

Nguyen, K., Nasouri, R., Bennett, C., Matamoros, A., Li, J., Montoya, A. 2019. Galvanizing Induced Distortion in Steel Plate Girders. I: Effects of Girder Geometry. Journal of Bridge Engineering, 24(12): 04019110.

Peric, M., Tonkovic, Z. Rodic, A. Surjak, M. Garasic, I., Boras, I., Svaic, S. 2014. Numerical analysis and experimental investigation of welding residual stresses and distortions in a T-joint fillet weld. Materials and Design, 53: 1052–1063.

QustomWeld 2020, Abaqus/CAE-based plugin.

Rakgate, S.M. Dundu, M. 2018. Strength and ductility of simple supported R/C beams retrofitted with steel plates of different width-to-thickness ratios. Engineering Structures, 157, 192-202.

Sause, R. Fahnestock, L.A. 2001. Strength and ductility of HPS-100W I-girders in negative flexure. Journal of Bridge Engineering, 6(5): 316-323

Selvaraj, J. Madhavan, M. 2018. Retrofitting of Structural Steel Channel Sections Using Cold-Formed Steel Encasing Channels. J. Perform. Constr. Facil., 32(4): 04018049.

Selvaraj, J. Madhavan, M. 2019. Strengthening of laterally Restrained Steel Beams Subjected to Flexural Loading Using Low-Modulus CFRP. J. Perform. Constr. Facil., 33(3): 04019032.

Subramanian, L. P., White, D. W. 2017. Resolving the disconnect between lateral torsional buckling experimental tests and test simulations, and design strength equations. Journal of constructional steel research, 128: 321–334.

Subramanian, L. P., White, D. W. 2017. Reassessment of the Lateral Torsional Buckling

Resistance of Rolled I-Section Members: Moment Gradient Tests. Journal of Structural Engineering, 143(4): 04016203.

Subramanian, L. White, D.W, 2017. Reassessment of the Lateral Torsional Buckling Resistance of

I-Section Members: Uniform-Moment Studies. Journal of Structural Engineering, 143(3): 04016194.

Szewczyk, P. Szumigala, M. 2018. Static Equilibrium Paths Of Steel-Concrete Composite Beam Strenthened Under Load. Civil and environmental engineering reports, 28(2); 101–111.

Tall, L. 1989. The reinforcement of steel columns. Eng J, AISC. 26(1): 33–7.

Tide RHR. 1990. Reinforcing steel members and the effects of welding. AISC Eng J, 4th Quarter:129–31.

Vild, M. Bajer, M. 2016. The effect of preload magnitude, Procedia Engineering, 161; 343 – 348.

Vild, M. Bajer, M. 2016. Strengthening of Steel Columns under Load: Torsional-Flexural Buckling, Advances in Materials Science and Engineering, Hindawi Publishing Corporation.

Wu, Z. Grondin, GY. 2002. Behaviour of steel columns reinforced with welded steel plates, Structural Engineering Report 250, Department of Civil & Environmental Engineering, University of Alberta.

Yossef, N. M. 2015. Effect of Reducing Deflection of Steel I-Beams Strengthened While Loading. International Journal of Engineering Research & Technology (IJERT), 4; 573-580.

Yossef, N. M. 2015. Strengthening Steel I-Beams by Welding Steel Plates before or While Loading. International Journal of Engineering Research & Technology (IJERT), 4; 545-550.

Yuan-qing, W. Liang, Z. Rui-xiang, Z. Xi-yue, L. Yong-jiu, Sh. 2015. Behavior of I-section steel beam welding reinforced while under load. Journal of constructional steel research, 106: 278–288.